

Use of Thermal Integrity Profiling (TIP) in Drilled Shaft Evaluation



January 2022
Final Report

Project number TR202015
MoDOT Research Report number cmr 22-002

PREPARED BY:

Andrew Boeckmann

R. Andrew Yeskoo

Paul Axtell

Dan Brown and Associates

PREPARED FOR:

Missouri Department of Transportation

Construction and Materials Division, Research Section

TECHNICAL REPORT DOCUMENTATION PAGE

1. Report No. cmr 22-002		2. Government Accession No.		3. Recipient's Catalog No.	
4. Title and Subtitle Use of Thermal Integrity Profiling (TIP) in Drilled Shaft Evaluation				5. Report Date December 2021 Published: January 2022	
				6. Performing Organization Code	
7. Author(s) Andrew Boeckmann, https://orcid.org/0000-0003-1243-4677 R. Andrew Yeskoo Paul Axtell				8. Performing Organization Report No.	
9. Performing Organization Name and Address Dan Brown and Associates 6424 Baum Dr. Knoxville, TN 37619-6039				10. Work Unit No.	
				11. Contract or Grant No. MoDOT project # TR202015	
12. Sponsoring Agency Name and Address Missouri Department of Transportation (SPR-B) Construction and Materials Division P.O. Box 270 Jefferson City, MO 65102				13. Type of Report and Period Covered Final Report (April 2020-December 2021)	
				14. Sponsoring Agency Code	
15. Supplementary Notes Conducted in cooperation with the U.S. Department of Transportation, Federal Highway Administration. MoDOT research reports are available in the Innovation Library at https://www.modot.org/research-publications .					
16. Abstract Thermal Integrity Profiling (TIP) methods have emerged as a viable concrete integrity test method alternative to crosshole sonic logging (CSL). The objective of this study was to evaluate TIP methods for potential implementation on MoDOT drilled shaft projects. The study included a review of experience from previous research and project applications as well as collection of new data from a MoDOT project application. Together, the previous studies and the new research indicate TIP and CSL are generally complementary, with TIP more effective for identifying defects outside the reinforcing cage and weak concrete defects and CSL more effective for identifying defects within the reinforcing cage and soft bottom conditions. However, the results of this study indicate soft bottom conditions may be detectable with TIP methods, especially if temperature versus time records at the bottom of the shaft are evaluated. This research also included implementation of fiber optic methods for collecting TIP data. Laboratory and field results indicate fiber optic methods result in similarly accurate temperature results compared with conventional TIP, although practical limitations generally mean the fiber optic methods do not produce as complete of a time record. Cost data was also analyzed, indicating conventional TIP may result in cost savings compared to CSL, which is primarily a result of savings associated with remote data collection for many TIP projects. Finally, recommended specifications for MoDOT implementation of TIP methods were developed. The proposed specifications are included as an appendix.					
17. Key Words Drilled shaft, Deep foundation, Concrete, Concrete integrity, Thermal integrity profiling, Fiber optic, Crosshole sonic logging			18. Distribution Statement No restrictions. This document is available through the National Technical Information Service, Springfield, VA 22161.		
19. Security Classif. (of this report) Unclassified.		20. Security Classif. (of this page) Unclassified.		21. No. of Pages 121	22. Price

Use of Thermal Integrity Profiling (TIP) in Drilled Shaft Evaluation

Andrew Boeckmann, R. Andrew Yeskoo, and
Paul Axtell

December 2021

Copyright

Authors herein are responsible for the authenticity of their materials and for obtaining written permissions from publishers or individuals who own the copyright to any previously published or copyrighted material used herein.

Disclaimer

The opinions, findings, and conclusions expressed in this document are those of the investigators. They are not necessarily those of the Missouri Department of Transportation, U.S. Department of Transportation, or Federal Highway Administration. This information does not constitute a standard or specification.

Acknowledgements

The authors gratefully acknowledge the entities and personnel listed below for their significant contributions to the work.

Financial Support

Missouri Department of Transportation

MoDOT Personnel

Lydia Browning
Tom Fennessey
Jennifer Harper
Jacob Kloepfinger
Suresh Patel
Brent Schulte

Pile Dynamics, Inc.

Travis Coleman
George Piscalko
Jim Zammataro

Drilled Shaft Construction

Andrew Wilder and Cory Patterson of KCI Construction Company
Subsurface Constructors Incorporated

University of California – Berkeley

Kenichi Soga

Dan Brown and Associates

David Graham
Erik Loehr
Mark Madgett

Abstract

Thermal Integrity Profiling (TIP) methods have emerged as a viable concrete integrity test method alternative to crosshole sonic logging (CSL). The objective of this study was to evaluate TIP methods for potential implementation on MoDOT drilled shaft projects. The study included a review of experience from previous research and project applications as well as collection of new data from a MoDOT project application. Together, the previous studies and the new research indicate TIP and CSL are generally complementary, with TIP more effective for identifying defects outside the reinforcing cage and weak concrete defects and CSL more effective for identifying defects within the reinforcing cage and soft bottom conditions. However, the results of this study indicate soft bottom conditions may be detectable with TIP methods, especially if temperature versus time records at the bottom of the shaft are evaluated. This research also included implementation of fiber optic methods for collecting TIP data. Laboratory and field results indicate fiber optic methods result in similarly accurate temperature results compared with conventional TIP, although practical limitations generally mean the fiber optic methods do not produce as complete a time record. Cost data were also analyzed, indicating conventional TIP may result in cost savings compared to CSL, which is primarily a result of savings associated with remote data collection for many TIP projects. Finally, recommended specifications for MoDOT implementation of TIP methods were developed. The proposed specifications are included as an appendix.

Executive Summary

Thermal Integrity Profiling (TIP) methods have emerged as a viable alternative to the Crosshole Sonic Logging (CSL) method used by many agencies for concrete integrity testing. TIP methods are used to identify potential defects as zones of lower temperature within a drilled shaft during concrete curing. Unlike CSL, TIP methods can be used to identify potential defects outside the reinforcing cage. However, there are challenges associated with interpretation of TIP results, and questions regarding its sensitivity to defects, particularly at the bottom of a drilled shaft.

The goal of this research project is to support potential implementation of TIP methods for MoDOT projects. The primary objective of the research is to evaluate the effectiveness, accuracy, and cost of using TIP and CSL to identify defects. An additional objective is to compare the accuracy and cost of TIP performed with conventional thermal wire and TIP performed with fiber optic methods.

Previous Work

A number of previous studies have been performed to evaluate the effect of defects on TIP results. Four studies involving the use of intentional defects were presented in the literature review. The studies generally indicate that TIP results can be used to effectively identify defects installed outside the reinforcing cage. In most of the studies, the defects consisted of sandbags tied to the outside of the drilled shaft reinforcing cage. Various configurations were included, with the volume of sand generally corresponding to about 10 to 15 percent of the shaft cross-sectional area.

A Wisconsin DOT study comparing TIP and CSL resulted in the conclusion that the tests are generally complimentary in terms of defect detectability, with TIP more effective for identifying weak concrete defects and defects outside the reinforcing cage and CSL more effective for identifying soft bottom conditions and defects within the reinforcing cage. The Wisconsin DOT study concluded soft bottom conditions were not readily detectable with TIP on the basis of research test shafts as well as project experience with drilled shafts for the Zoo Interchange project in Milwaukee. Finally, the Wisconsin DOT study showed the importance of considering TIP results in terms of temperature versus time, rather than just temperature versus depth, which is the more common evaluation technique.

Field Study

TIP methods were performed on two drilled shafts at each of two bridge sites. The first bridge, Ewing Ave., included 3.5-ft diameter shafts with 3-ft diameter rock sockets. The total length of the shafts was approximately 20 ft, with half the length in the socket and half above. The second bridge, Ramp F, included 6-ft diameter shafts with 5.5-ft diameter rock sockets. The total length of the shafts was about 90 ft, with approximately 20-ft long sockets. All shafts were permanently cased down to the top of the rock socket. In addition, telescoping temporary casings were used for the Ramp F shafts.

TIP results show peak temperatures of about 115 °F for the Ewing Ave. shafts, which peaked around 15 hours after concrete placement, and 125 °F for the Ramp F shafts, which peaked after 30 hours. Temperatures at the top of the shafts were greatest, a result of significant overpour resulting in greater diameter. Temperatures were greater within the shafts than in the sockets, a result that was expected based on the diameter difference. For many depths, the TIP results also indicate a significant difference in temperature from one side of the shaft to the other, a result that indicates reinforcing cage eccentricity based on construction observations. Eccentricity is not surprising considering the heavy cages were supported on the bottom of the shaft (rather than hanging off the casing or using a crane) and the use of small rebar chairs as centralizers (rather than wheel centralizers).

Much of the TIP data analysis focused on the results at the bottom of the shafts, where soft bottom conditions were observed for one of the two shafts at each bridge site. Soft bottom conditions were identified based on weighted tape soundings and were also supported by subsequent CSL test results. Interestingly, the soft bottom conditions existed in the two shafts for which SONICaliper results indicated significant lack of verticality in the cased portions of the shafts. In addition to making cage eccentricity more likely, lack of verticality could have made achieving a proper casing seal difficult, which would make soft bottom conditions more likely.

Having one shaft with soft bottom conditions and one without is ideal for evaluating the detectability of soft bottom conditions using TIP methods. Contrary to the results of previous studies, including the Wisconsin DOT study, soft bottom conditions were potentially identifiable in the TIP records from this field study. However, the potential for identification of the soft bottom conditions varied with the TIP interpretation method. Strictly looking at the temperature-depth profile, which is the typical process in current commercial practice, is unlikely to reveal the soft bottom conditions because the effect of the soft bottom is difficult to discern from roll-off. Evaluation of the effective radius profiles is more promising, with notable reductions in effective radius at the bottom of the affected shafts. However, the effective radius approach is sensitive to curve-fitting parameters and volume inputs. The soft bottom conditions are most evident from evaluation of the temperature versus time records for the bottommost TIP sensors, which revealed a more gradual increase in temperature for the shafts with soft bottom conditions. It is uncertain if the more gradual increase would be detected as a soft bottom response without the benefit of comparison with the clean bottom shafts.

An important caveat to identification of soft bottom conditions for both TIP and CSL is the need for measurements at or very near the bottom of the shaft. CSL results will not identify soft bottom conditions if the access tubes terminate above the affected zone. Similarly, the effect of soft bottom conditions for Ewing Shaft 3 and Ramp F Bent 6 were likely more evident because the bottommost TIP sensors were just above the base of the shaft and likely surrounded by sediment for Ramp F Bent 6.

Fiber Optic TIP Methods

Previous work has demonstrated the potential for using distributed fiber optic sensing as an alternative to conventional TIP methods. An advantage of the fiber optic system is the ability to use the same system to measure mechanical strain as well as temperatures. Mechanical strain is useful for load testing and performance data. Another advantage of the fiber optic system is relatively inexpensive expendable material costs (the cable), although these are often offset by expensive analysis costs.

A laboratory study was performed to compare temperatures measured by fiber optic and conventional TIP methods from a water bath involving known temperatures. Measured temperatures for both systems were remarkably accurate. During the field study, measured temperature with depth between conventional and fiber optic TIP systems also compared favorably, with an average difference of less than 2 °F. While the conventional TIP system resulted in a continuous record of temperature versus time, the fiber optic measurements were only recorded during times when testing personnel were on site to operate equipment.

Installation of fiber optic thermal cables on the reinforcement cage is similar to the process of installation of conventional TIP wire. If the fiber optic thermal cable is appropriately selected, it can match or exceed the robustness and resistance to breakage of TIP wire. Monitoring of the fiber optic thermal cable during curing remains a challenge, relying on both a reliable, “clean” power supply as well as a secure monitoring location for the analyzer given its high value as compared to the TIP data logger. This challenge has been solved in the UK by deploying the fiber optic analyzer in a small CONEX or similar shipping container which can be left on site, unattended, for long periods of monitoring. Identifying qualified personnel to perform fiber optic testing in Missouri may require out-of-state consultants.

Cost

Published cost data and cost data from the field component of this work suggest the cost of implementing TIP methods may be less than the cost of implementing CSL methods. The cost of TIP wire, generally \$5/ft as of the date of this report, is similar to the cost of steel tubes for CSL. However, TIP data is generally collected remotely via datalogging equipment that is simple to install and can generally be managed by personnel already on site. CSL data is generally collected by technicians or engineers, who often incur travel expenses. Requirements to grout CSL tubes also results in greater costs for CSL tests.

TIP and CSL Ability to Detect Defects

TIP and CSL are complementary test methods. Neither test provides a perfectly reliable assessment of drilled shaft integrity, but combined, they can be used to detect most conceivable defects. The complementary nature of the two tests is reflected in the table below. Relatively severe soft bottom conditions are detectable with TIP when sensors are at or just above the base of the shaft and the temperature versus time records are evaluated.

Ability to Detect Relatively Modest Defects

Defect Type	TIP	CSL
Inclusions in cage interior	Difficult to detect	Readily detectible
Defects outside reinforcing cage	Readily detectible	Not detectible
Soft bottom	Potentially detectible	Readily detectible
Weak concrete	Readily detectible	Difficult to detect
Tremie breach	Potentially detectible	Readily detectible

Recommendations

TIP methods should be an allowable concrete integrity test method that could be used as an allowable alternative to CSL or in conjunction with CSL. A logical approach would be to allow both test methods, with the specific method for any given project selected on the basis of project considerations, e.g. anticipated shaft installation challenges and/or design assumptions. Both test methods should be used for technique shafts. Additional recommendations implemented in the specification (Appendix H) include:

- TIP testing should be performed using sacrificial wires, not the probe method.
- TIP interpretation should include (1) review of all available and accurate construction records, including drilling records, bottom-of-shaft inspection forms, and concrete volume logs, (2) review of the TIP results (temperature and effective radius) versus depth, and (3) review of temperature versus time results for any depth with suspected imperfections based on (1) and (2).
- Effective radius results can be used to evaluate TIP results but should not be used to infer concrete cover or otherwise determine the precise shape of the shaft.
- Evaluations of TIP results should be based on relatively open-ended language that prefers professional judgment over rigid quantitative criteria. Any results suspected as potential imperfections should be identified in the TIP report and trigger evaluation by the Engineer of Record. The Engineer of Record should identify the results as either permissible or requiring further investigation or remediation.

In addition to the proposed TIP specification language, a recommendation pertaining CSL was offered: CSL results interpretation should include consideration of relative energy decrease as well as arrival time. The recommendations also note that integrity testing (TIP, CSL, or both) is not an adequate or acceptable replacement for qualified and diligent field inspection, particularly during final clean-out, cleanliness verification, and concrete placement activities.

Table of Contents

Copyright	iii
Disclaimer	iv
Acknowledgements	v
Abstract	vi
Executive Summary	vii
1. Introduction	1
2. Review of Literature	3
2.1 Terminology	3
2.2 Crosshole Sonic Logging (CSL)	3
2.3 Thermal Integrity Profiling	5
2.3.1 Example TIP Records	5
2.3.2 Time to Peak Temperature	7
2.3.3 Probe versus Wire	7
2.3.4 Distributed Fiber Optic Sensing for Thermal Integrity Profiling	8
2.3.5 Interpretation of TIP Results	12
2.4 Gamma Gamma Logging (GGL)	17
2.5 Acceptance Criteria for CSL and TIP	17
2.6 Previous Research regarding TIP Sensitivity to Defects	20
2.6.1 Florida DOT Study by Mullins et al. (2007)	20
2.6.2 Iowa DOT Study by Ashlock and Fotouhi (2014)	22
2.6.3 Schoen et al. (2018)	25
2.6.4 Wisconsin DOT Study by Boeckmann and Loehr (2018, 2019)	26
2.7 Agency Experiences with TIP	28
2.7.1 WisDOT: Zoo Interchange	29
2.7.2 South Carolina DOT	31
2.7.3 Other Agencies	31
2.8 Cost of TIP and CSL	31
3. Fiber Optic Laboratory Research	33
4. Field Testing Program	36
4.1 Project Selection	36
4.2 Drilled Shaft Design Details	36
4.2.1 Overview of Drilled Shafts and Testing	36
4.2.2 Subsurface Conditions	37
4.2.3 Reinforcing Cage	38

4.2.4 Concrete Mix Design and Specifications.....	39
4.3 Drilled Shaft Construction.....	39
4.3.1 Drilling.....	39
4.3.2 Installation of Conventional TIP, Fiber Optic TIP, and Reinforcing Cages.....	42
4.3.3 Concrete Placement	47
4.3.4 Evidence of Imperfections from Construction Observations.....	51
4.4 Performance of Integrity Test Methods.....	51
4.4.1 TIP Testing	51
4.4.2 Fiber Optic Thermal Monitoring	52
4.4.3 CSL Testing	54
4.4.4 SONICaliper Testing	54
4.5 Cost of TIP and CSL	55
5. Results of Field Research	57
5.1 Conventional TIP Results.....	57
5.2 Fiber Optic TIP Results.....	66
5.3 CSL Results.....	68
5.4 SONICaliper Results	70
6. Interpretation of Results	73
6.1 Comparison of Temperatures from Fiber Optic and Conventional TIP.....	73
6.2 Analysis of TIP Time Records at the Base of Shafts	74
6.3 Comparison of Radius Interpretations: Concrete Volume Log, TIP, and SONICaliper	77
7. Summary, Conclusions & Recommendations	80
7.1 Summary of Findings	80
7.1.1 TIP and CSL Sensitivity to Defects based on Previous Research	80
7.1.2 TIP and CSL Sensitivity to Defects based on this Research	81
7.1.3 Conventional TIP Procedures	82
7.1.4 Fiber Optic TIP Methods	82
7.1.5 Cost.....	83
7.2 Conclusions	83
7.3 Recommendations for Integrity Testing.....	85
7.3.1 Potential Approaches to Implementing TIP.....	86
7.3.2 TIP Test Procedures and Use of Probe	87
7.3.3 TIP Test Interpretation.....	87
7.3.4 Acceptance Criteria	88
7.3.5 Fiber Optic TIP	88
7.3.6 CSL Recommendations	89

References.....	90
Appendix A – Construction Plans for Ewing Ave. Bridge (A8851).....	A-1
Appendix B – Construction Plans for Ramp F Bridge (A8854).....	B-1
Appendix C – As-built Drawings for Drilled Shafts with TIP.....	C-1
Appendix D – Concrete Placement Logs.....	D-1
Appendix E – Conventional TIP Reports from PDI TIP Reporter Software.....	E-1
Appendix F – Crosshole Sonic Logging Test Reports.....	F-1
Appendix G – SONICaliper Test Reports.....	G-1
Appendix H – Proposed Specification Language	H-1

List of Figures

Figure 2-1: Drilled shaft cross-sections showing access tubes and ray paths for (a) small-diameter shaft with four access tubes and (b) large-diameter shaft with eight access tubes. From Boeckmann and Loehr (2018).....	4
Figure 2-2: (a) Time record for a single depth and single access tube pair; (b) plots of FAT (red line, left) and relative energy (blue line, right) versus depth. Modified from ASTM (2016).....	4
Figure 2-3: Example TIP result from Mullins (2010).....	6
Figure 2-4: Example TIP result from Piscsalko et al. (2016): (a) TIP record and (b) core photograph from a depth of 90 ft.	6
Figure 2-5: (a) Backscattered light phenomenon and (b) Brillouin optical time-domain analyzer function (from Soga, 2014).	9
Figure 2-6: Distributed fiber optic sensing cable installation for a drilled shaft in the United Kingdom...	10
Figure 2-7: Hourly concrete curing temperature change with depth (de Battista 2016). Each line represents a different measurement time.	11
Figure 2-8: Drilled shaft temperatures as a function of radial position and shaft radius. From Mullins (2013).....	13
Figure 2-9: Example concrete volume record from FHWA’s Drilled Shaft manual (Brown et al., 2018).	14
Figure 2-10: TIP data used for example temperature-radius model by Mullins and Winters (2011).	15
Figure 2-11: Example Level 2 temperature-radius model from Mullins and Winters (2011). Model is based on the data from Figure 2-10.	15
Figure 2-12: Example effective radius analysis from Mullins and Winters (2011) using TIP data from the example of Figure 2-10 and the temperature-radius model shown in Figure 2-12.	16
Figure 2-13: Curve fitting at roll-off zones at top of shaft (TOS) and bottom of shaft (BOS) from Johnson (2014).	17
Figure 2-14: CSL evaluation criteria recommended by DFI (2018).....	20
Figure 2-15: Results of FDOT TIP study by Mullins et al. (2007), as presented by Mullins and Winters (2011).....	21
Figure 2-16: TIP results for Test Shaft 1 from Ashlock and Fotouhi (2014): (a) temperature and (b) effective radius.....	23
Figure 2-17: TIP results for Test Shaft 2 from Ashlock and Fotouhi (2014): (a) temperature and (b) effective radius.....	23
Figure 2-18: CSL results for Test Shaft 2 from Ashlock and Fotouhi (2014).	24
Figure 2-19: CSL results for Test Shaft 2 from Ashlock and Fotouhi (2014).	24

Figure 2-20: Example TIP result showing decreases in temperature at two known defect locations: (a) 14 hours and (b) 34 hours, the peak time. From Schoen et al. (2018).	26
Figure 2-21: Temperature and temperature difference versus time based on results from Boeckmann and Loehr (2018).	28
Figure 2-22: Temperature versus time for the bottom of shafts from Boeckmann and Loehr (2018).	28
Figure 3-1: Photograph of the water bath testing setup.	33
Figure 3-2: Photograph of the cable configuration within the water bath.	33
Figure 3-3: Photograph of the cable routing at the access port within the water bath lid.	34
Figure 3-4: Fiber optic peak frequency during water test. Each line represents a different time during the test.	34
Figure 3-5: Recorded temperature during the water bath test from the two measurement systems.	35
Figure 4-1: Plan view of Ewing Ave. bridge.	37
Figure 4-2: Partial plan view of Ramp F overpass bridge.	37
Figure 4-3: Drilled shaft cross-section for Ewing Ave. shafts: (a) within permanently cased section and (b) in uncased rock socket.	38
Figure 4-4: Drilled shaft cross-section for Ramp F shafts: (a) within permanently cased section and (b) in uncased rock socket.	38
Figure 4-5: Excavated shaft for Ramp F Bent 6 with the permanent (innermost) 72-inch casing and temporary 84-inch casing shown.	41
Figure 4-6: Ramp F Bent 6 shaft after welding an extension piece to the top of the permanent casing. In this photo, the temporary casings have been removed and the ground near the shaft has been excavated to provide a safe working space for reinforcing cage and concrete placement.	41
Figure 4-7: Conventional TIP wires affixed to the reinforcing cage for the Ramp F Bent 6 drilled shaft.	43
Figure 4-8: Conventional TIP wires affixed to the outside of the reinforcing cage for the Ramp F Bent 6 drilled shaft.	43
Figure 4-9: Schematic diagram of the fiber optic cable routing for a single loop / vertical pair.	44
Figure 4-10: Thermal fiber optic cables pre-installed on bottom section of reinforcement cage, with bundles for final vertical attached to the side of the cage.	45
Figure 4-11: Lowering of the reinforcing cage for the Ramp F Bent 6 shaft, with the TIP and thermal fiber optic cable spread radially around the shaft.	45
Figure 4-12: Reinforcing cage placement for the Ramp F Bent 5 drilled shaft: (a) lower half of cage suspended with the crane, (b) lower half of cage resting on casing, and (c) top half of cage aligned with bottom half prior to engaging mechanical bar splices.	46
Figure 4-13: Reinforcing steel chairs used as centralizers for the Ramp F Bent 5 drilled shaft.	47
Figure 4-14: Concrete slump test performed for Ramp F Bent 5 drilled shaft.	47

Figure 4-15: Concrete placement for Ewing Ave. Shaft 2.....	48
Figure 4-16: Concrete placement for Ewing Shaft 3: (a) Gap between the outside of the permanent casing and the ground surface; (b) overpouring concrete at the end of placement.	49
Figure 4-17: Concrete is transferred from concrete truck to pump truck.....	49
Figure 4-18: Placement of concrete by tremie in the drilled shaft for Ramp F Bent 5.	50
Figure 4-19: Concrete for Ramp F Bent 5 drilled shaft is over-poured.	50
Figure 4-20: Concrete volume curve for the drilled shaft at Ramp F Bent 6.....	51
Figure 4-21: TIP wires connecting into a TAG box (left) and TAP box (right). The boxes are attached to the top of the reinforcing cage for the Ramp F Bent 5 drilled shaft.	52
Figure 4-22: Photograph of the fiber optic analyzer setup in the rear of the cargo van.....	53
Figure 4-23: Raw fiber optic data from Ramp F, Bent 6, with thermal loops networked in series. Different lines correspond to different time stamps.	53
Figure 4-24: CSL testing is performed on the shaft for Ramp F Bent 5.	54
Figure 4-25: Performance of SONICaliper test: (a) overview and (b) caliper device within shaft.	55
Figure 5-1: Temperature versus depth for Ewing Shaft 2: (a) time of peak temperature, (b) half the time of peak temperature.....	59
Figure 5-2: Temperature versus depth for Ewing Shaft 3: (a) time of peak temperature, (b) half the time of peak temperature.....	59
Figure 5-3: Temperature versus depth for Ramp F Bent 5: (a) time of peak temperature, (b) half the time of peak temperature.....	60
Figure 5-4: Temperature versus depth for Ramp F Bent 6: (a) time of peak temperature, (b) half the time of peak temperature.....	60
Figure 5-5: Temperature difference versus depth for Ewing Shaft 2.....	61
Figure 5-6: Temperature difference versus depth for Ewing Shaft 3.....	61
Figure 5-7: Temperature difference versus depth for Ramp F Bent 5.	62
Figure 5-8: Temperature difference versus depth for Ramp F Bent 6.	62
Figure 5-9: Effective radius versus depth at half peak for Ewing Ave. (a) Shaft 2 and (b) Shaft 3.	65
Figure 5-10: Effective radius versus depth at half peak for Ramp F (a) Bent 5 and (b) Bent 6.	65
Figure 5-11: Fiber optic temperature versus depth for Ewing Shaft 2: (a) 7 hours after time of peak temperature, (b) half the time of peak temperature.....	66
Figure 5-12: Fiber optic temperature versus depth for Ewing Shaft 3: (a) 7 hours after time of peak temperature, (b) half the time of peak temperature.....	67

Figure 5-13: Fiber optic temperature versus depth for Ramp F Bent 6: (a) time of peak temperature, (b) 6 hours prior to half the time of peak temperature..... 67

Figure 5-14: Example CSL result for Ramp F Bent 6 (Tube Pairing 1-2)..... 70

Figure 5-15: SONICaliper shaft profiles for Ewing Ave.: (a) Shaft 2 and (b) Shaft 3. 71

Figure 5-16: SONICaliper shaft profiles for Ramp F: (a) Bent 5 and (b) Bent 6. 72

Figure 6-1: Fiber optic and conventional TIP thermal profiles at three times during curing of Ramp F Bent 6. 73

Figure 6-2: Temperature vs time at the bottom of shaft for Ewing Ave.: (a) Shaft 2 and (b) Shaft 3. 76

Figure 6-3: Temperature vs time at the bottom of shaft for Ramp F: (a) Bent 5 and (b) Bent 6. 77

Figure 6-4: SONICaliper and TIP effective radius interpretations in Ewing Ave. rock sockets: (a) Shaft 2 and (b) Shaft 3..... 78

Figure 6-5: SONICaliper and TIP effective radius interpretations in Ramp F rock sockets: (a) Bent 5 and (b) Bent 6. 79

List of Tables

Table 1-1: Advantages and limitations of TIP and CSL for evaluation of concrete integrity from Boeckmann and Loehr (2018). Table contents are revised in Chapter 7.	2
Table 2-1: Comparison of probe and wire methods. From Boeckmann and Loehr (2018).	8
Table 2-2: Acceptance criteria for CSL and TIP from various sources.	18
Table 2-3: Summary of defect characteristics from Ashlock and Fotouhi (2014) study.	22
Table 2-4: Summary of the ability to detect various types of relatively modest defects for TIP and CSL from Boeckmann and Loehr (2018). Table contents are revised in Chapter 7.	27
Table 2-5: Summary of concrete integrity testing results for the six shafts at Zoo Interchange that were cored. Defects were confirmed in five of the six shafts; all five were remediated via grouting. From Boeckmann and Loehr (2018).....	29
Table 2-6: Information from other transportation agencies with relevant TIP experience. From Boeckmann and Loehr (2018).....	31
Table 2-7: Summary of cost information from Hyatt et al. (2019).	32
Table 4-1: Concrete mix design specifications.	39
Table 4-2: Omnisens fiber optic analyzer reading settings.	52
Table 4-3: Summary of average unit price information from Hyatt et al. (2019) and the field testing program of this research.....	56
Table 5-1: Summary of conventional TIP testing results.....	63
Table 5-2: Summary of CSL anomalies identified in Appendix F.	69
Table 7-1: Summary of the ability to detect various types of relatively modest defects for TIP and CSL. Modified from Boeckmann and Loehr (2018).	84
Table 7-2: Significant advantages and limitations of TIP and CSL methods. Modified from Boeckmann and Loehr (2018).....	85

1. Introduction

Recent years have witnessed a significant increase in the diameters and depths commonly specified for drilled shafts, driven by demands for greater load capacity and facilitated by advances in drilling technology. The larger shafts result in challenging concrete pours requiring large volumes of concrete to maintain workability throughout long duration pours and along long flow paths through congested reinforcing cages. Concrete integrity test methods can augment post-installation assurance that drilled shaft concrete is sound, making the methods a useful complement to appropriate agency concrete mix design, construction, and QA/QC practices.

Thermal Integrity Profiling (TIP) methods have emerged as a viable alternative to the Crosshole Sonic Logging (CSL) method used by many agencies for concrete integrity testing. Whereas CSL uses geophysical measurements to identify zones of defective concrete, TIP methods identify defective zones using temperature measurements. Hydration of cement generates significant heat, so depths with defective concrete are expected to yield temperature reductions.

Boeckmann and Loehr (2018) summarized the advantages and limitations of CSL and TIP testing as shown in Table 1-1. One of the most significant differences between the two test methods is the zone of concrete within the shaft that is tested. CSL results are unaffected by defects outside the reinforcing cage since the ultrasonic wave is measured between access tubes affixed to the cage (typically on the inside of the transverse reinforcement). TIP results should conceivably be influenced by defects anywhere within the shaft cross-section, and especially defects outside the reinforcing cage since such defects disproportionately affect one or two wires. That TIP can detect defects outside the reinforcing cage is significant since concrete outside the reinforcing cage is critical for shaft side resistance, structural integrity, and durability. The background information presented in Table 1-1 is updated in Chapter 7 based on the results of this research.

Table 1-1: Advantages and limitations of TIP and CSL for evaluation of concrete integrity from Boeckmann and Loehr (2018). Table contents are revised in Chapter 7.

	Advantages	Limitations
TIP	<ul style="list-style-type: none"> • Can identify defects outside the reinforcing cage. • In addition to identifying defects, data can be used to indicate misalignment of reinforcing cage. • Tests can generally be performed within a day after concrete placement, resulting in potential construction schedule advantages. • Temperature information may provide additional value for large-diameter shafts subject to mass concrete considerations. 	<ul style="list-style-type: none"> • No information about soft bottom conditions. • Ability to detect defects in the center of the shaft may be limited. • Challenges interpreting test data: <ul style="list-style-type: none"> ○ Distinguishing defects from nuisance effects. ○ Acceptance criteria not well established. • Test window closes within days of concrete placement; optimal test time varies by project. This limitation is mostly insignificant for the wire method.
CSL	<ul style="list-style-type: none"> • Relatively long history of experience. • Reliably identifies concrete defects within central core of shafts. • Relatively simple interpretation. 	<ul style="list-style-type: none"> • No information outside reinforcing cage: <ul style="list-style-type: none"> ○ Cannot detect defects outside cage. ○ No indication of cage misalignment. • Relatively frequent “false positives,” particularly due to debonding of concrete. • Must wait 3 days to perform test, potentially impacting schedule.

The primary concerns regarding TIP methods relate to interpretation of TIP results:

- What is the detection ability of TIP?
- How sensitive are TIP results to various types of defects?
- Does temperature roll-off at the top and bottom of a shaft preclude identification of defects in these zones?
- Does temperature roll-off along the shaft (e.g. due to diameter changes) preclude identification of defects or increase the likelihood of false positives?
- How should TIP records be evaluated?

The goal of this research project is to support potential implementation of TIP methods for MoDOT drilled shaft projects. The primary objective of the research is to evaluate the effectiveness, accuracy, and cost of using TIP and CSL to identify defects in drilled shafts for MoDOT. An additional objective is to compare the accuracy and cost of TIP performed with conventional thermal wire and TIP performed with fiber optic methods.

The research objectives were achieved through evaluation of previous TIP experience from research and practice as well as through collection of new data from field research. The field research involved performing TIP and CSL testing on four production shafts, two from each of two bridge sites in St. Louis. Both conventional and fiber optic methods were used for TIP.

Background regarding CSL and TIP testing, including fiber optic methods, is provided in Chapter 2 of this report, which also summarizes acceptance criteria for both. Chapter 3 summarizes the results of a laboratory study of fiber optic TIP methods. Chapter 4 describes the field testing program, the results of which are presented in Chapter 5. Results of the field research are interpreted and discussed in Chapter 6, and conclusions and recommendations are presented in Chapter 7.

2. Review of Literature

Information about methodology, advantages, and limitations of CSL and TIP test methods are presented in this chapter. Various acceptance criteria for both tests are also presented. Also included in the chapter is a summary of cost data.

2.1 Terminology

This report adopts the terminology recommended in FHWA's GEC 15 *Acceptance Procedures for Deep Foundations of Transportation Structures* (Brown et al., anticipated 2022):

- An ***anomaly*** is an irregularity in the results of a concrete integrity test method. An anomaly may or may not represent an imperfection in the deep foundation.
- An ***imperfection*** is an unintended deviation in the constructed foundation element from the plan. An imperfection may or may not be a defect. "Imperfection" is synonymous with "flaw," as flaw is defined in the Deep Foundation Institute's "Terminology and Evaluation Criteria of Crosshole Sonic Logging (CSL) as Applied to Deep Foundations" (2018) white paper. "Imperfection" is preferred here to avoid confusion that can result from use of "flaw" and "defect."
- A ***defect*** is an imperfection that rises to the level of rendering the foundation insufficient or inadequate to perform as designed. Designation of an imperfection as a defect typically requires engineering analysis.

2.2 Crosshole Sonic Logging (CSL)

CSL (ASTM D6760, 2016) is the most common concrete integrity test performed for drilled shafts. The test involves measuring the passage of ultrasonic waves through access tubes attached to opposite sides of the shaft reinforcing cage as depicted in Figure 2-1. Incongruities in the resulting signal indicate potential anomalies of the concrete within the shaft reinforcing cage; concrete between reinforcing bars and outside the reinforcing cage is not evaluated. In the 2015 FHWA study of drilled shaft concrete practices (Boeckmann and Loehr), all 13 of the study agencies reported using CSL for concrete integrity testing for at least some drilled shafts, and eight of the 13 agencies reported using CSL in all shafts.

The area of the shaft investigated using CSL depends on the number of access tubes, as shown in Figure 2-1. The figure depicts CSL access tubes positioned inside the reinforcing cage for two shafts, one small-diameter shaft with four tubes and one large-diameter shaft with eight tubes. Assuming all access tube pairings are tested, the proportion of the shaft that is investigated is significantly greater for eight tubes than for four tubes. The greater number of tubes is associated with better coverage in the zone just inside of the reinforcing cage, as well as smaller zones of uninspected concrete between the ray paths. Importantly, the area outside the reinforcing cage is not inspected by CSL, regardless of the number of access tubes. In addition, the required personnel time to perform the test generally increases with the number of tube pairings, although new technology involving simultaneous analysis of more than two tubes (involving more than two probes) reduces the time required for large shafts.

Access tubes for CSL testing are typically 2 in. diameter, Schedule 40 steel pipe. PVC pipe is also sometimes used, but PVC pipe is more susceptible to concrete debonding and pipe deformation, both of which produce false positive results. The number of access tubes included on reinforcing cages generally increases with shaft diameter, with many agencies requiring one tube per foot of shaft diameter and a minimum of four tubes for small shafts. The tubes should be water-filled to prevent debonding, and for operation of the test probes during the test.

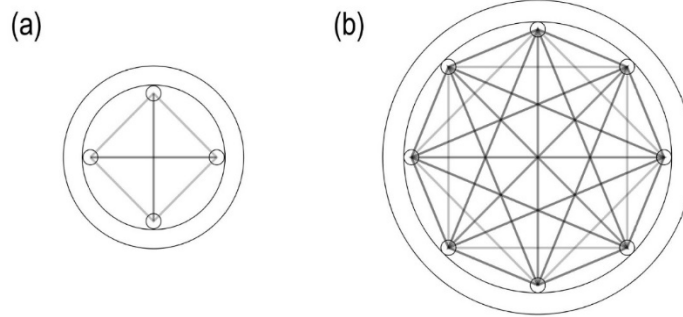


Figure 2-1: Drilled shaft cross-sections showing access tubes and ray paths for (a) small-diameter shaft with four access tubes and (b) large-diameter shaft with eight access tubes. From Boeckmann and Loehr (2018).

During the test, a source probe and receiver probe (geophones) are simultaneously raised from the bottom of separate access tubes. Per ASTM D6760, a common pulley equipped with a depth-encoding device is used to raise the probes. Ultrasonic pulses are sent from the source to the receiver as the probes are raised, and the ultrasonic response from the receiver is recorded for many depths. An example time record is shown in Figure 2-2(a) (ASTM, 2016). From each time record, the first arrival time (FAT) is interpreted, typically automatically by proprietary test software (rather than by test personnel). From the FAT, wave velocity can be interpreted by dividing the distance between tubes by the FAT. The relative energy is also commonly calculated for each time record from the amplitude of the pulses. The test is repeated for each combination of access tubes. The most common method for reporting results is to plot profiles with depth of FAT or wave velocity and relative energy for each combination of access tubes. An example profile set (FAT and relative energy) is shown in Figure 2-2(b) (ASTM, 2016). Spikes in arrival time and/or relative energy can be used to identify defective concrete, as discussed at the end of this chapter. For the record of Figure 2-2(b), spikes near 2, 8, and 14 m would likely be interpreted as anomalies.

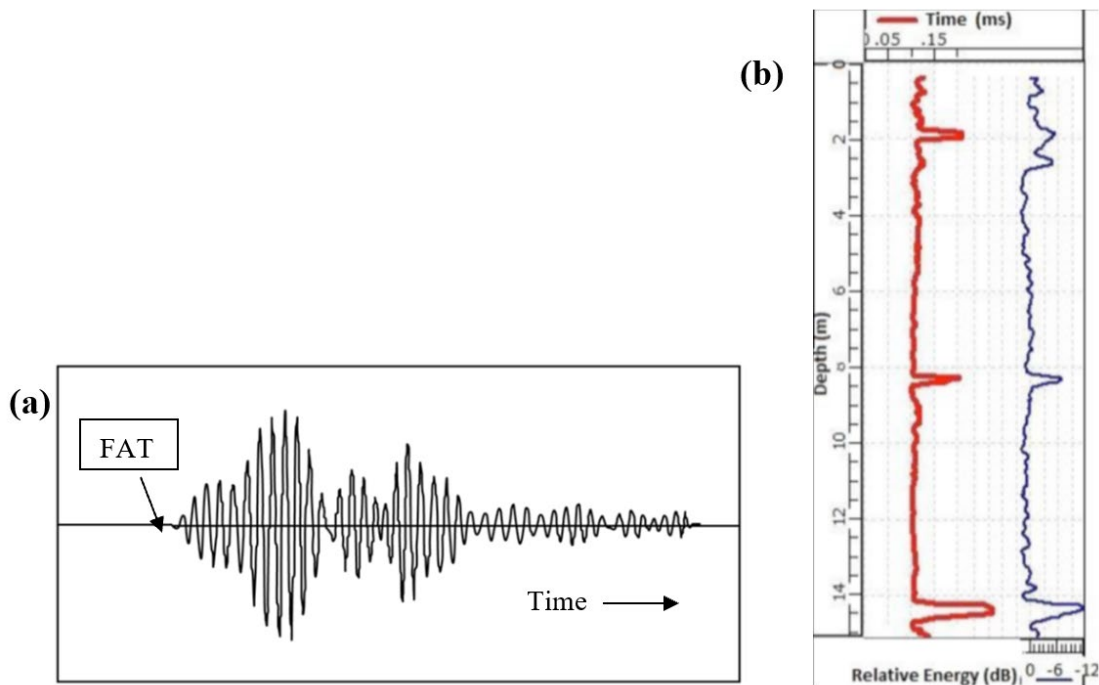


Figure 2-2: (a) Time record for a single depth and single access tube pair; (b) plots of FAT (red line, left) and relative energy (blue line, right) versus depth. Modified from ASTM (2016).

2.3 Thermal Integrity Profiling

TIP methods (ASTM D7949, 2014) originated at the University of South Florida from work for the Florida DOT (Mullins et al., 2007). TIP test methods involve measuring drilled shaft temperature versus depth during concrete curing. Hydration of cement generates heat that increases shaft temperatures during curing. Defective or absent concrete results in less heat generation and therefore lower temperatures whereas bulges in the shaft produce greater temperatures. TIP results are also used to evaluate the centrality of the reinforcing cage.

Temperatures are measured along the length of the reinforcing cage using either a probe lowered down access tubes on the cage or, more commonly, using temperature sensors along sacrificial wires tied to the cage. Similar to CSL, the number of access tubes or wires generally increases with shaft diameter, one tube or wire per foot of shaft diameter is often specified, and a minimum of four tubes or wires is often required.

The 2015 FHWA study of drilled shaft concrete practices found that TIP methods were not as common as CSL, with six of 13 agencies indicating experience with TIP methods. The agencies generally expressed an interest in further implementation of TIP methods. One of the agencies, Washington State DOT (WSDOT), has incorporated TIP methods into its standard specifications.

2.3.1 Example TIP Records

Example TIP results for a drilled shaft with sound concrete are shown in Figure 2-3. The example case was documented by Mullins (2010). The data are from a 10 ft diameter shaft with 10 access tubes, with data collected by the probe method. The top 15 ft of the access tubes were in the stick-up length of the casing, which did not contain concrete but was likely heated by heat radiating from the top of the concrete. Below the top of concrete, the temperatures are relatively consistent, with a few noteworthy exceptions. First, a slight increase in average temperature is evident at 32 ft. Mullins explains that this blip corresponds to the groundwater depth at the time of drilling, when some minor sloughing occurred prior to slurry introduction. Second, the temperature variation from one tube to the next indicates eccentricity of the reinforcing cage, which causes some tubes to be closer to the center of the shaft (and therefore warmer) while tubes on the opposite side are further from the center (and therefore cooler). Third, temperatures decrease near the top and bottom of the concrete in the so-called “roll-off” zones. Roll-off occurs because heat flow at the ends of the shaft is dominated by longitudinal flow of heat out of the shaft, whereas along the rest of the shaft, heat flow is primarily radial out the sides of the shaft, which are insulated by soil and/or rock.

Example TIP results with a zone of defective concrete are shown in Figure 2-4. The example case was documented by Piscsalko et al. (2016). The TIP data were recorded for a 10 ft diameter by 125 ft long drilled shaft with 10 TIP wires. A significant decrease in temperatures was observed in the TIP data at a depth of 90 ft (Figure 2-4(a)). The shaft was cored to investigate the potential defect. As shown in the photograph of Figure 2-4(b), the core results confirmed segregated concrete at 90 ft. The shaft was subsequently repaired by grouting.

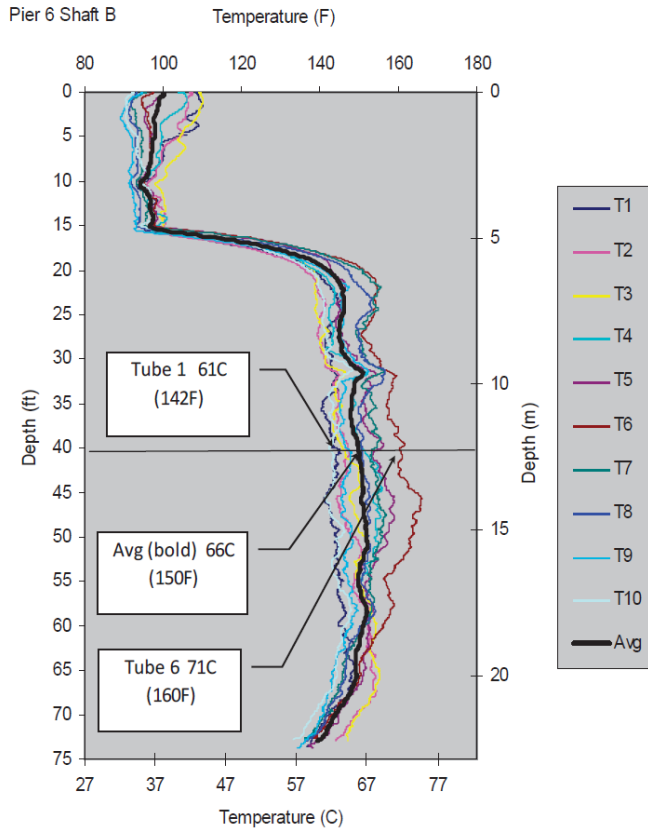


Figure 2-3: Example TIP result from Mullins (2010).

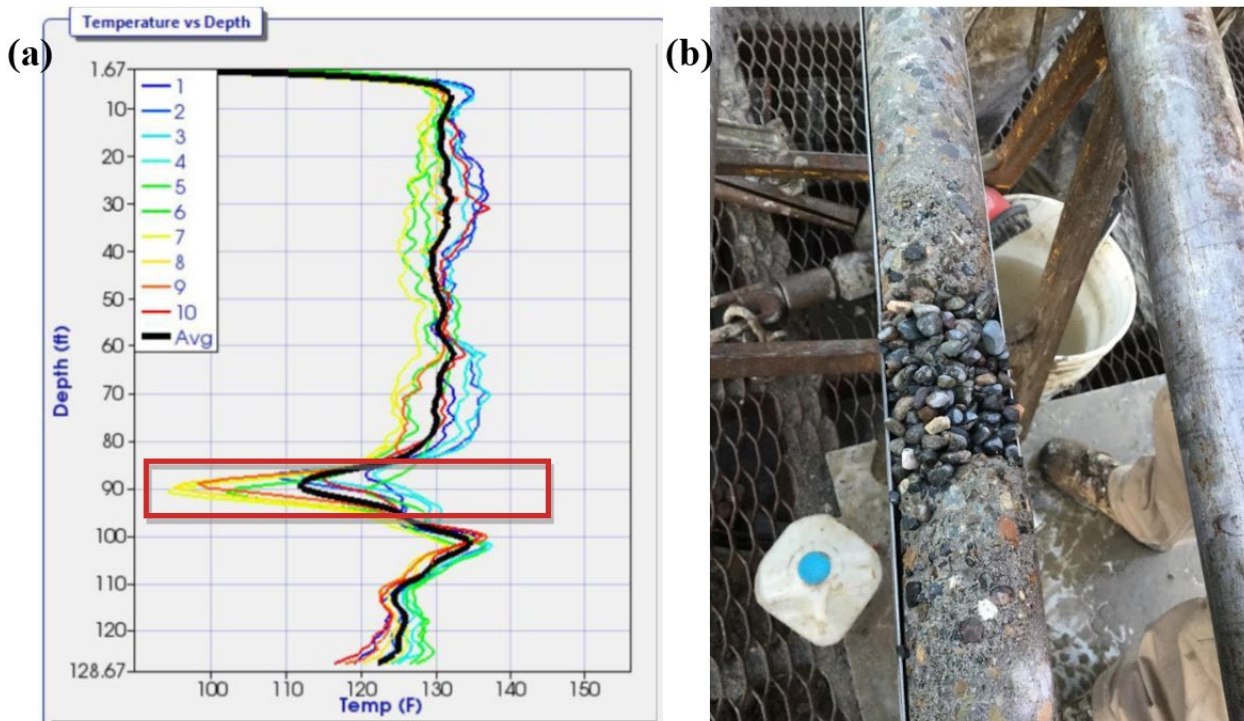


Figure 2-4: Example TIP result from Pisciaino et al. (2016): (a) TIP record and (b) core photograph from a depth of 90 ft.

2.3.2 Time to Peak Temperature

The testing window for TIP methods is limited to the period of elevated temperatures in the drilled shaft concrete. The time to peak drilled shaft concrete temperature is variable. Drilled shaft concrete temperatures often peak in less than one day, but it is also common for peak temperatures to develop within one to three days, or even longer for some shafts. The time to peak temperature is greater for larger shafts, and it also varies considerably with concrete mix parameters. The ASTM standard recommends testing “near the time of peak temperature in the concrete.” Since the time to peak cannot be known ahead of time (although it can be predicted), the ASTM standard recommends a testing window extending from 12 hours to D days, where D is the shaft diameter in feet. As discussed in Section 2.6.4, Boeckmann and Loehr (2018, 2019) demonstrated that evaluation of TIP data at one-third to one-half of the time to peak temperature is more effective for identifying imperfections.

Although references to “peak temperature” are included in virtually every TIP report and throughout published literature regarding TIP methods, no definition of peak temperature has been formally defined in any of the publications. It is important to note that during concrete curing, temperatures within a drilled shaft vary spatially—with depth and with distance from the center of the shaft cross-section—and with time. In addition, there is interaction between these effects. In other words, different locations within the shaft experience maximum temperatures at different times. Therefore, any given point in time may represent pre-peak, peak, or post-peak conditions, depending on location. These complications present challenges for defining peak temperature.

Several potential definitions of peak temperature are possible:

1. The maximum temperature observed in any of the TIP wires (or probes) at any depth (i.e. the single greatest measurement of all temperatures recorded).
2. The maximum temperature at any depth for the average temperature profile (i.e. the profile defined by averaging results from each of the wires).
3. The maximum temperature, averaged for all depths and all wires.

The second definition above was used for this project. For the purpose of interpreting TIP data, the peak temperature is primarily of interest as a means of normalizing the test interpretation time (e.g. evaluating records at the time of peak temperature, at half peak, after peak, etc.). As discussed in the Section 2.3.4 below, the interpretation of TIP data is typically based on shaft temperatures at a single point in time.

It is possible that for many projects, the time to peak temperature would be similar for all three definitions above, but significant differences are also conceivable. The middle definition is likely to produce the most consistent definitions of time to peak temperature. The first definition is likely susceptible to cage misalignment, or simply to measurement outliers. In contrast, the last definition “averages out” significant effects like changes in diameter, casing, groundwater, and geology. Averaging these effects may be inappropriate when it could be more effective to define multiple peak temperatures (e.g. one time for a narrower portion near the bottom of a shaft and a later time for the top part of the shaft).

2.3.3 Probe versus Wire

As explained above, TIP measurements can be taken along the reinforcing cage either with a probe lowered down access tubes (Method A in ASTM D7949) or with sacrificial wires with temperature gages, typically spaced at 1 ft increments (Method B). Access tubes for the probe method can be the same as those used for CSL testing, but the tubes must be dewatered before inserting the temperature probe. PVC pipes can also be used as access tubes. A summary of advantages and disadvantages of the probe and wire methods are summarized in Table 2-1 (Boeckmann and Loehr, 2018). Because TIP methods are premised

on temperature development during curing, the window for testing is limited to the period of elevated temperatures as described previously. The test window limitation is significant for the probe method, which requires testing personnel to actively collect data whereas the wires are equipped with loggers that record data from the time of logger installation. Because of the testing window limitation, decreases in wire costs, and improvements in wire construction (i.e. reduced wire breakage as reported in Chapter 3), wire method implementations of TIP have greatly surpassed probe methods (J. Zammataro, personal communication, Nov. 14, 2017).

Some consultants have taken to performing TIP testing by suspending TIP wires in CSL access tubes, attempting to simultaneously realize (1) the advantages of maintaining the ability to perform subsequent CSL testing with (2) the time record from the wires (and without the expense of the probe). However, Schoen et al. (2018) showed convincingly that the effect of defects on measured temperatures is greatly diminished when wires are suspended in access tubes. In addition, the ASTM standard does not include the suspended wire approach. The suspended wire approach is therefore not recommended and was not evaluated in the field research.

Table 2-1: Comparison of probe and wire methods. From Boeckmann and Loehr (2018).

	Advantages	Limitations
Thermal Probe (Method A)	<ul style="list-style-type: none"> • Access ducts support TIP as well as CSL. • Probe can be reused or rented. 	<ul style="list-style-type: none"> • Difficult or impossible to detect defects if collection occurs too far before or after peak shaft temperatures develop. • Time-consuming data collection. • Difficulties interpreting data for large shafts due to temperature changes during data collection time. • Initial equipment cost.
Wire (Method B)	<ul style="list-style-type: none"> • Nearly continuous record of temperatures: <ul style="list-style-type: none"> ○ Improves interpretation. ○ Eliminates risk of missing peak temperatures. ○ Additional data may be useful for thermal modeling. • Data collection is simple. 	<ul style="list-style-type: none"> • Cannot perform CSL unless access tubes are installed separately. • Wires are sacrificial. • Data collected at relatively larger intervals (typically 1 ft).

2.3.4 Distributed Fiber Optic Sensing for Thermal Integrity Profiling

In addition to the use of electrical temperature sensors, either in probe or wired sensors, distributed fiber optic sensing (DFOS) technology can use reflected light within embedded fiber optic cables to produce temperature profiles within a drilled shaft. The installation method of the fiber optic cable is similar to that of conventional TIP wire, with the fiber optic cable attached to the reinforcement cage at equally distributed verticals around the circumference. The only difference during installation is that the fiber optic cables are typically installed in loops, with each vertical thermal cable completing a partial or series of circumferential turns at the bottom of the reinforcing cage before returning to the top of the reinforcing cage in another vertical. This allows the fiber optic cables to be networked together for interrogation on a single channel, rather than requiring a switch.

DFOS refers to a variety of different sensing technologies which allow the interaction of light along a fiber optic cable to be used to measure various physical parameters along the cable length. In each of

these systems, the cable itself is the sensing instrument, with a single fiber optic analyzer at one end of the cable serving as the light source, receiver, and data logger. When light is sent through a fiber optic cable, several types of scattering occur to a small proportion of the transmitted light within the fiber. This scattering is continuous along the fiber and takes place throughout the entire length. Of the scattered light, a small portion is reflected back toward the source, a phenomenon referred to as backscattering. A diagram illustrating the backscattering phenomenon is shown in Figure 2-5 (Soga, 2014). By carefully recording differences in the backscattered light, measurements of physical phenomenon along the cable length can be made. The types of DFOS technology are Raman scattering, which is proportional to temperature changes, Rayleigh scattering, which is proportional to vibration or dynamic rate-of-strain, and Brillouin scattering, which is proportional to strain and temperature changes.

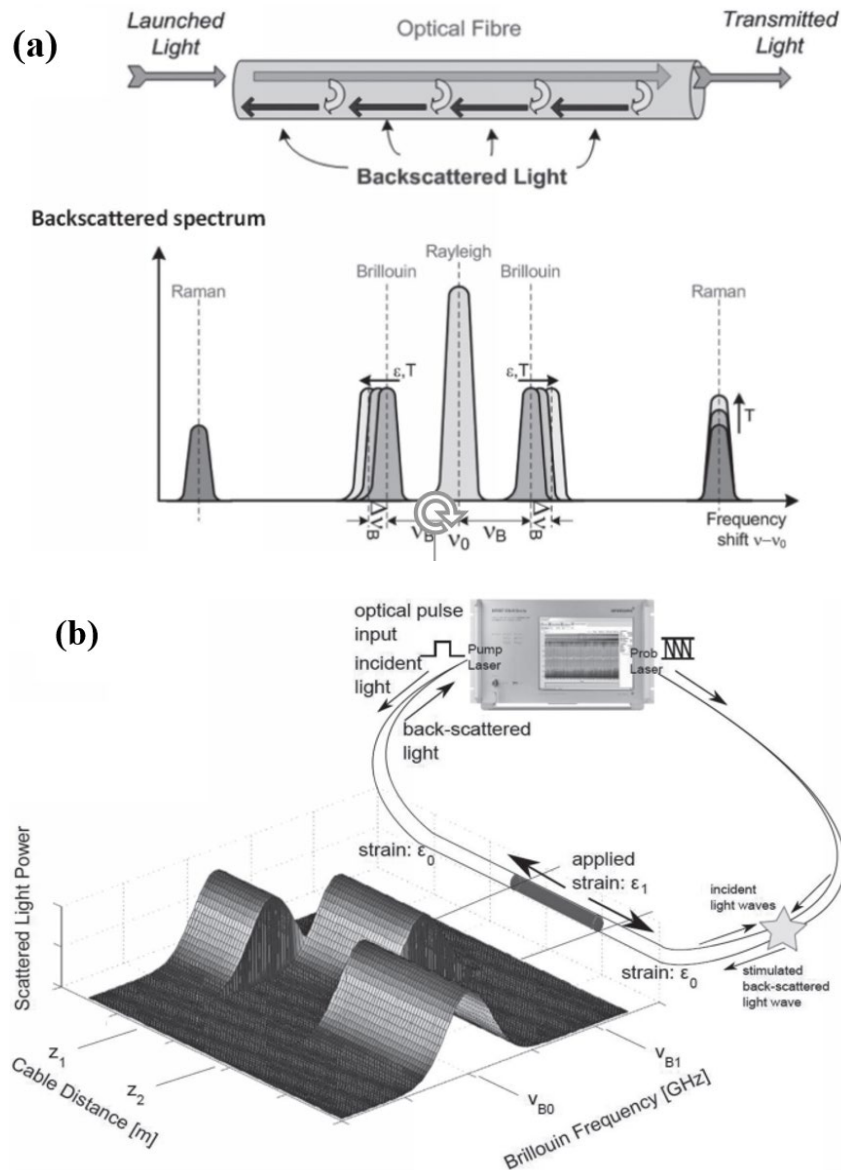


Figure 2-5: (a) Backscattered light phenomenon and (b) Brillouin optical time-domain analyzer function (from Soga, 2014).

Brillouin-based DFOS has been used for strain monitoring within deep foundations as early as the mid-2000s (Klar, 2006; Ouyang, 2015). The combination of commercial analyzer availability, small spatial and temperature/strain resolution, and the ability to measure both temperature change (e.g., during curing) and strain (e.g., during load testing or service loading) offer a wide array of capabilities and benefits for foundation monitoring. For a given reading, a matrix of peak Brillouin frequency with distance along the fiber is generated. The frequency is proportional to the strain along the fiber optic cable at each readout point. Changes in the frequency over time are proportional to changes in strain at that point, either mechanical strain or thermal strain. Different cable designs are available which either directly transfer external strains to the fiber core for mechanical strain measurement or cable packaging with a strain break for thermal strain measurement. As shown in Figure 2-6, the application of Brillouin-based DFOS for deep foundation monitoring was developed through a series of joint research projects in the United Kingdom, with the primary participants being the University of Cambridge and Cementation Foundations Skanska. While these early deployments focused on measurements of strain within the length of the piles, temperature sensing cables were included in some of the instrument piles to allow for thermal compensation of the mechanical strain measurements.



Figure 2-6: Distributed fiber optic sensing cable installation for a drilled shaft in the United Kingdom.

Thermal DFOS' first published use for thermal integrity measurements of subsurface structures was in 2016 when thermal fiber optic systems were used to monitor concrete curing in piles as part of larger pile testing program (de Battista, 2016). Results are shown in Figure 2-7. Loose-tube fiber optic cables were deployed vertically along the pile reinforcement, with multiple verticals arranged equally around the reinforcement perimeter.

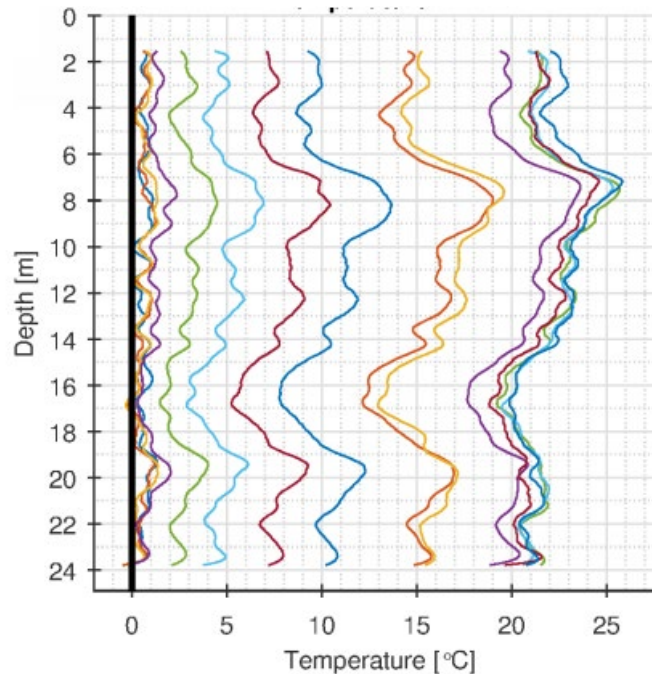


Figure 2-7: Hourly concrete curing temperature change with depth (de Battista 2016). Each line represents a different measurement time.

DFOS thermal monitoring practices were further developed in 2017 by researchers at the Centre for Smart Infrastructure & Construction (CSIC), a research group operating within the University of Cambridge (Rui, 2017). The work combined the deployment of fiber optic thermal monitoring within deep foundations to measure temperature curing with one-dimensional modeling of the heat generation and dissipation to estimate concrete cover. Conventional TIP wires were deployed in parallel with the fiber optic system. The monitoring results compared favorably between the two systems. Work is ongoing at the University of Bath and the University of California, Berkeley, to create a code package to automate the processing and numerical analysis of fiber optic thermal data during curing to generate the predicted pile shape with depth. Separately, Cementation Foundations Skanska has incorporated the use of fiber optics monitoring into their foundations practice under the CemOptics offering in the United Kingdom, including thermal integrity testing as well as strain measurements (Fisher, 2017). The approach of using fiber optic sensors for thermal integrity testing was granted a U.S. patent in 2018; however it has not yet been deployed commercially in the United States.

Additional research has been done to conceptually explore the use of thermal DFOS monitoring for pile integrity testing using a spiral fiber configuration rather than the more conventional vertical. This work was first undertaken in 2018 at the Missouri University of Science and Technology (Zhong, 2018) and was advanced in 2021 by researchers at Southeast University in Nanjing, China (Deng, 2021). Although both efforts specifically highlight the use of thermal DFOS for temperature monitoring, the focus is on numerical modeling of the spiral configuration of the temperature measurements rather than any unique feature or application of fiber optics. It is not clear from the publications if field deployment of the spiral design has been tested.

In most applications, the output of a fiber-optic based thermal monitoring program is a set of temperature measurements within the pile with depth and time. This output is analogous to the temperature records generated by conventional TIP wire sensors and can be post-processed and interpreted similarly.

2.3.5 Interpretation of TIP Results

The fundamental concept that is the basis for TIP – drilled shaft concrete temperatures can be used to identify defective concrete – is fairly simple, but interpreting the results of TIP tests can be less so, particularly if a quantitative interpretation is required. In a report for WSDOT regarding TIP testing, Mullins and Winters (2011) established four levels of TIP interpretation:

- Level 1 – Direct observation of the temperature profiles
- Level 2 – Superimposed construction logs and concrete yield data
- Level 3 – Three dimensional thermal modeling
- Level 4 – Signal matching numerical models to field data

Most TIP applications use Level 1 and/or Level 2 interpretation, both of which are detailed below. Level 3 and Level 4 interpretations are less common: none of the many published project applications of TIP included Level 3 or 4 analysis. Mullins and Winters did not outline Level 3 and Level 4 analysis procedures in the WSDOT report, but they did apply Level 3 analyses to the test cases they interpreted. In addition, details of a thermal modeling approach for drilled shafts are provided in the original TIP development report by Mullins et al. (2007).

Level 1 analysis is a qualitative assessment of TIP data. The discussion of the examples in the previous section could be considered Level 1-type analyses. In short, TIP results for the example from Figure 2-3 indicated sound concrete with no major concerns, but the results for the example of Figure 2-4 indicated a potential imperfection at a depth of 90 ft. Importantly, Level 1 analysis of the second example would be sufficient to trigger action (the coring that was performed). Mullins and Winters describe effects that can be considered during a Level 1 assessment. The list below includes items from their report as well as some supplementary considerations:

- Changes in shaft diameter, as indicated by the average temperature. Diameter changes could be part of the shaft design (e.g. telescoping casing), incidental to construction (e.g. temporarily cased segments of the shaft typically have a slightly greater diameter than uncased sections of the same nominal diameter), or indicate imperfections (e.g. bulging or necking).
- Proper cage alignment, as indicated by relative uniformity among wire temperatures.
- Roll-off zones at the top and bottom of the shaft. Mullins and Winters note the length of each roll-off zone is typically within one shaft diameter.
- Groundwater table
 - Greater temperatures at the location of the groundwater table can be produced by bulging, especially in granular materials (e.g. Figure 2-3)
 - Saturated materials have greater thermal conductivity; all else equal, greater temperatures would generally be anticipated above the groundwater table.

The engineer's responsibility during a Level 1-type assessment is to evaluate how trends in the observed TIP data can be explained by effects like those explained above. The responsibility further includes evaluating how significant any deviations are, and whether they warrant further action, but this responsibility is common to all levels of TIP interpretation, and to other integrity tests.

Level 2 (and Level 3 and 4) assessments are based on interpretations of “effective radius,” which Mullins and Winters defined as the predicted radius that would produce the observed temperature in the TIP data. The concept behind the effective radius approach is to “convert” the observed temperatures to shaft radius at each wire and for every depth. The effective radius values are often used to report average shaft diameter, cage eccentricity, and concrete cover, all of which are more meaningful parameters for evaluating concrete integrity than raw concrete temperature. Pile Dynamics, Inc. (PDI), which

manufacturers the most common TIP equipment, has adopted the effective radius approach within its TIP software, so it is common to see plots of effective radius presented with temperature plots in TIP reports.

The premise of the effective radius approach is that concrete temperatures near the edge of a drilled shaft are strongly influenced by two factors: shaft radius and radial position, defined as the distance from the center of the shaft. This concept can be observed in Figure 2-8. The graph in Figure 2-8 is from Johnson (2016), who based the graph on results of analytical thermal models by Mullins (2013). The sloping surfaces shown in the figure represent significant increases in temperature with (1) increasing shaft radius and (2) decreasing distance from the shaft center. Applied to TIP, this means that depths of greater-than-average measured temperatures could be explained by either (1) the shaft being larger or (2) the measurement points being closer to the center of the shaft. These explanations correspond to the yellow circle points in Figure 2-8 being (1) further right along the black dashed line or (2) being closer to the center along the solid red line. By incorporating multiple TIP wires (or access tubes), it is possible to distinguish between the two effects at a given depth: (1) increases in temperature due to larger shaft radius would be indicated by increases in the average wire temperature whereas (2) increases in temperature due to wire location would be indicated by differences in the temperatures among the various wires.

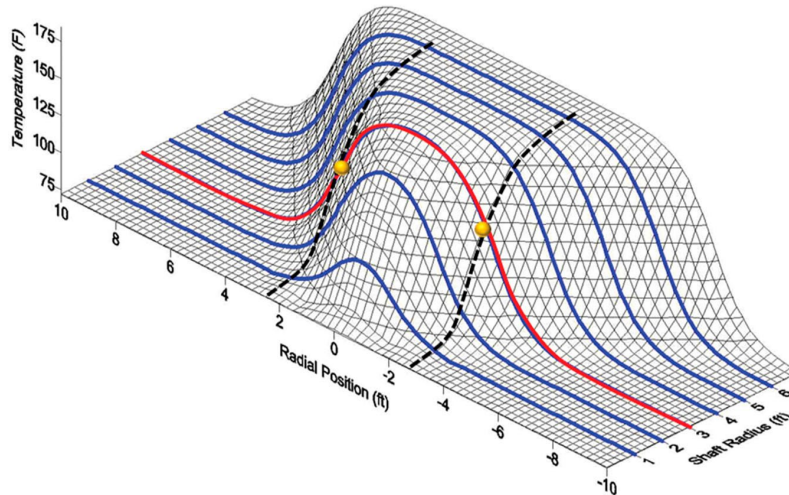


Figure 2-8: Drilled shaft temperatures as a function of radial position and shaft radius. From Mullins (2013).

Practically, the effective radius premise for TIP interpretations is implemented through temperature-radius models, which are relationships used to infer radius from temperature measurements. There are several methods for creating temperature-radius models. Level 2 assessments create the models empirically using TIP results and concrete volume records from the drilled shaft installation. Concrete volume information is a recommended component of drilled shaft construction QA/QC procedures (e.g. FHWA's Drilled Shaft manual; Brown et al., 2018). A useful means for conveying concrete volume information is to plot the cumulative volume of concrete placed versus depth. An example concrete volume plot is shown in Figure 2-9. The plot includes points for each volume measurement, which typically represents the volume placed from one concrete truck. The plot also shows the theoretical volume for the design shaft, which is generally less than the actual volume. The slope of the actual volume versus depth line corresponds to the cross-sectional area of the shaft, from which the shaft radius can be calculated. Thus, for each line segment on the concrete volume plot, one shaft radius value can be interpreted.

Level 3 analyses are similar to Level 2, but the temperature-radius model is developed using a thermal model rather than using the concrete volume measurements. Level 4 analyses contain all of the components of a Level 3 analysis. In addition, the thermal model for a Level 4 analysis is calibrated so that predicted temperatures are consistent with TIP measurements. The temperature versus radius model used to interpret the effective radius values is based on the calibrated thermal model. No examples of Level 4 analyses were found in the literature.

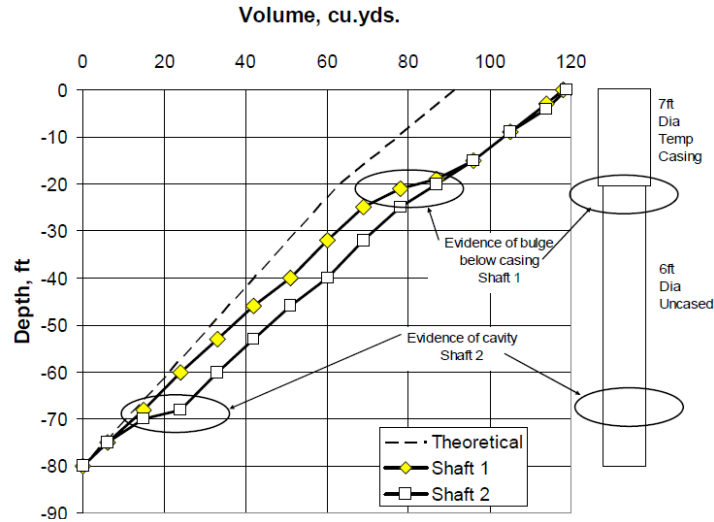


Figure 2-9: Example concrete volume record from FHWA’s Drilled Shaft manual (Brown et al., 2018).

Example temperature-radius data for a Level 2 assessment by Mullins and Winters (2011) are shown in Figure 2-10, which is a profile of TIP and shaft diameter values with depth for a 7 ft diameter shaft. The heavy black line in the figure is the average temperature from the TIP data, and the pink line with square dots is the shaft diameter as interpreted from the concrete volume log. There appears to be significant correlation between the average temperature and the shaft diameter, as the shape of both plots is similar. The correlation is confirmed by the temperature-radius model shown in Figure 2-11. The temperature-radius relationship used for the data is from linear regression.

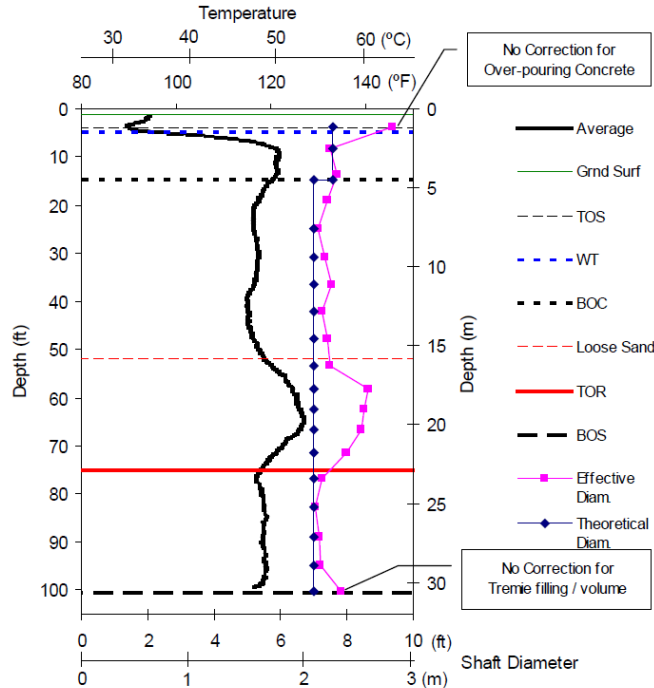


Figure 2-10: TIP data used for example temperature-radius model by Mullins and Winters (2011).

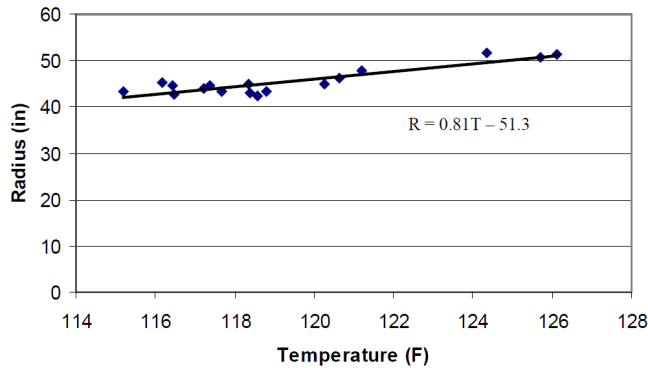


Figure 2-11: Example Level 2 temperature-radius model from Mullins and Winters (2011). Model is based on the data from Figure 2-10.

Figure 2-12 shows the results of applying the temperature-radius model from Figure 2-11 to all of the TIP data collected for the shaft in order to produce effective radius values. Specifically, each TIP temperature measurement is used in the regression equation to infer the effective radius with depth for each TIP access tube. Also shown in Figure 2-12 is the design radius of 3.5 ft, represented by a vertical blue line. The effective radius interpretation implies the overall average shaft radius is greater than design, since most points are to the right of the blue line. This implication follows directly from the observation that the total volume of concrete placed was greater than the theoretical volume. The vertical dashed black line in Figure 2-12 represents the design cage location; the distance between the dashed black line and the solid blue line, 6 in., is the design concrete cover distance. Accordingly, the effective radius results near a depth of 50 ft imply a complete loss of cover at TIP access tubes t3 and t4.

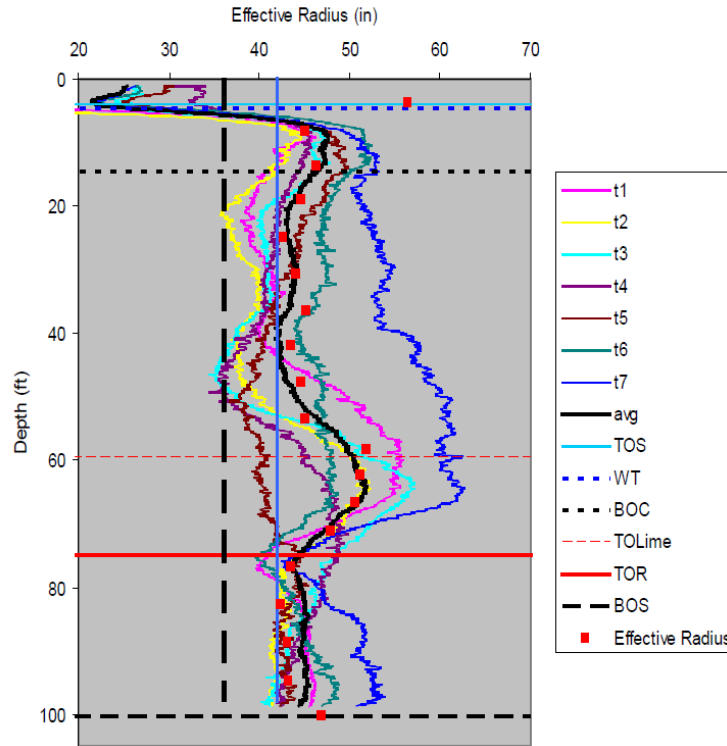


Figure 2-12: Example effective radius analysis from Mullins and Winters (2011) using TIP data from the example of Figure 2-10 and the temperature-radius model shown in Figure 2-12.

Johnson (2016) also notes that the empirical temperature-radius models (e.g. the model shown in Figure 2-11) only apply to zones where heat flow is predominantly out the sides of the shaft with negligible longitudinal (vertical) heat flow. The roll-off zones at the top and bottom of every shaft violate this assumption, as do several other potential shaft “transition” scenarios: changes in diameter, changes in geology, presence of groundwater, and likely others. To account for the roll-off and transition zones, Johnson (2014, 2016) describes a curve-fitting approach depicted in Figure 2-13. The approach involves fitting a hyperbolic tangent function to the TIP measurements and then calculating “corrected” temperatures from the difference between measurements and the fitted curve. The corrected temperatures are essentially normalized to the temperatures just below the top roll-off zone or just above the bottom roll-off zone. The corrected temperatures were conceived to represent the temperatures that would be expected without the longitudinal heat flow, and therefore to be useful both for developing temperature-radius models (e.g. as in Figure 2-11) and for interpreting TIP measurements.

In Figure 2-13, the black points represent TIP measurements, the solid red line is the fitted hyperbolic tangent function, and the dashed blue line is the corrected temperatures. Because the hyperbolic curves fit the measured data at the top and bottom of the shaft well, the corrected temperatures in the roll-off zones are similar to the temperatures just outside the roll-off zones. If the agreement between measured temperatures and the fitted hyperbolic tangent curve were weaker, corrected temperatures would deviate from the temperatures outside the roll-off zones. The TIP software implemented by PDI applies the corrected temperature adjustments at the top and bottom of each shaft by default. It also includes an option to include adjustments at user-specified depths for transitions between the ends of the shaft.

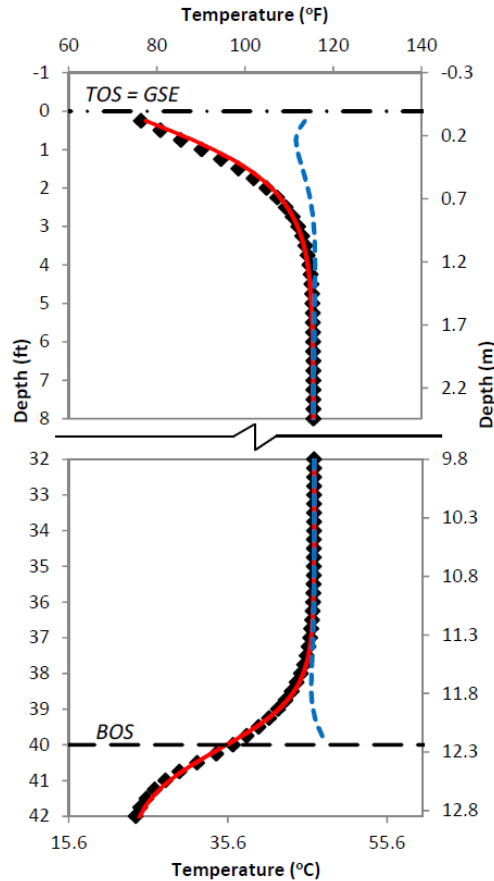


Figure 2-13: Curve fitting at roll-off zones at top of shaft (TOS) and bottom of shaft (BOS) from Johnson (2014).

2.4 Gamma Gamma Logging (GGL)

A third concrete integrity test method, Gamma Gamma Logging (GGL), is also available but commonly used only in California. The GGL test measures gamma rays to interpret concrete integrity in a zone approximately 3 in. around PVC access tubes attached to the reinforcing cage. The test is useful for evaluating concrete in the cover zone, but it does not identify defects in the center of the cage. In addition, there are practical drawbacks: it requires a nuclear source and it requires PVC access tubes that cannot be bundled with vertical reinforcement on the reinforcing cage, so it complicates cage design and increases cage congestion.

2.5 Acceptance Criteria for CSL and TIP

A critical aspect of concrete integrity tests is acceptance criteria: the methodology for evaluating the interpreted test results to reach a conclusion of either accepting the concrete placement or requiring further action (e.g. engineering analysis, coring, etc.). State transportation agency specifications, research reports, project reports, and TIP literature were reviewed to identify both suggested and adopted acceptance criteria for CSL and TIP. Results of the review are summarized in Table 2-2.

Table 2-2: Acceptance criteria for CSL and TIP from various sources.

Source	CSL	TIP
ASTM	No specific criteria. “How one applies the results obtained using this standard is beyond its scope.”	No specific criteria. “Interpretation ...should contain proper engineering judgment and experience.”
Washington State DOT Standard Specifications (2022)	<p><u>Good:</u> No signal distortion and decrease in signal velocity of 10% or less.</p> <p><u>Questionable:</u> Minor signal distortion and lower signal amplitude with a decrease in velocity between 10 and 20%.</p> <p><u>Poor:</u> Severe signal distortion and much lower signal amplitude with a decrease in signal velocity of 20% or more.</p>	<p><u>Satisfactory:</u> 0 to 6% reduction in effective shaft radius and cover criteria met.</p> <p><u>Questionable:</u> effective local radius reduction >6%, effective local average diameter reduction >4%, or cover criteria not met.</p>
Florida DOT Standard Specifications (2022)	Velocity reduction greater than 30% is not acceptable without 3D tomography and subsequent engineering analysis.	No specific criteria, but requires reports to indicate “unusual temperatures, including cooler local deviations from the average at any depth [or] from the overall average over the entire length.” Reports must also include “a conclusion stating whether the tested shaft is free from integrity defects, meets the minimum concrete cover and diameter requirements by the specifications and the cage is properly aligned.” Thermal modeling (i.e. Level 3 interpretation) is required to satisfy report requirements, which include “theoretical temperatures.”
Mullins et al. (2009) Draft Specifications for FDOT <i>Note: Not implemented (per above row)</i>	N/A	Included two potential criteria, both of which require thermal modeling: (1) “Test results with deviations greater than 5 degrees over a 1 ft length shall be further evaluated using Signal Matching Analyses to determine the possible shaft cross-section loss.” (2) “Drilled shafts with either insufficient cover or 5 degree Fahrenheit reduction from the model norm over a length of shaft at least 2 ft in length will not be accepted without an engineering analysis.”
Likins and Mullins (2011)	<p><u>Good:</u> Velocity reduction less than or equal to 10%.</p> <p><u>Questionable:</u> Velocity reduction between 11 and 29%.</p> <p><u>Poor:</u> Velocity reduction 30% or greater.</p>	<p><u>Good:</u> No reduction in effective radius.</p> <p><u>Questionable:</u> Radius reduction less than or equal to 1 in.</p> <p><u>Poor:</u> Radius reduction greater than 1 in.</p>

Source	CSL	TIP
Piscalko et al. (2016)	N/A	<u>Satisfactory</u> : 0 to 6% reduction in effective radius and local cover criteria satisfied. <u>Anomaly</u> : Greater than 6% reduction in effective radius or local cover criteria not satisfied.
GRL Engineers Documentation (2015)	N/A	<p><u>Good</u>: First Arrival Time (FAT) increase less than 10%; energy reduction less than 6 dB</p> <p><u>Questionable</u>: FAT increase between 10 and 20%; energy reduction between 6 and 9 dB</p> <p><u>Flaw</u>: FAT increase between 20 and 30%; energy reduction between 9 and 12 dB</p> <p><u>Defect</u>: FAT increase greater than 30%; energy reduction greater than 12 dB</p>
PDI Documentation (2017)	N/A	No specific criteria, but requires potential local anomalies be reported. Local anomalies are indicated by “locally low temperatures relative to the average temperature at that depth, or average temperatures significantly lower than the average temperatures at other depths.”
Deep Foundations Institute (2018)	N/A	Defines three rating classes graphically (Figure 2-14) based on combinations of FAT increase (%) and energy reduction (dB). Class A ratings are acceptable, Class B ratings are conditionally acceptable, and Class C ratings are highly abnormal.

The CSL evaluation criteria recommended by DFI (2018) are presented in Figure 2-14. Whereas many of the criteria summarized in Table 2-2 include only consideration of arrival time increases, the criteria recommended by DFI includes consideration of both arrival time and energy reduction. The criteria establish three classes:

- Class A, Acceptable
- Class B, Conditionally Acceptable: “assessment is needed to determine the significance of results relative to shaft performance,” which should include consideration of the depth(s) and tube pairing(s) affected.
- Class C, Highly Abnormal. Class C ratings generally require evaluation by the Engineer of Record, likely more invasive testing (e.g. coring), and potentially remediation.

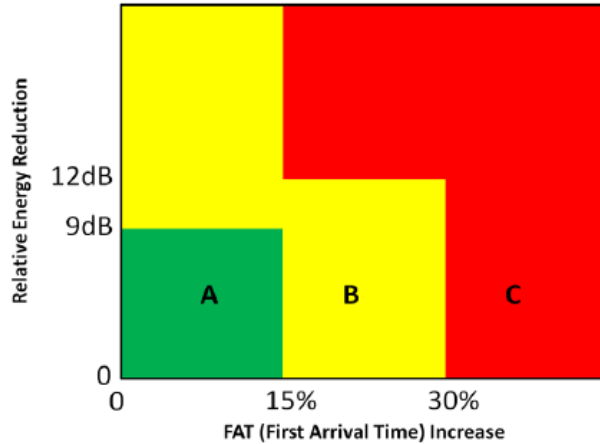


Figure 2-14: CSL evaluation criteria recommended by DFI (2018).

Table 2-2 reveals significant differences in the states of practice for interpretation of CSL and TIP:

- Acceptance criteria for CSL are relatively consistent. The criteria are generally based on quantitative interpretation of measured values (arrival times) and values calculated directly from the measurements (velocity and energy). There are some ambiguities in the interpretation:
 - How is the “baseline” arrival time or energy measurement for calculation of percent change determined?
 - Should the Engineer consider anomalies based on either arrival time (velocity) or energy, or must both quantities be anomalous to trigger the various action levels?
- Compared to CSL, acceptance criteria for TIP are less explicit, with many TIP specifications either not establishing acceptance criteria or recommending acceptance based on the Engineer’s judgment. The quantitative acceptance criteria that have been implemented are primarily based on inferred values of effective radius rather than direct measurements of temperature. The effective radius is calculated from the techniques described in the previous section.

That the state of practice for interpretation of TIP is less quantitative and perhaps less consistent than CSL is not surprising considering TIP methods are newer. The more subjective criteria for TIP may also be a result of the nature of TIP data, with concrete temperatures influenced by many factors.

2.6 Previous Research regarding TIP Sensitivity to Defects

One of the primary objectives of this research is to evaluate the ability of TIP to detect concrete defects. In addition to performing field research to investigate TIP sensitivity, a review of literature and engineering practice was performed to identify previous related works. The review was conducted prior to the field research in order to improve the experimental design of this project (Chapter 4). Results of the review are presented in this chapter.

Several previous studies have been conducted to investigate the ability of TIP measurements to identify drilled shaft defects. Three such studies are presented in this section.

2.6.1 Florida DOT Study by Mullins et al. (2007)

The original study of TIP by Mullins et al. (2007) included construction of a test shaft with planned defects to evaluate TIP sensitivity. The 4 ft diameter, 25 ft deep test shaft was installed in relatively uniform, saturated sandy soil. Two defects were installed, both consisting of bagged native soil tied to the

outside of the reinforcing cage. The cross-sectional area of each defect represented approximately 10% of the shaft. The shallower defect, at a depth of 8 ft, had bags tied to two opposite sides of the reinforcing cage as shown at the bottom of Figure 2-15. The deeper defect, at a depth of 17 ft, had all bags tied on one side of the reinforcing cage, centered around Tube 1 as shown in Figure 2-15.

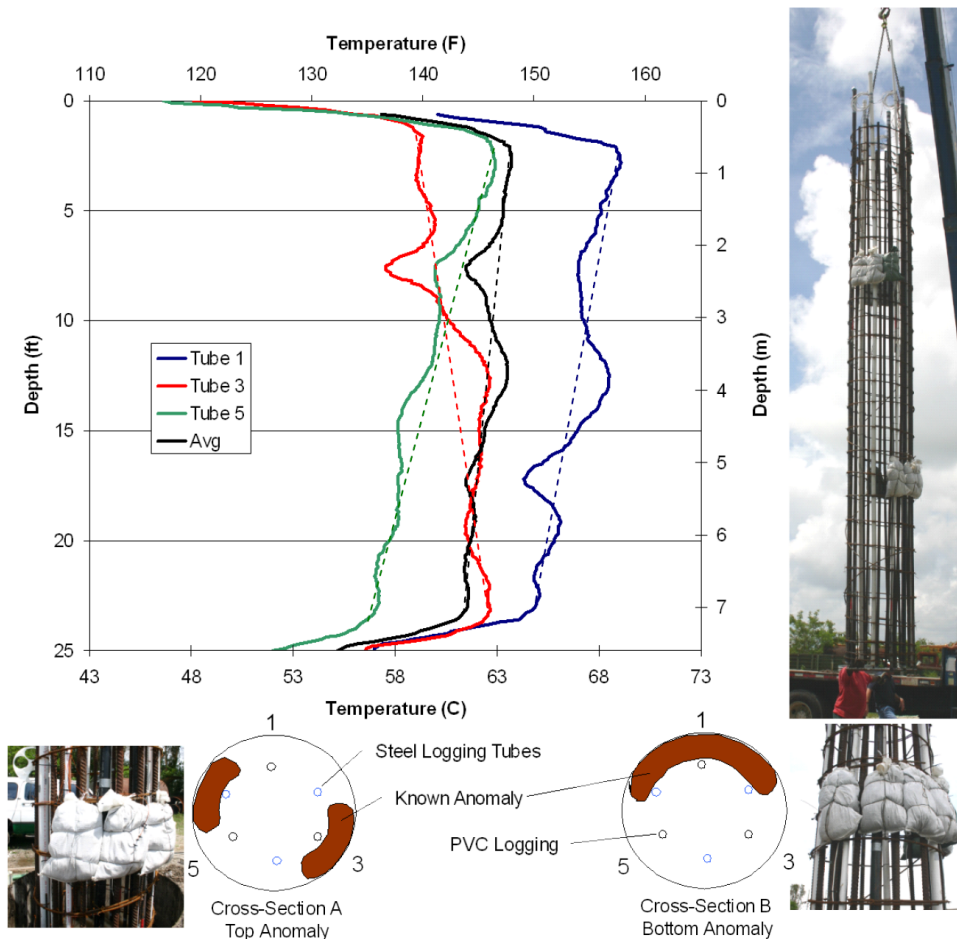


Figure 2-15: Results of FDOT TIP study by Mullins et al. (2007), as presented by Mullins and Winters (2011).

Mullins et al. performed TIP testing by probe every 3 hours. Results of the TIP testing 15 hours after concrete placement are shown in Figure 2-15. The exact peak time is not clear from the original reporting, but it is likely around the time shown in Figure 2-15 (15 hours). Before examining the influence of the defects on TIP temperatures, it is worth noting the wide variation in temperatures among the three access tubes. Mullins and Winters (2011) attributed the variation to poor cage alignment, which could also explain the tendency for tube temperatures to increase or decrease with depth.

It is helpful to consider the effect of cage alignment when evaluating the effect of the defects, which is why Mullins and Winters included the dashed lines in Figure 2-15. Temperature decreases were observed in all three tubes at the top defect, but the decrease was most significant in Tube 3. The temperature in Tube 3 decreased to 137° F at the defect depth, but it is uncertain what the temperature might have been without the defect. If the dashed line of Figure 2-15 is correct, the decrease was only 4° F, but the temperature without the defect could likely have been greater than implied by the dashed line considering the curvature of the Tube 3 temperature profile. It is similarly difficult to evaluate the effect of the bottom

defect. There is a clear decrease in temperature in Tube 1 near the bottom defect to about 149° F. If the dashed line is correct, this represents approximately a 3° F decrease, but it is likely the temperature that would have been observed without the defect would have been greater than implied by the dashed line based on the curvature of the profile. If the presence of the defects were not known, it is not certain the bottom defect would be detected, especially considering temperatures in Tube 3 were above average.

2.6.2 Iowa DOT Study by Ashlock and Fotouhi (2014)

Ashlock and Fotouhi (2014) conducted research for the Iowa DOT that investigated the sensitivity of TIP and CSL to defects. The research included two 5 ft diameter, 80 ft long shafts installed at a site near Des Moines with approximately 45 ft of sand over interbedded shale, limestone, and sandstone. The top 11 ft of the test shafts were temporarily cased with a 6 ft diameter casing. Each test shaft included two defects, which are summarized in Table 2-3. All defects were installed on the inside of the reinforcing cage and concentrated on one side of the cage (rather than concentrically around the cage). The defects were small, at 3 to 8% of shaft cross-sectional area. For comparison, the defects by Mullins et al. (2007) represented 10% of cross-sectional area. For Test Shaft 1, the defects consisted of hardened concrete cylinders with low cement content to achieve compressive strength around 600 psi. The defects for Test Shaft 2 were cylinders filled with sand, gravel, and water in similar proportion to the first test shaft concrete mix, but without cement.

Table 2-3: Summary of defect characteristics from Ashlock and Fotouhi (2014) study.

	Type of Defect	Defect Depth, ft	Size of Defect, % of cross section
Test Shaft 1	Cylinders of weak concrete	8	3
		29	4
Test Shaft 2	Cylinders of aggregate and water	15	8
		32	8

Ashlock and Fotouhi performed TIP testing via the probe method. Results of TIP testing are shown in Figure 2-16 for Test Shaft 1 and Figure 2-17 for Test Shaft 2. Results include temperatures as well as effective radius interpretations according to the Level 2 method outlined in Chapter 2. For Test Shaft 1, there was no perceptible decrease in temperature or effective radius at either defect location. For Test Shaft 2, the TIP response is dominated by cage misalignment, which resulted in temperature variations as great as 25° F among tubes near the shaft mid-height. Such variation makes interpretation of a temperature change due to the defects challenging. There is perhaps a modest decrease in temperatures near Tube 3 for both defects, but this decrease is at most 3° F for the top defect and 2° F for the bottom defect. These decreases are considerably less than the significant increase in temperatures near a depth of 45 ft. SONICaliper results and concrete volume log results indicate a bulge at this depth corresponding to about a 4 or 5 in. radius increase. A bi-directional load testing cell (“O-cell”) was included in both test shafts. For both shafts, the temperature decreases due to the O-cell were greater than those due to the intentional defects.

CSL results from Ashlock and Fotouhi (2014) are presented in Figure 2-18 for Test Shaft 1 and in Figure 2-19 for Test Shaft 2. CSL results for Test Shaft 1 showed no significant increase in arrival time for either defect. For Test Shaft 2, an increase in arrival time of approximately 25% was observed for both defects. Such an increase straddles the line between questionable and actionable, depending on acceptance criteria (Table 2-2).

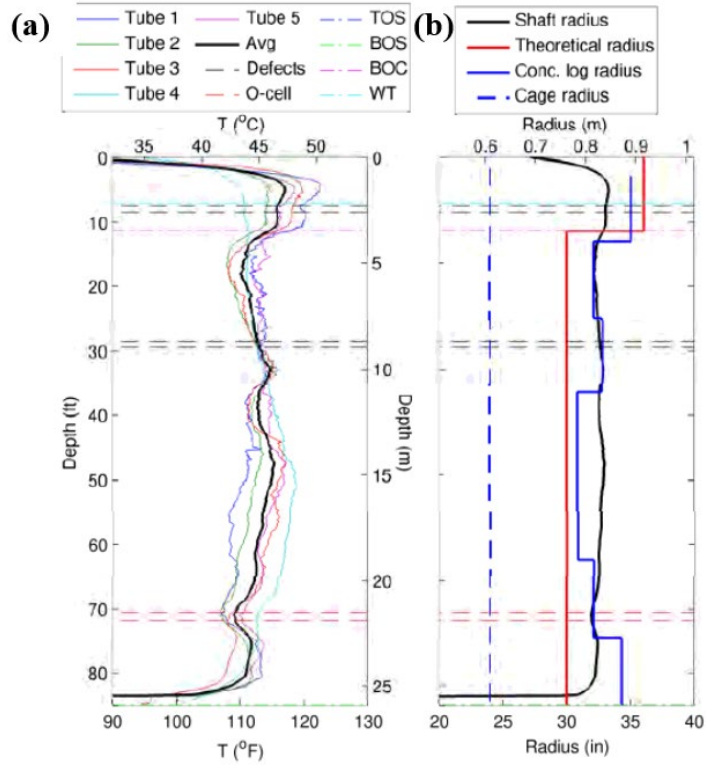


Figure 2-16: TIP results for Test Shaft 1 from Ashlock and Fotouhi (2014): (a) temperature and (b) effective radius.

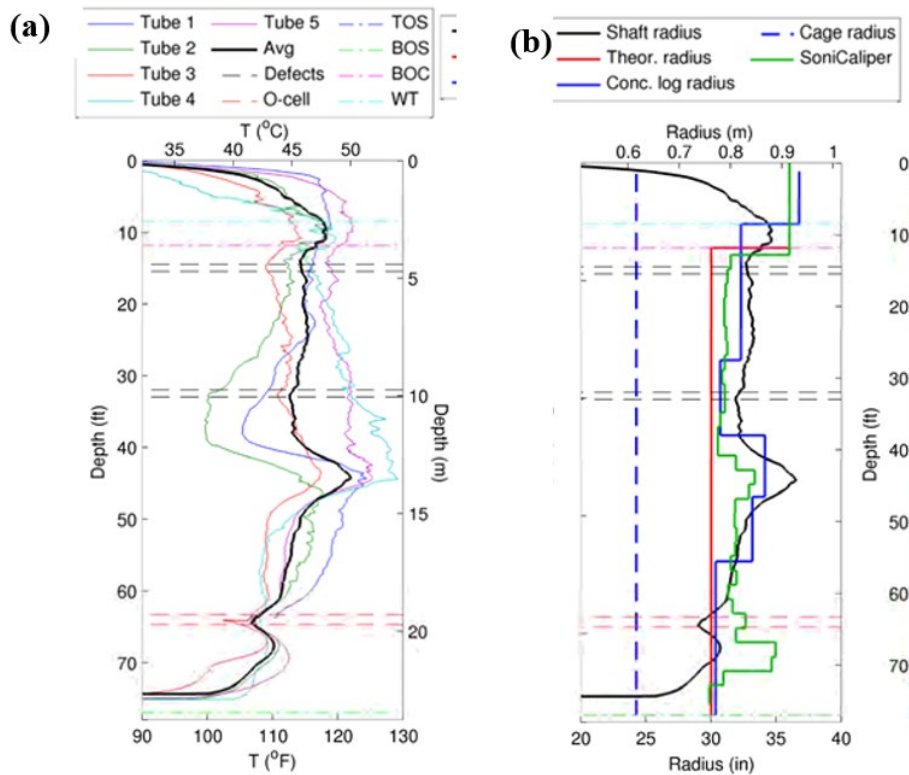


Figure 2-17: TIP results for Test Shaft 2 from Ashlock and Fotouhi (2014): (a) temperature and (b) effective radius.

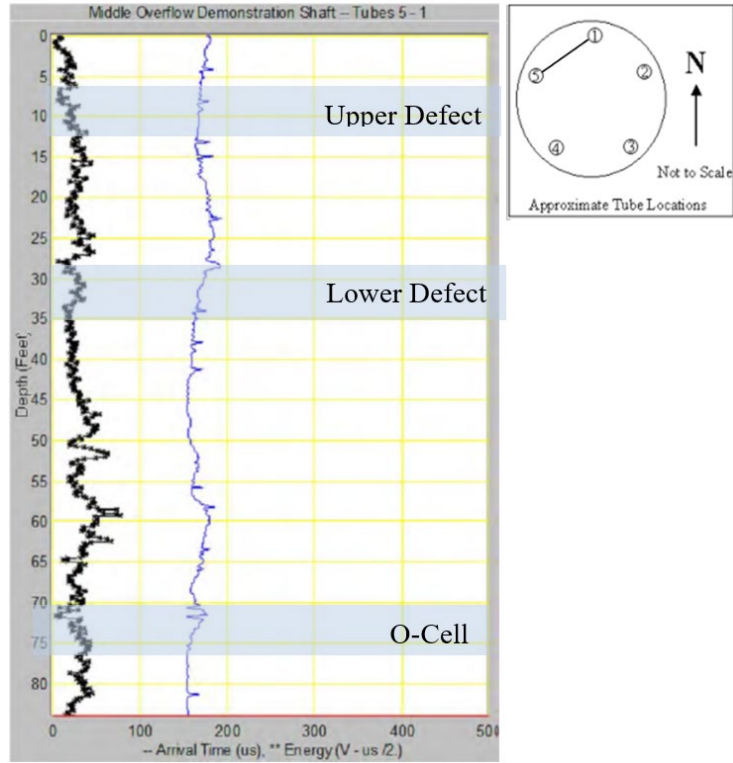


Figure 2-18: CSL results for Test Shaft 2 from Ashlock and Fotouhi (2014).

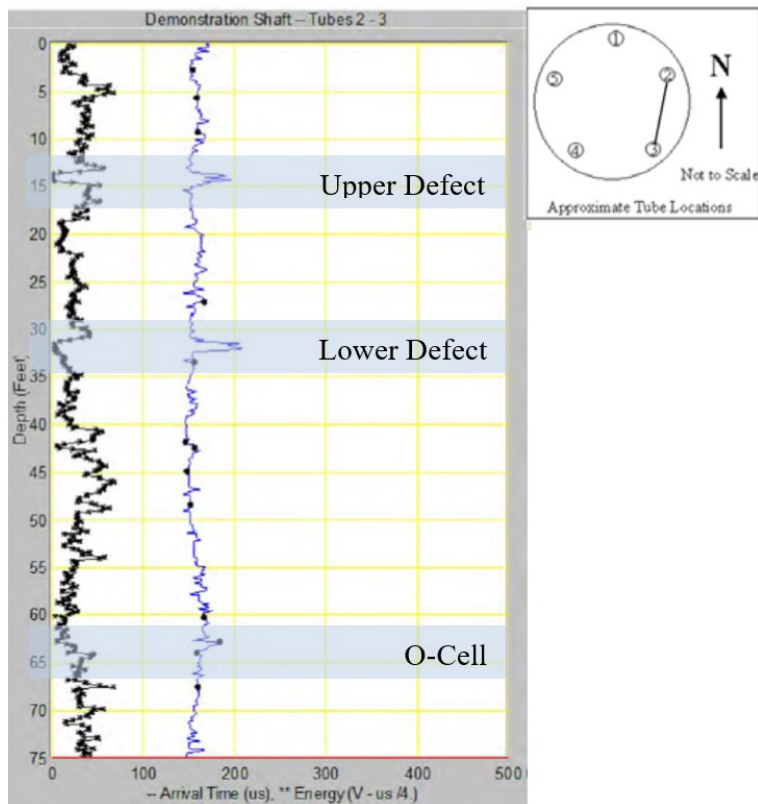


Figure 2-19: CSL results for Test Shaft 2 from Ashlock and Fotouhi (2014).

2.6.3 Schoen et al. (2018)

Schoen et al. (2018) documented TIP testing for a 102 ft long by 5 ft diameter drilled shaft in South Carolina. The shaft was constructed as a design-phase load test shaft. Schoen et al. installed known defects consisting of gravel-filled concrete bags attached to the inside of the reinforcing cage at depths of 3 ft and 21 ft below the top of shaft. The gravel bags represented approximately 15% of the shaft cross-sectional area and were attached to only one side of the reinforcing cage (rather than concentrically around the entire cage).

TIP records for the shaft are shown in Figure 2-20. Figure 2-20(a) shows temperatures 14 hours after concrete placement, and Figure 2-20(b) shows temperatures at the peak time of 34 hours. Both defects are clearly evident at 14 hours. The top defect resulted in a 12° F decrease in temperature in Wire 5, and the bottom defect resulted in a decrease of approximately 14° F, assuming the temperature without defects would have been halfway between the temperature above and the temperature below the bottom defect. At 14 hours, the reduction in the average temperature is modest at both defects. At about 5° F, the decreases in average temperature are noticeable, but not necessarily sufficient to cause concern without considering the reductions at Wire 5.

Evidence of the defects at the peak time of 34 hours (Figure 2-20(b)) is considerably weaker. For the top defect, there is limited evidence of a defect, with only a 2 or 3° F decrease at Wire 5. One might reasonably conclude the cage was off-center at the top of the shaft since the average temperature profile is relatively consistent and the wire temperatures are relatively evenly distributed about the average. For the bottom defect, the reduction in temperature at Wire 5 was about 8° F, a notable decrease, but only slightly more than half the decrease observed at 14 hours.

CSL was also performed on the shaft documented by Schoen et al. CSL plots were not presented in the research paper, but Schoen et al. note that CSL testing indicated both defects. Schoen et al. noted that the CSL testing firm was aware of the defects.

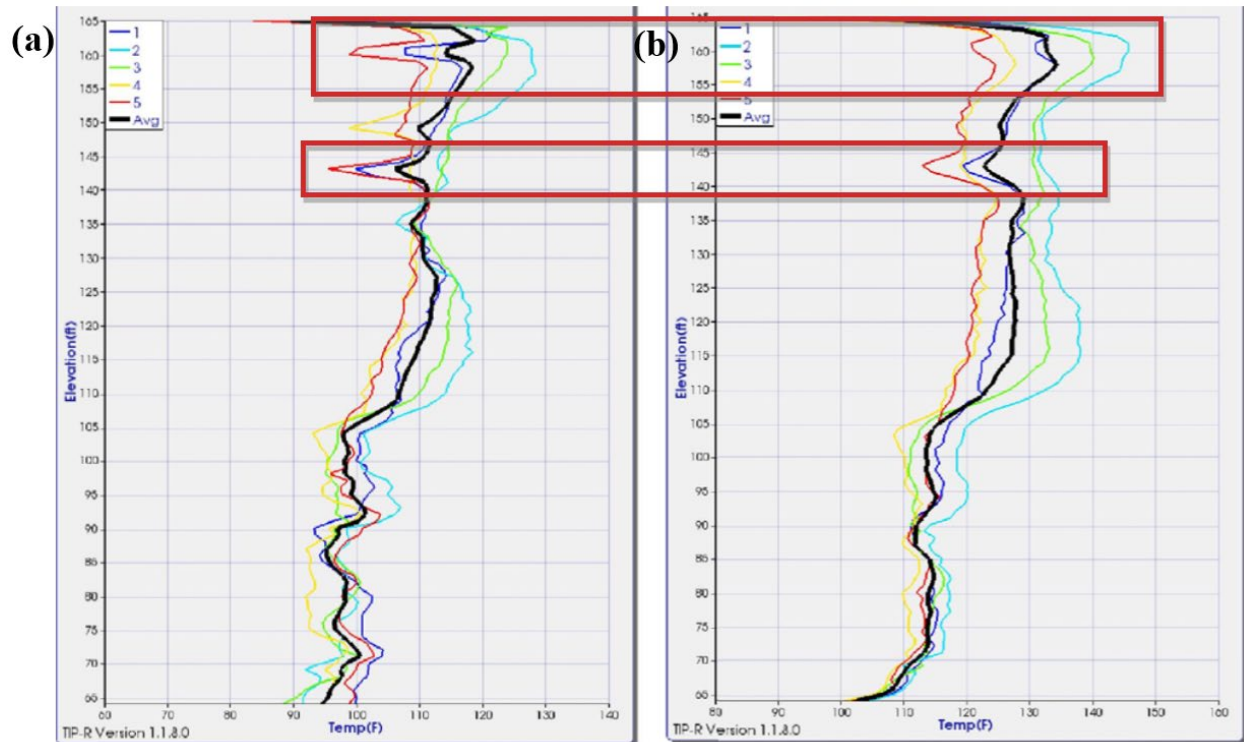


Figure 2-20: Example TIP result showing decreases in temperature at two known defect locations: (a) 14 hours and (b) 34 hours, the peak time. From Schoen et al. (2018).

2.6.4 Wisconsin DOT Study by Boeckmann and Loehr (2018, 2019)

Boeckmann and Loehr performed a research study evaluating TIP and CSL for the Wisconsin DOT. Results of the research are presented in a research report (2018) and a journal article (2019). The study involved construction of three 3-ft diameter by approximately 30-ft long drilled shafts, two of which included 4 or 5 intentional defects (the test shafts) and one of which included one intentional defect (the control shaft). Conventional TIP testing by both wire and probe methods was performed; CSL testing was also performed. The defects were intended to replicate common drilled shaft construction issues:

- Soft bottom conditions were mimicked by pouring sand into the bottom of the shaft
- Soil inclusions within concrete were mimicked by tying sandbags to the reinforcing cage. Some of the sandbags were tied outside the reinforcing cage; others were tied inside.
- A tremie breach was mimicked by removing the tremie pipe during concrete placement for one shaft and then pouring sand in the shaft before re-inserting the tremie.
- Weak concrete was created by mixing additional water into the concrete placed at the top of each of the test shafts.

The results indicated soft bottom conditions were identifiable with CSL methods, but not TIP methods. Soil inclusions outside the reinforcing cage were readily identifiable from TIP results, but not from CSL methods; the opposite was true of soil inclusions inside the reinforcing cage. Effects of the tremie breach were also identifiable in the CSL results but not the TIP results. Weak concrete was clearly identifiable in the TIP results, but not the CSL results.

As shown in Table 2-4, Boeckmann and Loehr concluded TIP and CSL methods are generally complementary: TIP is more effective for identifying some types of defects, CSL is more effective for

others, and likely any significant defect should be identifiable by at least one of the two tests. Boeckmann and Loehr therefore recommended selecting integrity tests based on project-specific considerations. Selection of the appropriate integrity test should consider the likelihood of potential types of defects as well as the consequence of potential types of defects, according to Boeckmann and Loehr. In addition, Boeckmann and Loehr recommend performing both test methods for method (a.k.a. technique or demonstration) shafts, which are sometimes constructed for large projects.

Table 2-4: Summary of the ability to detect various types of relatively modest defects for TIP and CSL from Boeckmann and Loehr (2018). Table contents are revised in Chapter 7.

Defect Type	TIP¹	CSL¹
Inclusions in cage interior	Difficult to detect	Readily detectible
Defects outside reinforcing cage	Readily detectible	Not detectible
Soft bottom	Not detectible	Readily detectible
Weak concrete	Readily detectible	Difficult to detect
Breach of tremie pipe	Potentially detectible	Readily detectible

¹*Detection ability assessments are generally based on relatively small defects. Detection ability assessments would likely be greater for more significant defects.*

A significant technical finding from Boeckmann and Loehr was the utility of TIP time records for identifying drilled shaft defects. Results for four of the defects are shown in Figure 2-21. The plot includes the temperature difference for each of the four defects versus time, with the temperature difference defined between the sensor nearest the intentional defect and a nearby sensor deemed to be unaffected by the defect. For reference, a line representing temperature for the average of all sensors at the peak temperature depth is also included in the plot.

Boeckmann and Loehr observed that different defects have different temperature difference versus time shapes, a finding they speculated could be used to identify various “signatures” associated with different types of defects. Boeckmann and Loehr also observed that the temperature differences are generally greatest at a time between one-third and one-half of the time to peak temperatures; they noted the time for the greatest temperature difference was generally around the time of maximum temperature rise (i.e. the steepest portion of the dashed line in the figure). Based on the observation that temperature difference reduces to near zero by the time of peak temperature for several of the defects, Boeckmann and Loehr recommend evaluating TIP records at half peak time.

As shown in Figure 2-21, Boeckmann and Loehr also plotted the temperature versus time at the bottom of each shaft. Because the results are similar for all three shafts, including the control shaft, which had no soft bottom, Boeckmann and Loehr concluded TIP could not be used to identify soft bottom conditions, at least for severity of the soft bottom conditions included in the test shafts. Each test shaft included 420 lbs of sand at the bottom.

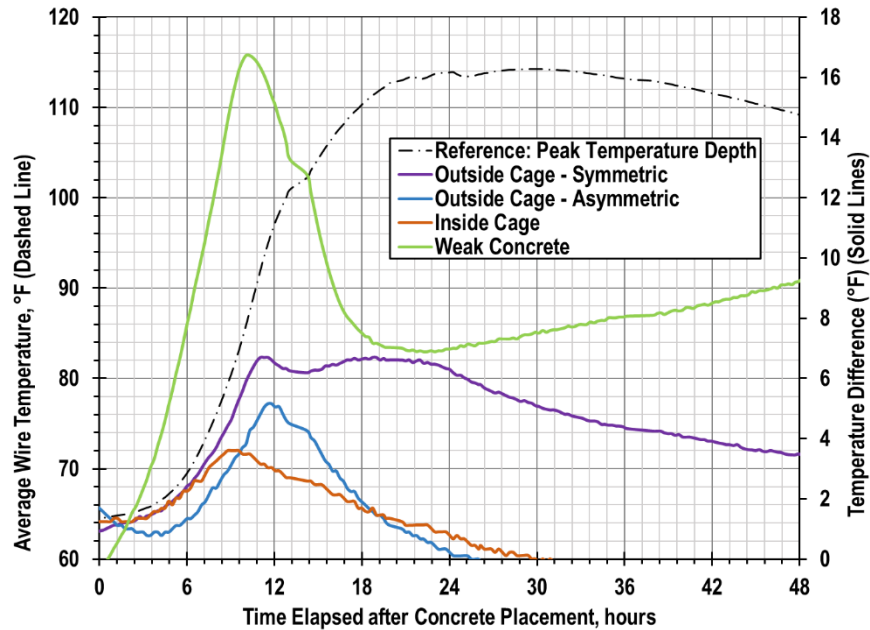


Figure 2-21: Temperature and temperature difference versus time based on results from Boeckmann and Loehr (2018).

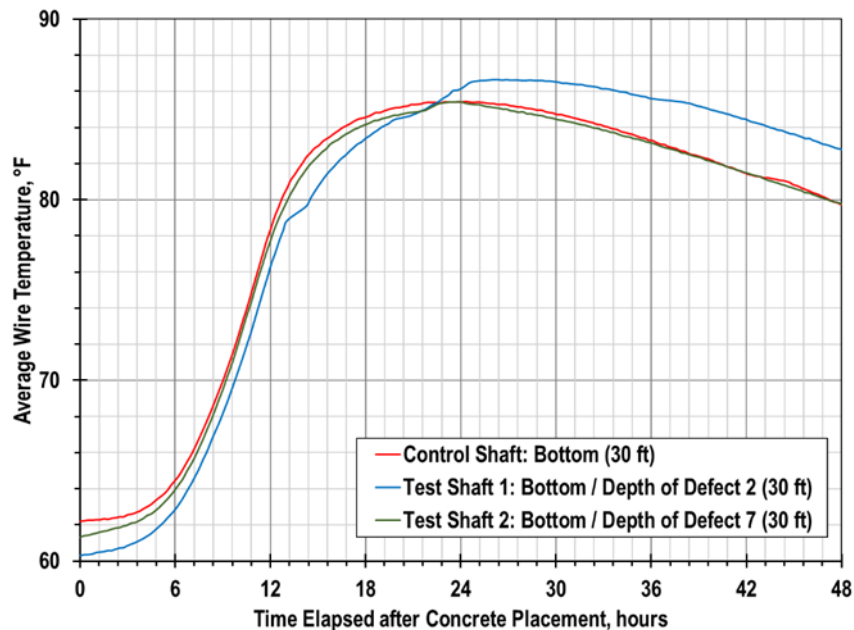


Figure 2-22: Temperature versus time for the bottom of shafts from Boeckmann and Loehr (2018).

2.7 Agency Experiences with TIP

Project applications of TIP offer another opportunity to evaluate TIP sensitivity to defects. Project applications are not controlled (or quasi-controlled) like the research projects described in the previous section, but they offer practical lessons and a quantity of data not frequently encountered in research projects. Most of the information in this section is derived from the WisDOT Zoo Interchange project, but TIP lessons from other transportation agencies are also documented.

2.7.1 WisDOT: Zoo Interchange

Boeckmann and Loehr (2018) also reviewed drilled shaft installation records, results of CSL and TIP tests, and, where applicable, results of coring and concrete remediation for the Zoo Interchange project drilled shafts outside Milwaukee. The shafts were 8 or 10 ft in diameter, with lengths varying from 30 to greater than 100 ft. The shafts were installed using temporary casing, and a tremie pipe was used to place concrete in the water-filled shafts. Table 2-5 summarizes results for the six shafts for which coring was completed in response to potential defects indicated in CSL and/or TIP test results. For five of the six shafts, coring confirmed defects, which were remediated by grouting.

Table 2-5: Summary of concrete integrity testing results for the six shafts at Zoo Interchange that were cored. Defects were confirmed in five of the six shafts; all five were remediated via grouting. From Boeckmann and Loehr (2018).

Shaft	Field Notes	CSL Results	TIP Results	Coring Results	Comments
WS07	Nothing unusual noted.	Spike in arrival times for many pairs on NW side of shaft in the top 5 to 10 ft. Coring recommended.	Perhaps some temperature deviations, but difficult to interpret in zone near top of shaft.	One core of top of shaft did not reveal any defects.	Core could have missed a defect? Core in SW quadrant; CSL indicated NW. Otherwise, could indicate CSL overly sensitive?
NE01	Tremie breached at a depth of 42 ft.	Spike in arrival times for 20 of 28 pairs at depth of tremie breach. Recommend further review by engineer and possibly coring.	No data below 35 ft due to “unknown failures” of five wires.	Two of three cores revealed 6 in. defect zones at the depth of the tremie breach.	
ES03	Tremie breached at a depth of 37 ft.	Spike in arrival times for all 45 pairs at depth of tremie beach. Coring recommended.	Temperature dips at depth of breach deemed “provisionally acceptable, if the minimum cover meets the design requirements and CSL test results indicate acceptable integrity.”	Three of four cores revealed 6 in. defect zones at the depth of tremie breach.	
ES12	Evidence of soft bottom (cage sinking slowly for last 6 in.).	Spike in arrival times for all 28 pairs at base of shaft. Coring recommended.	Difficult to discern temperature decreases at base of shaft from typical “roll-off.” Roll-off zone is 6 ft, less than 8 ft diameter. Interpreted radius values at base were less than design, but similar deviations were noted at other depths. Further engineering analysis recommended for shaft.	Defects in all four cores for 1.5 ft near bottom of shaft.	“Further engineering analysis” was a common recommendation in TIP reports. The recommendation was not specific to a particular depth.

Shaft	Field Notes	CSL Results	TIP Results	Coring Results	Comments
WN11	Nothing unusual reported.	Spike in arrival times for 29 of 45 pairs at bottom of shaft. Recommend further review by engineer and possibly coring.	Difficult to discern temperature decreases at base of shaft from typical “roll-off.” The TIP report concluded the shaft concrete integrity was acceptable.	Two of three cores revealed defect zones about 6 in. thick.	
WN06	6 in. of silt noted at bottom of shaft before pour.	Spike in arrival times for 40 of 45 pairs at the base of shaft. Recommend further review by engineer and possibly coring.	No TIP test – wires broke during shaft installation.	Two of three cores revealed defect zones about 6-in. thick.	

The only shaft in which coring did not confirm defects, WS07, is potentially a false positive CSL result. A false positive would be consistent with reports of CSL being overly sensitive, particularly near the top of drilled shafts where the effects of bleed water are most prevalent. However, it is certainly possible that the core location missed a real defect, especially considering the core location was near the edge of the zone indicated by the anomalous tube pairings (rather than being in the center of that zone). For two of the five shafts with confirmed defects, NE01 and ES03, the depth of defective concrete is consistent with the depth of a tremie breach. For both shafts, the CSL report recommended coring, although one such recommendation was conditional upon the engineer’s review. For one shaft with a tremie breach, there was no TIP test because the wires failed; for the other, there was a notable dip in shaft temperatures at the depth of the breach, but the TIP report recommended “provisionally accepting” the shaft since the effective radius indicated almost 4 in. of concrete cover. For the other three shafts with defective concrete (ES12, WN11, WN06), defects occurred at the bottom of the shaft, presumably because of accumulation of soft material at the base of the shaft in the time between drilling and concrete placement. For all three, CSL reports recommended coring, with two of the recommendations conditional upon the engineer’s review. For one of the shafts, there was no TIP test because of wire failure; for the other two, TIP recommended further engineering analysis or acceptable integrity. It is difficult to discern lower temperatures due to soft bottom conditions because the temperature gradient is steep in the roll-off zone.

TIP was not an effective integrity test for identifying defects in the Zoo Interchange shafts. Specifically, Boeckmann and Loehr observed:

- Broken wires were a recurring issue for the Zoo Interchange project. The manufacturer of the TIP wires for Zoo Interchange and all other projects encountered has indicated a new wire design with cable strain relief has greatly reduced these issues. The improvement has been confirmed with other users of TIP wires, who report about 1 to 2% breakage with the new wires in a recent project with a large number of TIP tests. In addition, the manufacturer reports further improvement in the TIP wire design will result in even fewer instance of breakage.
- It is difficult to detect defects in the top and bottom of shafts from TIP testing. Boundary conditions (loss of heat to air or soil) produce a roll-off zone with significant vertical temperature gradients. It is difficult to isolate temperature effects from a potential defect from the roll-off temperature gradients, especially since the length of the roll-off zone varies.
- Reports of CSL results were generally more informative and included clearer recommendations compared to the reports of TIP results. Testing was performed by two different firms, so it is difficult to discern whether the differences were a result of different firms having different reporting standards, the lack of standard interpretation and acceptance criteria for TIP (see Section 2.5), or both.

2.7.2 South Carolina DOT

In the 2015 FHWA study regarding drilled shaft concrete (Boeckmann and Loehr, 2015), South Carolina DOT (SCDOT) was described as having allowed TIP as an alternative to CSL for several years. SCDOT implements TIP via special provisions, but the agency is considering adding TIP to its standard specifications. The agency has observed significant bleed water in many large-diameter shafts. The bleed water has been observed through coring to produce “thumb size” bleed channels that result in significant CSL anomalies (hence coring) but generally not significant concern regarding the shaft’s structural integrity. SCDOT has used TIP in large part because of the high incidence of coring based on CSL report recommendations.

2.7.3 Other Agencies

In addition to SCDOT, seven other state DOTs with TIP experience were contacted by Boeckmann and Loehr (2015). Three agencies (Missouri DOT, Minnesota DOT, Utah DOT) did not have any data to share. Florida DOT referenced reports by Mullins (e.g. Mullins et al., 2007). Information from the three agencies that offered information is summarized in Table 2-6.

Table 2-6: Information from other transportation agencies with relevant TIP experience. From Boeckmann and Loehr (2018).

Agency	Experience with TIP Testing	Other Comments
Washington DOT	<p><u>Manette Bridge</u>: TIP data confirmed soil caving that was observed prior to concrete placement (higher temperatures due to larger shaft). No CSL testing on project.</p> <p><u>I-5 M-Street</u>: TIP identified bulge of concrete and cage racking near tip. No CSL testing on project.</p> <p><u>Portland Ave, Pier 9</u>: TIP showed temperature dips of 35° F at depths of 100 ft in the 120 ft long shaft. Coring indicated segregated concrete with strengths of 1800 psi adjacent to 9000 psi concrete. Not clear from field logs what caused defect. No CSL testing on project.</p> <p><u>Portland Ave, Pier 1</u>: CSL and TIP performed side-by-side on five shafts. Neither test indicated any significant anomalies in any of the shafts; no coring was performed.</p>	In January 2017, WSDOT updated its standard specifications to include TIP as an allowable CSL alternative (see Table 2-2). WSDOT intends to keep using CSL test, but likes TIP as an alternative, especially for larger, deeper shafts. Indicated cost of TIP is comparable to CSL.
Nevada DOT	<p><u>US95/CC-215 Interchange</u>: CSL and TIP performed side-by-side on Shaft 8. Neither test indicated significant defects, and no coring was performed.</p>	
Louisiana DOTD	<p>CSL and TIP used side-by-side for a test shaft in 2013. No defects were reported for either test. Subsequent load test did not reveal any structural deficiencies.</p>	Agency noted TIP can be useful when cage is too congested for CSL tubes.

2.8 Cost of TIP and CSL

The cost of TIP testing depends on drilled shaft diameter, project size, the number (percentage) of shafts to be instrumented, and likely other factors. Assuming the wire method is used, material costs are associated with the sacrificial thermal wires and the equipment used to collect and analyze data from the wires. The equipment can be rented or purchased. In 2021, a general unit price for estimating the delivered (not installed) cost of thermal wires is \$5 per foot, plus \$25 for each individual wire and any freight expenses. Labor costs for the wire method result from three tasks: installing the wires on the

reinforcing cage, collecting the data, and analyzing the data. In addition to material and labor costs, there may also be mobilization and travel expenses for each test method.

Comparison of TIP and CSL costs likely depends on the scale of the project. Hyatt et al. (2019) performed a project-specific cost comparison for CSL and TIP for a project involving seven 5-ft diameter shafts ranging from 60- to 76-ft long. Unit cost data from Hyatt et al. are presented in Table 2-7. For CSL, the greatest costs are generally incurred for the access tubes, subsequent grouting, and engineering, with installation labor also a contributor. For TIP, costs of wire per foot are about half of the cost of CSL tubes per foot from Hyatt et al., including grouting in the CSL tube cost. For all seven project shafts, Hyatt et al. reported total costs of materials, installation labor, and engineering of \$43,900 for CSL and \$21,800 for TIP. In other words, the total cost of CSL testing was twice the total cost of TIP testing.

The most significant factors in the cost difference are costs associated with grouting CSL tubes (about \$8,000 for all seven shafts), and the difference in engineering costs (about \$8,500 for all seven shafts). Engineering costs were defined by Hyatt et al. to include mobilization costs and data collection costs, which likely explains the large difference between the two test methods. Whereas TIP data can often be collected by the contractor or other on-site personnel, CSL typically requires mobilizing technicians to the site to perform testing. The unit costs presented in Table 2-7 are updated in Chapter 4 to include the results of the field testing program of this project. The discussion in Chapter 4 also addresses the cost of fiber optic TIP methods.

Table 2-7: Summary of cost information from Hyatt et al. (2019).

Test	Item	Unit	Range of Cost	Average Cost
CSL	Access Tubes	LF	\$6.00 to \$7.00	\$6.50
	Access Tube Cap	each tube	\$9.50 to \$10.00	\$9.75
	Installation Labor	each tube	\$135.00 to \$145.00	\$140.00
	Post Grouting	LF	\$3.15 to \$3.25	\$3.20
	Engineering	each shaft		\$1,845.00
TIP	Wire	LF	\$4.00 to \$6.00	\$5.00
	Connector	each wire	\$20.00 to \$30.00	\$25.00
	Installation Labor	each wire	\$115.00 to \$125.00	\$120.00
	Engineering	each shaft		\$608.50

3. Fiber Optic Laboratory Research

Prior to the field deployment of the DFOS thermal system, a laboratory test was conducted to confirm the accuracy of the fiber optic measurements and compare the results with the more conventional thermal wire. The same fiber optic thermal cable and type of fiber optic analyzer were used for the laboratory test as for the field research (Chapter 4). A large water bath, shown in Figure 3-1, was used to control the temperature at incremental set points, ranging from 77° to 176°F (25° to 80°C) in 9°F (5°C) increments. Approximately 30 ft of fiber optic cable and TIP wire were submerged within the water bath, with an additional 2 to 3 monitoring points outside the bath at room temperature.

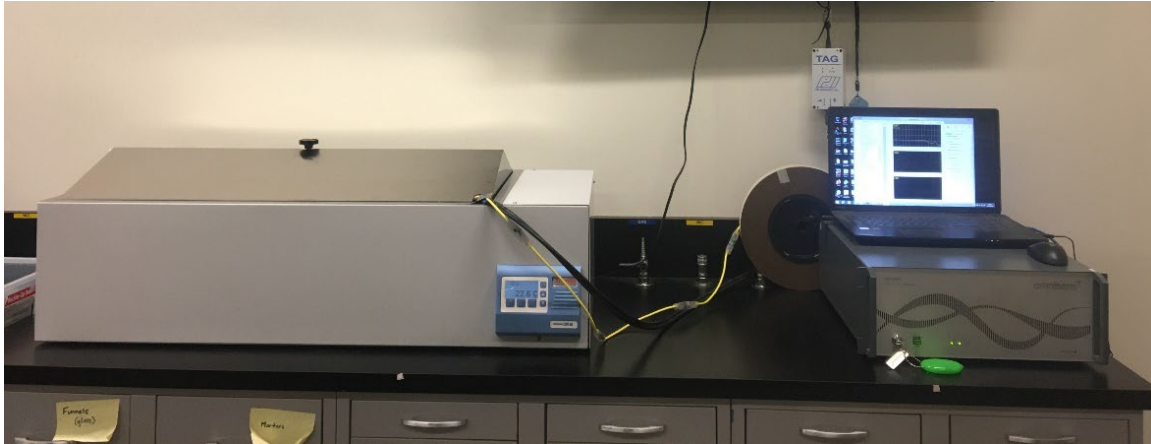


Figure 3-1: Photograph of the water bath testing setup.

Within the water bath, the two cable types were coiled in loops of approximately 10 inches in radius in the center of the bath, as shown in Figure 3-2. The cables were taped to the bottom tray of the bath to prevent flotation and keep the cables fully submerged during the test. A series of baseline readings were taken using the fiber optic analyzer to confirm that no significant bending strain was imparted on the fiber optic thermal cable. The cables exited the water bath at a small cutout in the lid, where they were routed to the respective reading systems, as shown in Figure 3-3.



Figure 3-2: Photograph of the cable configuration within the water bath.

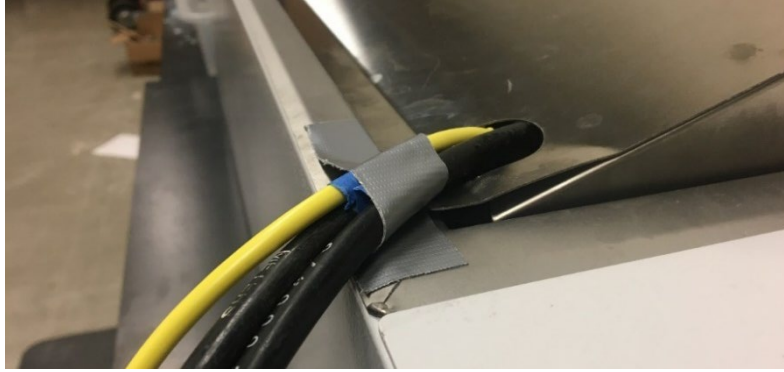


Figure 3-3: Photograph of the cable routing at the access port within the water bath lid.

The temperature set points during the test were manually recorded, with a minimum of 3 readings from the fiber optic analyzer at each set point. The TIP data logger was set to read automatically at 1-minute intervals. The holds at each temperature were a minimum of 12 minutes long to allow for 3 full thermal fiber optic readings, each taking approximately 4 minutes to complete. No fiber optic readings were taken during the transitions between temperature set points, although the TIP data logger continued to take readings during these transitions. The ambient air temperature within the laboratory was also automatically recorded using a digital thermometer.

While the TIP data logger records in temperature Fahrenheit, the fiber optic analyzer outputs peak Brillouin frequency for each readout point along the cable, as shown in Figure 3-4. The conversion from frequency to temperature is a linear transformation. The slope is a standard value based on the coefficient of thermal expansion of the glass fiber core that falls within a narrow range for all telecommunications fiber. The slope value can be fine-tuned using laboratory testing in a water bath like this experimental setup. The offset can vary depending on the analyzer and specific cable and is best determined using a series of measurements at a known temperature. In this case, the temperature measurements on the fiber optic cable outside the water bath were compared to the measurements from the digital thermometer, and an offset was fit to minimize the difference between the two temperature records. This approach is identical to what was performed in the field testing, with the cable recorded temperatures outside of the drilled shafts fit to temperature measurements of the ambient air during readings.

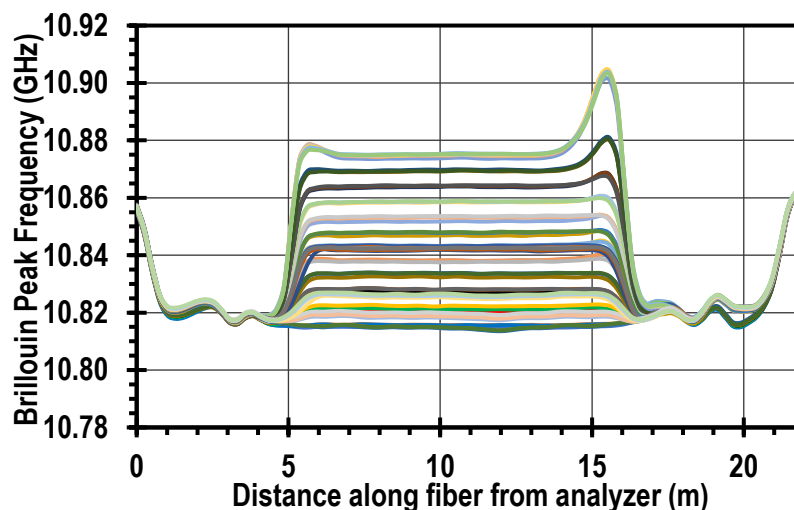


Figure 3-4: Fiber optic peak frequency during water test. Each line represents a different time during the test.

The section from approximately 6 to 16 meters in Figure 3-4 represents the 10 meters of thermal fiber optic cable within the water bath. The peak frequency within the majority of the submerged cable is horizontal and linear, indicating that the cable is experiencing uniform temperature and no external mechanical strain. The two peaks of higher frequency (and associated higher temperature) represent the points where the thermal fiber optic cable entered and exited the water bath. Upon inspection after the testing, it was noted that the cable in these areas was resting directly upon the metal tub of the water bath (Figure 3-3), which was experiencing hotter temperatures than the water itself. At the rim of the bath, one of the thermal cables is on top of the other. The cable that was in direct contact with the tub of the bath is shown as the higher peak within the data readout.

Following the conversion of the raw fiber optic frequency data into temperature, the results between the TIP thermal wire and the distributed fiber optic system could be compared. For the purposes of the comparison, a single measurement point for each system at the center of the submerged portion was chosen for plotting. The measured temperature for the two systems is shown in Figure 3-5.

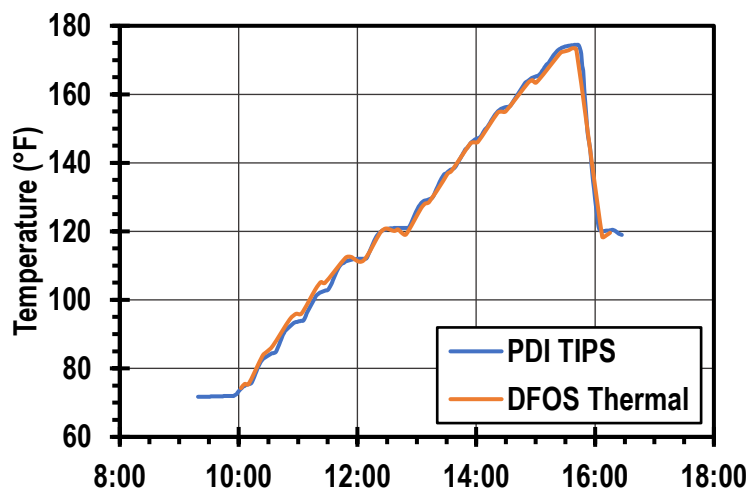


Figure 3-5: Recorded temperature during the water bath test from the two measurement systems.

As can be seen in Figure 3-5, the two systems recorded very similar temperatures. The average deviation between the two systems during temperature hold periods (excluding records during temperature transitions) was less than 0.1°F. The fiber optic cable took a longer time to equilibrate at the water bath temperature than the TIP sensors, lagging the water temperature by approximately 2-4 minutes and 2-3°F as compared to the temperature set point. This analysis was compared for all measurement points for both systems and the results were similar within the submerged portion.

One area of difference that is important to note is in sections of high thermal gradient, or a concentrated temperature change. This is most evident at the entry and exit of the water bath, although the temperature spike from the water bath tub partially conceals the true magnitude. As can be seen in the transition, the temperature readings going from the water to the ambient air extend over 1-2 meters. This is due to the spatial resolution limitation of how the fiber optic analyzer functions. For each reading, the Brillouin frequency peak represents a “sample” of the fiber optic cable. While the sample is not quite an arithmetic average, the reading output is influenced by the measured strain or temperature within this length. The spatial resolution of the analyzer was set at 0.75 m. Therefore, for a reading just at the edge of the water bath at a high temperature, the reading is influenced by both the water temperature and the ambient air temperature. This creates a smoothing effect that can be seen in the lower temperature data. The extension of this effect at higher temperatures from the artificial peak is instead believed to be conduction within the cable, as opposed to a real artifact of the fiber optic reading method.

4. Field Testing Program

Field research was performed to further evaluate the sensitivity of TIP to drilled shaft defects and the potential agency-wide implementation of TIP for drilled shaft integrity testing. The field research involved performing TIP on two drilled shafts at each of two bridge sites in St. Louis. Both conventional and fiber optic TIP methods were used. All four of the tested shafts are production shafts (i.e. they will support the superstructure to be constructed in 2021). Because production shafts were tested rather than installing experimental test shafts, there were no intentional defects included in the shafts. CSL testing was also performed on each of the shafts, as is typical for MoDOT production shafts. This chapter describes the field research project selection as well as design, construction, and testing of the drilled shafts. Results are presented in the next chapter.

4.1 Project Selection

Eleven candidate bridge projects were identified by MoDOT as including drilled shaft foundations and being scheduled for letting during a time period conducive with the research project schedule (i.e. letting between late 2020 and early 2021). Among the eleven candidates, two options emerged as having the most potential research value: (1) bridge A7742 in Montgomery County and (2) bridges A8854 and A8851 in St. Louis City. The first option was viewed favorably because the drilled shafts were designed neglecting base resistance, which raised the possibility of including intentional defects at the base of the shafts. The second option was viewed favorably because the two bridges were part of one combined construction project, making it feasible to test shafts with different diameters, albeit with additional testing mobilizations required. Ultimately, the second option was selected because the likelihood of including intentional defects in the Montgomery County bridge was deemed poor, and because the Montgomery County shafts were small, with rock sockets only 2.5 ft in diameter and 9 ft in length.

4.2 Drilled Shaft Design Details

Design information relevant to TIP testing is presented in this section, which includes subsections for an overview, reinforcing cage information, and concrete mix design. Within each subsection, information is presented for both bridges. Plans for both bridges are presented in the appendices: Appendix A for Ewing Ave. and Appendix B for Ramp F.

4.2.1 Overview of Drilled Shafts and Testing

Ewing Ave. bridge (A8854), shown in Figure 4-1, is a two-span structure carrying Ewing Ave. over Interstate I-64 in St. Louis City. The intermediate bent is supported on 3.5-ft diameter shafts with 3-ft diameter rock sockets. The shafts extend about 10 ft through soil with permanent casing above the 10-ft long socket in limestone. Shafts 2 and 3 of the intermediate bent were instrumented for both conventional and fiber optic TIP testing. CSL and SONICaliper were also performed on both shafts.

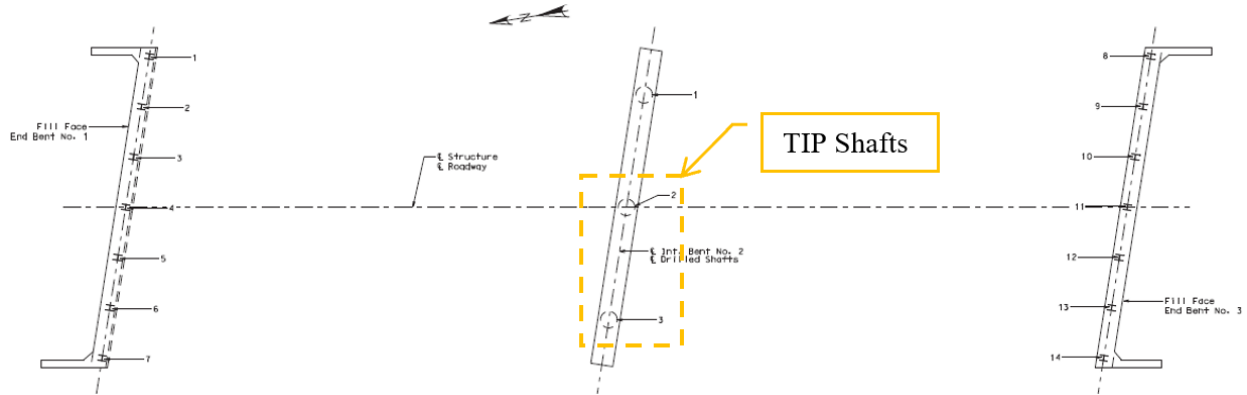


Figure 4-1: Plan view of Ewing Ave. bridge.

Ramp F overpass bridge (A8854), shown in part in Figure 4-2, is a seven-span structure that will provide access to eastbound I-64 from 22nd St. Each of the intermediate bents is or will be supported by a single drilled shaft. All shafts include a 6-ft diameter permanently cased section down to rock and an 18-ft long by 5.5-ft diameter socket in limestone. TIP testing was performed on the shafts supporting Bents 5 and 6, with conventional TIP testing on both shafts and fiber optic on only the Bent 6 shaft. CSL and SONICaliper testing were performed on both shafts. The permanently cased sections of the shafts for both Bents 5 and 6 are about 70 ft long.

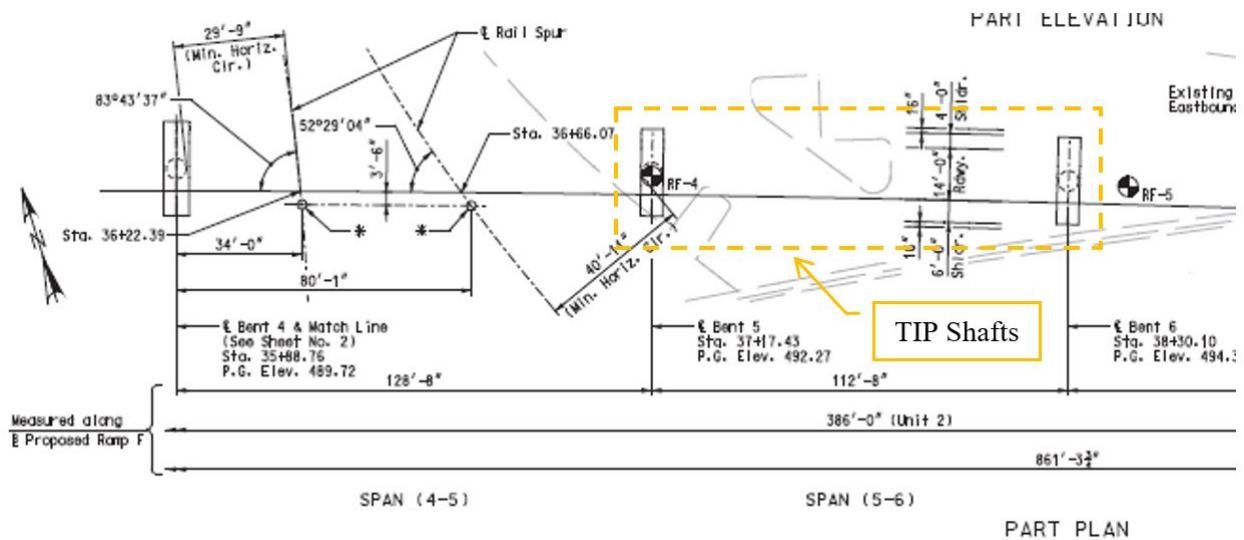


Figure 4-2: Partial plan view of Ramp F overpass bridge.

4.2.2 Subsurface Conditions

Subsurface conditions at each bridge are documented in the boring logs shown at the end of the bridge plan sets included in Appendix A (Ewing Ave.) and Appendix B (Ramp F). Shafts for both bridges are permanently cased through overburden soil with rock sockets in limestone. For the Ewing Ave. shafts, there is approximately 10 ft of lean clay fill material above limestone. The Ramp F Bent 5 shaft was installed through 27 ft of clay and rubble fill above 41 ft of clay above the limestone rock socket. The Ramp F Bent 6 shaft was installed through 22 ft of clay and rubble fill above 22 ft of native clay above 21 ft of limestone and fat clay above the limestone rock socket. At the time of construction, groundwater was

less than 10 ft deep for all shafts except Ramp F Bent 6. Groundwater filled the excavated shaft for Ramp F Bent 6 to about 30 ft below the ground surface.

4.2.3 Reinforcing Cage

Cross-sections for Ewing Ave. and Ramp F drilled shafts are shown in Figure 4-3 and Figure 4-4, respectively. For all shafts, the section through soil is permanently cased, and the rock sockets are uncased. The reinforcing cages for the Ewing Ave. shafts include 12 No. 10 reinforcing bars with 4.5 inches of concrete cover within the casing and 1.5 inches of concrete cover within the rock socket. Design clear spacing between vertical bars was 7.3 inches. The reinforcing cages for the Ramp F shafts consist of 24 bundles of two No. 10 reinforcing bars with 6 inches of concrete cover within the casing and 3 inches of concrete cover within the rock socket. Design clear spacing between vertical bars was 5.3 inches. The reinforcing cages for the Ewing Ave. shafts are continuous through the shaft and rock socket, whereas the cages for the Ramp F shafts include mechanical bar splices about 40 ft below the top of the shaft. Transverse reinforcing steel for all shafts consists of No. 4 spirals, with a 3-inch pitch for Ewing Ave. and a 6-inch pitch for Ramp F, corresponding to 5.5 and 2.5 inches of clear space, respectively.

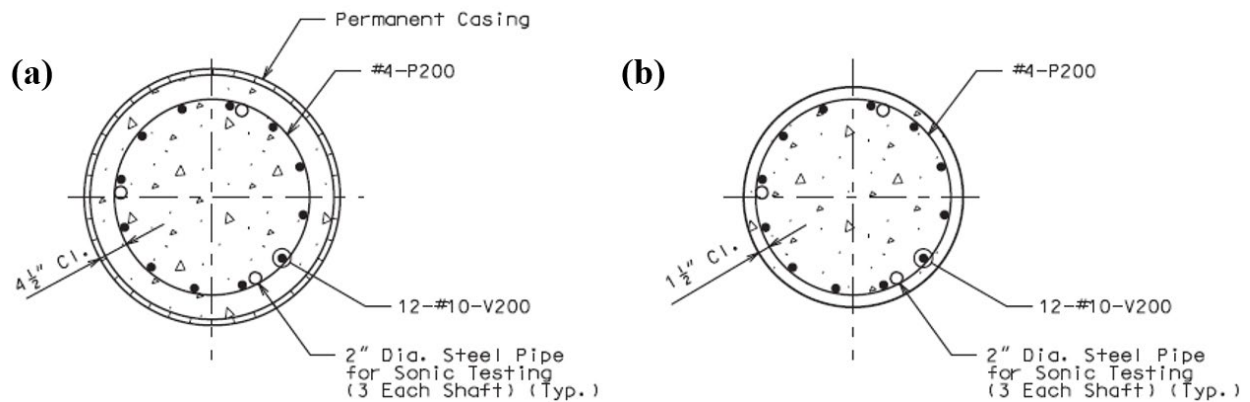


Figure 4-3: Drilled shaft cross-section for Ewing Ave. shafts: (a) within permanently cased section and (b) in uncased rock socket.

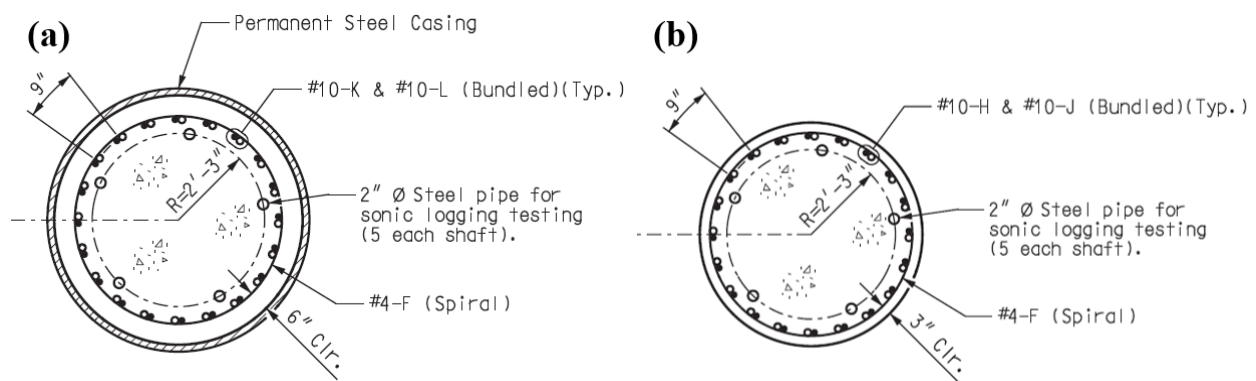


Figure 4-4: Drilled shaft cross-section for Ramp F shafts: (a) within permanently cased section and (b) in uncased rock socket.

4.2.4 Concrete Mix Design and Specifications

The same concrete mix design was used for drilled shafts at both bridges. The mix design specifications are presented in Table 4-1. The minimum clear space openings reported in the prior section for Ewing Ave. and Ramp F are respectively 3 and 7 times larger than the maximum coarse aggregate size, 0.75 inches. FHWA GEC 10 recommends a factor of at least 5 be used (Brown et al., 2018). The target slump upon arrival was 4 inches, with superplasticizer dosed upon arrival of the concrete to achieve a target slump closer to 8 inches. The actual slump was less, as described in Section 4.3.

Table 4-1: Concrete mix design specifications.

Material	Quantity per Cubic Yard of	Specification or Brand Name
Cement	555 lb	Portland Cement Type I/II
Fly Ash	150 lb	ASTM C618, Class C
Fine Aggregate	1,215 lb	MoDOT Class A
Coarse Aggregate	1,760 lb	MoDOT Grade E (Max coarse aggregate 0.75 inch)
Water (potable)	225 lb	
Air Entrainment Admixture	5 oz/cwt	Dravair 1400
Water Reducing Admixture	21 oz/cwt	Mira 95 (Type A and Type F)
Superplasticizer		Dosed at site to increase slump

4.3 Drilled Shaft Construction

The TIP shafts at the Ewing Ave. and Ramp F bridges were drilled in late May 2021, with concrete placement on May 25 for both Ewing Ave. shafts, May 27 for Ramp F Bent 6, and June 3 for Ramp F Bent 5. This section details the construction operations, including drilling the shaft excavation, installation of TIP equipment on reinforcing cages, placement of reinforcing cages in the shaft excavation, and placement of concrete. This section closes with a summary of the evidence of potential defects based on construction observations.

Information in this section is presented graphically in the appendices. Appendix C is as-built drawings of the completed shafts, showing relevant elevations and temporary casing diameters. Appendix D is the concrete placement logs, which include volume curves.

4.3.1 Drilling

All shafts were drilled using earth augers in soil and core barrels in rock. Drilling was completed using water as the drilling fluid. The results of drilling operations are depicted in the as-built records depicted in Appendix C.

Each Ewing Ave. shaft was installed by first drilling an oversized hole with a 48-inch auger through approximately 10 ft of fill. After excavating the soil, the 42-inch diameter permanent casing was twisted into the top of rock and the 3-ft diameter rock socket was excavated using a core barrel.

Telescoping casing was used for the Ramp F shafts, which extend through about 70 ft of soil and weathered rock above the rock socket. For both Ramp F shafts, the telescoping casing system consisted of a 90-inch diameter by 15-ft long temporary casing at the surface, an 84-inch by 25-ft long temporary

casing, and the 72-inch permanent casing extending from the top of concrete to the top of rock socket. A photograph of the telescoping casing for Ramp F Bent 6 after removal of the outermost casing is shown in Figure 4-5. The temporary casings were removed prior to placement of concrete.

The top of competent rock encountered during drilling for the Ramp F Bent 6 drilled shaft was 7 ft below where it was indicated in the inspection hole boring. (The inspection hole was drilled in the correct location, and the actual top of competent rock is consistent with the elevation that was indicated in the original plans, so it is likely the top of competent rock was misidentified during interpretation of the inspection hole log.) Because of the difference, the permanent casing for Bent 6 was too short, which is why the top of the inner casing is below the temporary casing in Figure 4-5. Acquiring an extension piece of permanent casing resulted in a delay of several days. After the delay for acquiring and welding on the extension casing (Figure 4-6), a clear image could not be observed from the inspection camera, resulting in further delays while the general contractor attempted to improve the image using flocculant and exchanges of water.

The drilling techniques are relevant to TIP because they affect temperature development. In particular, use of an oversized hole (at Ewing Ave.) and telescoping casings (at Ramp F) make it likely that air gaps exist between the soil and permanent casing. Air gaps would be limited to the length of shaft above groundwater, which was less than 10 ft below the top of concrete for all shafts except Ramp F Bent 6, where it was 28 ft. Trapped air would act as an insulator since the thermal conductivity of air is considerably less than that of soil.

Upon completion of drilling, the bottom of each shaft was cleaned using a cleanout bucket. However, for all shafts, the reinforcing cage was placed at least one day prior to concrete placement, which results in at least a 24-hour window for sedimentation to precipitate out of the fluid column prior to concrete placement. Soundings with a weighted tape were performed prior to concrete placement for all shafts. The soundings indicated solid rock for Ewing Shaft 2 and Ramp F Bent 5. For Ewing Shaft 3, the sounding indicated some significant sedimentation, especially on the north side of the base of the shaft. For Ramp F Bent 6, the base felt sticky across the bottom of the shaft prior to concrete placement. In addition, a MoDOT inspector reported 8 inches of sediment at the bottom of Ramp F Bent 6 based on comparison of the final drilled depth with the depth just prior to concrete placement. Sedimentation of the Ramp F Bent 6 shaft overnight between reinforcing cage installation and concrete placement was expected given the sedimentation that was observed during the period between the completion of drilling and approval of the video camera.



Figure 4-5: Excavated shaft for Ramp F Bent 6 with the permanent (innermost) 72-inch casing and temporary 84-inch casing shown.



Figure 4-6: Ramp F Bent 6 shaft after welding an extension piece to the top of the permanent casing. In this photo, the temporary casings have been removed and the ground near the shaft has been excavated to provide a safe working space for reinforcing cage and concrete placement.

4.3.2 Installation of Conventional TIP, Fiber Optic TIP, and Reinforcing Cages

Conventional TIP wires are typically installed on reinforcing cages prior to the reinforcing cage installation into the excavated shaft. The wires are attached to the cage using cable ties (a.k.a. zip ties). PDI recommends the wires be installed according to the procedure listed below. The guidance included in the procedure is intended to reduce the likelihood of wire damage during installation of the reinforcing cages. Damage is most commonly a result of the wire being pinched by lifting equipment, hitting the shaft sidewall during cage installation, or being struck by the tremie pipe during concrete placement.

1. TIP wires will be attached to longitudinal reinforcing bars. Identify the bars along which to route the TIP wires, taking care to avoid wire placement on any bars that will
 - a. Have lift points, i.e. avoid any bar with straps or lift chains.
 - b. Have centralizers.
 - c. Be adjacent to CSL tubes, although it is acceptable to place the wire on the side of the bar opposite the CSL tube.

Although the bars should generally be spaced evenly around the circumference of the reinforcing cage, it is better to satisfy (a) through (c) at the expense of perfectly even spacing.

2. Record the serial number and cage location for each wire.
3. Route TIP wires along longitudinal reinforcing bars on the inside of the reinforcing cage (i.e. inside the transverse reinforcing steel). Route the wires without cable ties while the reinforcing cage rests on the ground. Rules for routing wires:
 - a. The sensor at the bottom of cage is the first to come off spool. It should be placed 0.5-inch from the bottom of the bar.
 - b. Place the wire on the side of the longitudinal bar, not outside the cage.
 - c. Do not pull the wires into tension.
 - d. Do not move from one side of a bar to the other.
 - e. Do not cross bars.
 - f. Do not go around internal or external reinforcement (i.e. steel used to brace cage).
4. Tie wires using cable ties while the reinforcing cage rests on the ground. Rules for cable tying:
 - a. Tie bottom sensor with two cable ties attached tightly and directly on sensor. This is the only location with cable ties directly on the sensor, and the only location with cable ties as tight as possible by hand.
 - b. Use one cable tie between each sensor. Do not over-tighten ties; the wire should be able to slide a little.
 - c. Do not pre-tension wires. Wires should rest naturally on bar.
 - d. At the top of the reinforcing cage, wrap excess sensors and lead wire in a bundle and use cable ties to affix the bundle to a cage location that will be safe during concrete placement.
 - e. Ensure the vertical location of sensors is approximately the same for all wires.

Conventional TIP wires affixed to the Ramp F Bent 6 drilled shaft reinforcing cage resting on the ground surface are shown in Figure 4-7.

The conventional TIP wires for this research were placed according to the procedure above, with one significant exception: wires for the top half of the Ramp F shafts were attached to the reinforcing cages as the cages were lowered into the shaft. The resulting wire placement is shown in Figure 4-8. To accommodate placement as the reinforcing cages were lowered, the TIP wires were attached to the longitudinal bars on the outside of the cage (i.e. outside the transverse reinforcing steel). Placement as the cage was lowered was necessary because of the reinforcing cage being placed in two pieces with a mechanical bar splice near the midpoint. (An alternative to wiring the top half of the cage as it is lowered would be to wire the cage halves separately with an intentional wire splice, but this was not feasible for Ramp F because the bottom half of the reinforcing cage was cut upon completion of drilling.)



Figure 4-7: Conventional TIP wires affixed to the reinforcing cage for the Ramp F Bent 6 drilled shaft.



Figure 4-8: Conventional TIP wires affixed to the outside of the reinforcing cage for the Ramp F Bent 6 drilled shaft.

The fiber optic thermal cables were installed in a similar fashion as the conventional TIP wire. The main exception is that the fiber optic cables were installed on the exterior of the reinforcement cages, and each vertical cable was routed in a 1.5 circumference loop around the base of the cage before being routed up as a return in an opposite vertical, as shown in Figure 4-9. A total of 4 verticals (2 loops) were installed on the Ewing shafts, and a total of 6 verticals (3 loops) were installed on the Ramp F Bent 6 shaft. For all three shafts, all verticals except one were installed on the bottom reinforcement cage prior to the cage being picked for placement into the shaft excavation. The cable for the final vertical, located on the side of the reinforcing cage resting on the ground, was coiled and attached to the side of the cage during picking and was attached to the cage as it was lowered into the excavation, as shown in Figure 4-13.

For the Ramp F Bent 6 shaft, the total length of cable necessary was installed on the bottom reinforcing cage, with the excess coiled at the top of the cage. After the bottom cage was lowered into the shaft excavation, the coils were released from the side of the cage and spread radially around the pile bore. The cables were then attached to the upper section of the reinforcing cage as it was lowered into the shaft excavation along with the TIP wire.

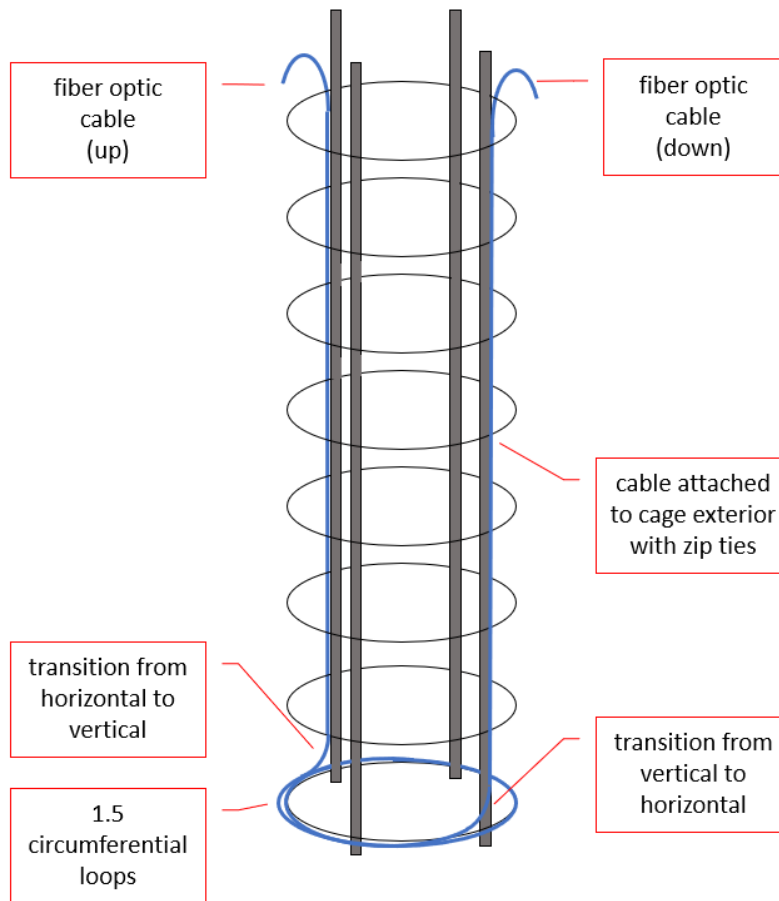


Figure 4-9: Schematic diagram of the fiber optic cable routing for a single loop / vertical pair.



Figure 4-10: Thermal fiber optic cables pre-installed on bottom section of reinforcement cage, with bundles for final vertical attached to the side of the cage.

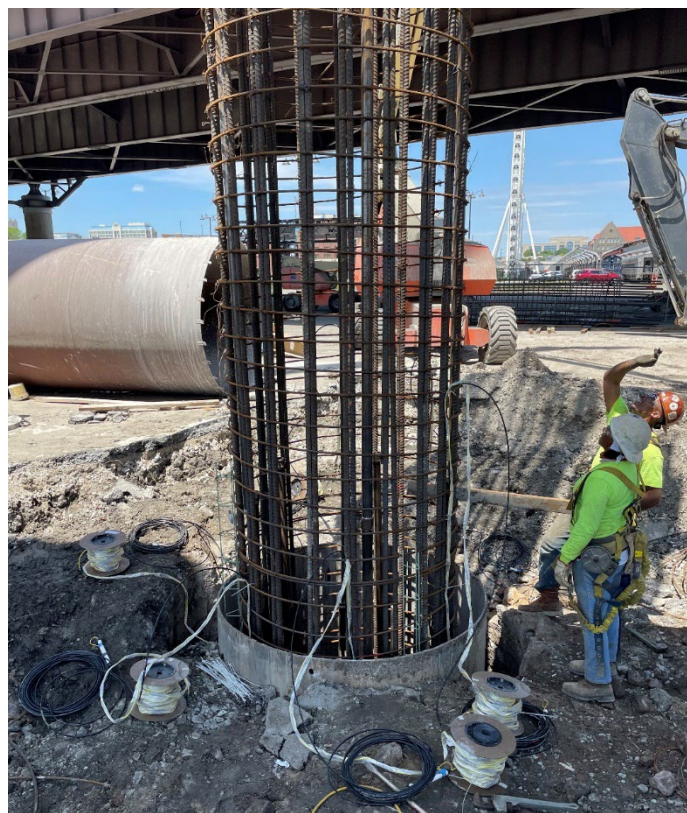


Figure 4-11: Lowering of the reinforcing cage for the Ramp F Bent 6 shaft, with the TIP and thermal fiber optic cable spread radially around the shaft.

For both Ewing Ave. and Ramp F, reinforcing cages were lowered into excavated shafts using a mobile crane. At Ramp F, the lower half of the cage was suspended with the crane and then supported on the permanent casing while the top half was connected, as shown in Figure 4-12. Rather than using drilled shaft centralizing devices, reinforcing steel chairs were attached to the reinforcing cages, as shown in

Figure 4-8 and Figure 4-13. The chairs were 2-inches deep within the rock socket and 4 to 5 inches deep above the rock socket. The chairs were installed at intervals of at least 10 ft, and likely greater at some depths. After the reinforcing cages were lowered into the excavated shaft, they rested on the base of the shaft (rather than being supported by the crane or hung off the casing). There were no bar “boots” on the bottom of the longitudinal bars, so the cage was resting directly on the base of the shaft.



Figure 4-12: Reinforcing cage placement for the Ramp F Bent 5 drilled shaft: (a) lower half of cage suspended with the crane, (b) lower half of cage resting on casing, and (c) top half of cage aligned with bottom half prior to engaging mechanical bar splices.



Figure 4-13: Reinforcing steel chairs used as centralizers for the Ramp F Bent 5 drilled shaft.

4.3.3 Concrete Placement

Concrete placement for all shafts occurred in the wet via a tremie pipe extended from a concrete pump truck. The tremie pipe was relatively small diameter, with an inner diameter of approximately 4.5 inches. For all shafts, a head of at least 10-ft of concrete was maintained above the bottom of the tremie during concrete placement, as is recommended (e.g. Brown et al., 2018). Results of concrete placement are documented in the concrete placement logs of Appendix D.

For each concrete pour operation, concrete slump was measured on a sample from the first concrete truck but not any of the subsequent trucks. This is consistent with standard specification requirements to test slump once per 100 cy for structural concrete. As shown in Figure 4-14, slump was measured to the average depth of the slumped concrete, rather than to the highest point. Measuring to the highest point would have resulted in lower slump values. For the Ewing Ave. shafts, the concrete slump was 6.75 inches. For the Ramp F Bent 5 shaft, the slump was between 6 and 7.5 inches. For the Ramp F Bent 6 shaft, the slump was 6.75 inches. These slump values were measured prior to the addition of high-range water reducer (a.k.a. super plasticizer).



Figure 4-14: Concrete slump test performed for Ramp F Bent 5 drilled shaft.

An initial attempt at concrete placement for the Ewing Ave. drilled shafts occurred on May 21, 2021. As concrete was placed in the first shaft, Ewing Ave. Shaft 1, the concrete displaced the reinforcing cage, lifting the cage visibly. The concrete had become unworkable, likely a result of low initial slump, high ambient temperatures, and significant delays due to several re-dosings of the first truck to satisfy air content specifications. Concrete placement for Shaft 1 was terminated so that the shaft could be re-drilled, and placement for Shafts 2 and 3 was postponed. As per the research plan, Shaft 1 did not have TIP testing; Shafts 2 and 3 had both conventional and fiber optic TIP testing. Concrete placement for Shafts 2 and 3, shown in Figure 4-15, was completed on May 25, 2021. Less than one truck's worth (appx. 9 cubic yards (cy)) was required for each of the Ewing Ave. shafts, so the curves shown in Appendix D for Ewing Ave. are not particularly informative. Over-pouring the shafts resulted in excess concrete filling the annular space between the ground and the outside of the permanent casing, as shown in Figure 4-16.



Figure 4-15: Concrete placement for Ewing Ave. Shaft 2.

Concrete placement for the Ramp F drilled shafts was also performed underwater via tremie. Concrete transfer from a concrete truck into the pump truck is shown in Figure 4-17. The concrete placement operation is shown in Figure 4-18, with water from the shaft displaced as concrete was placed. For both Ramp F shafts, the concrete was over-poured, as shown in Figure 4-19. The overpour results in a significant volume of concrete outside the shaft, which likely results in greater concrete temperatures near the top of the shaft.

During placement of the concrete, the depth to the top of concrete was observed between concrete trucks to develop concrete volume curves such as the one shown in Figure 4-20 for the Bent 6 shaft. The “x” points shown in the plot are the depths to top of concrete after each truck or set of trucks, assuming 9 cy per truck, which is consistent with the volume ordered. When trucks would arrive in close succession, their concrete was placed into the pump truck hopper concurrently or without a break in tremie concrete placement. When this occurred, the total volume from the trucks was combined for a single point on the curve. The black line on the concreting curve represents the theoretical volume of the shaft. All points are just below or just to the right of the theoretical curve, indicating the placed volume was slightly greater than the theoretical volume. Similar concrete volume curves are included for all shafts in Appendix C. The volume curves are used to interpret diameter in Chapter 6.



Figure 4-16: Concrete placement for Ewing Shaft 3: (a) Gap between the outside of the permanent casing and the ground surface; (b) overpouring concrete at the end of placement.



Figure 4-17: Concrete is transferred from concrete truck to pump truck.



Figure 4-18: Placement of concrete by tremie in the drilled shaft for Ramp F Bent 5.



Figure 4-19: Concrete for Ramp F Bent 5 drilled shaft is over-poured.

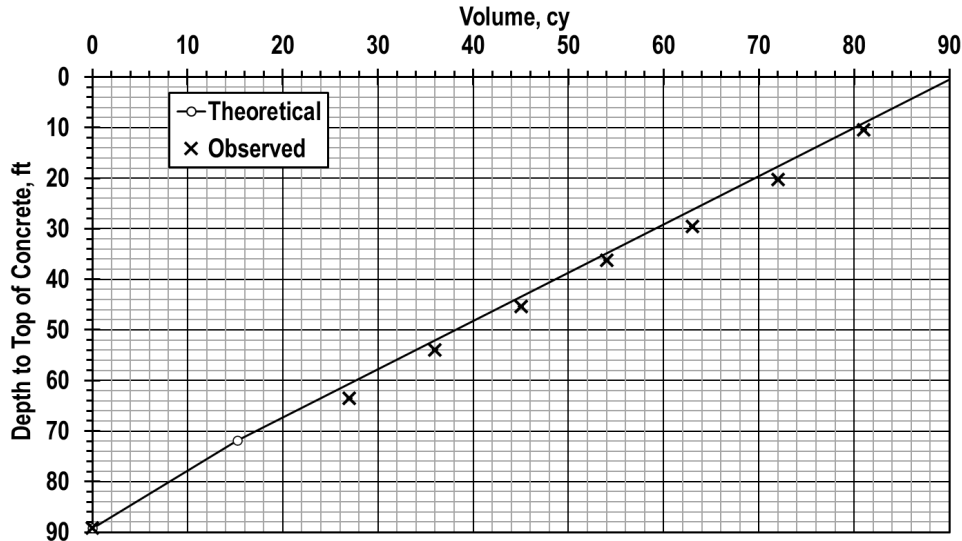


Figure 4-20: Concrete volume curve for the drilled shaft at Ramp F Bent 6.

4.3.4 Evidence of Imperfections from Construction Observations

Observation of drilling, reinforcing cage installation, and concrete placement were documented in this section. The primary evidence of potential imperfections is the weighted tape soundings of Ewing Shaft 3 and the shaft supporting Ramp F Bent 6. The former indicated potential sedimentation of the north side of the shaft; the latter indicated more significant sedimentation across the base of the shaft. A MoDOT inspector reported 8 inches of sediment at the bottom of Ramp F Bent 6 based on comparison of the final drilled depth with the depth just prior to concrete placement.

4.4 Performance of Integrity Test Methods

Both TIP and CSL were performed on Ewing Ave. Shafts 2 and 3 and Ramp F shafts for Bents 5 and 6. In addition, SONICaliper testing was performed on all four shafts.

4.4.1 TIP Testing

TIP testing was performed using the wire method, with wires and data collection equipment manufactured by PDI. For Ewing Ave., four wires were installed on each shaft. For Ramp F, six wires were installed on each shaft. All wires included one temperature sensor per foot of wire length. Installation of the TIP wires was documented in the previous section. Data collection for TIP was initiated after the reinforcing cages were installed within the excavated shafts but before concrete placement. It is also possible to delay data collection until after concrete placement to reduce the risk of damage during concrete placement, but it is advantageous to have a time record of concrete placement in the TIP data.

TIP data was collected remotely using PDI's wireless system. Temperatures were collected every 15 minutes, which is the default interval. The system includes one Thermal Access Port (TAP) box per TIP wire. The TAP boxes communicate wirelessly with a single Thermal Aggregator (TAG) box. The TAG box uses cellular networks to upload all TIP data to PDI's web-based system, which can be accessed remotely by any credentialed user. The TAG box is connected to one of the TIP wires; the TAG box also collects data from the wire, eliminating the need for a TAP box for that wire. A photograph showing a TAG box and TAP box attached to the top of the reinforcing cage for the Ramp F Bent 5 shaft is shown in Figure 4-21. At Ewing, one TAG box was used to collect data from both shafts. At Ramp F, one TAG box was used for each shaft.



Figure 4-21: TIP wires connecting into a TAG box (left) and TAP box (right). The boxes are attached to the top of the reinforcing cage for the Ramp F Bent 5 drilled shaft.

4.4.2 Fiber Optic Thermal Monitoring

The fiber optic thermal cables were monitored periodically for approximately 3 days after pouring for the shafts at Ewing Avenue and Ramp F, Bent 6. The analyzer used for the monitoring program was an Omnisens DITEST STA-R Fiber Optic Distributed Temperature and Strain Analyzer. The system operates in the BOTDA mode, connecting to both ends of the fiber optic cable during interrogation. The reading settings for the fiber optic analyzer are listed below.

Table 4-2: Omnisens fiber optic analyzer reading settings.

Spatial resolution (m)	1.0
Readout spacing (m)	0.2
Averaging	1000
Frequency window, start (GHz)	10.68
Frequency window, stop (GHz)	11.00
Frequency step (GHz)	0.50

At both sites, the fiber optic analyzer was operated from within the rear of a cargo van. This allowed the analyzer to be protected from the elements during operation, as well as to be secured for travel between the two field sites when the monitoring periods overlapped. The analyzer was powered using a portable battery power station with an integrated AC inverter. Monitoring was performed for approximately 10 hours per day, with the cables from the pile connected to the analyzer during monitoring. The readings were taken automatically on an approximate 15-minute interval, with a single operator present to ensure security for the equipment while on site. The data from the fiber optic readings was exported and backed up at the end of each day of monitoring.



Figure 4-22: Photograph of the fiber optic analyzer setup in the rear of the cargo van.

For all three shafts, the individual thermal fiber optic loops were connected in series so that the readings could be interrogated simultaneously on a single complete loop. For the Ewing Avenue shafts, the 2 thermal loops in each shaft were connected at the pile head, then the two shafts were connected so they could be interrogated on the same loop. At the Ramp F, Bent 6 shaft, the 3 thermal loops were connected together at the top of the pile head with the remaining free ends connected to the fiber optic analyzer. The distances along the fiber optic cable from the analyzer are referenced to specific locations in the piles, both in plan and depth, in a process referred to as “indexing.”

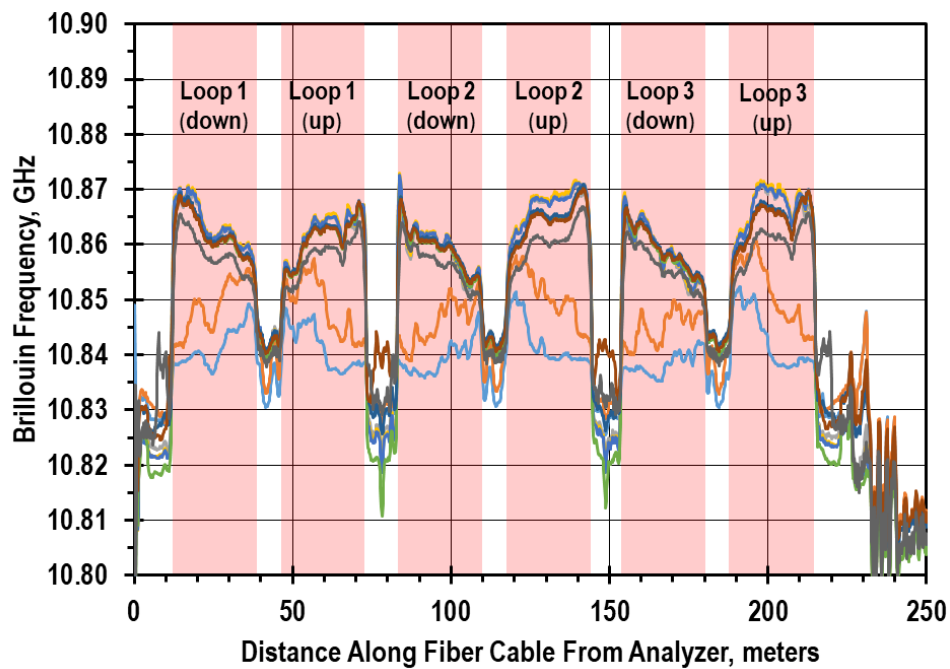


Figure 4-23: Raw fiber optic data from Ramp F, Bent 6, with thermal loops networked in series. Different lines correspond to different time stamps.

4.4.3 CSL Testing

CSL testing is typically performed on MoDOT drilled shafts. Accordingly, CSL testing was performed by others under contract with the general contractor for the Ewing Ave. and Ramp F bridges. Three CSL access tubes were included in each Ewing Ave. shaft; five access tubes were included in each Ramp F shaft. The access tubes are 2-inch diameter, Schedule 40 steel pipes. CSL testing was performed by testing all tube pairing combinations, resulting in three pairs for each Ewing Ave. shaft and ten pairs for each Ramp F shaft. A photograph of the CSL testing is shown in Figure 4-24. Behind the testing engineer, the pulley that is used to lower the CSL probes simultaneously is shown.



Figure 4-24: CSL testing is performed on the shaft for Ramp F Bent 5.

4.4.4 SONICaliper Testing

In addition to TIP and CSL, SONICaliper testing was performed on all four shafts. SONICaliper uses sonar technology to interpret the distance between the caliper device and the shaft side walls. The SONICaliper data can therefore be used to interpret shaft radius versus depth and the inclination (or eccentricity) of the shaft excavation. The test is performed by lowering the caliper device down the center of the shaft, stopping every 1 or 2 ft to collect shaft radius and eccentricity data. Performance of SONICaliper testing for Ewing Shaft 3 is shown in Figure 4-25.

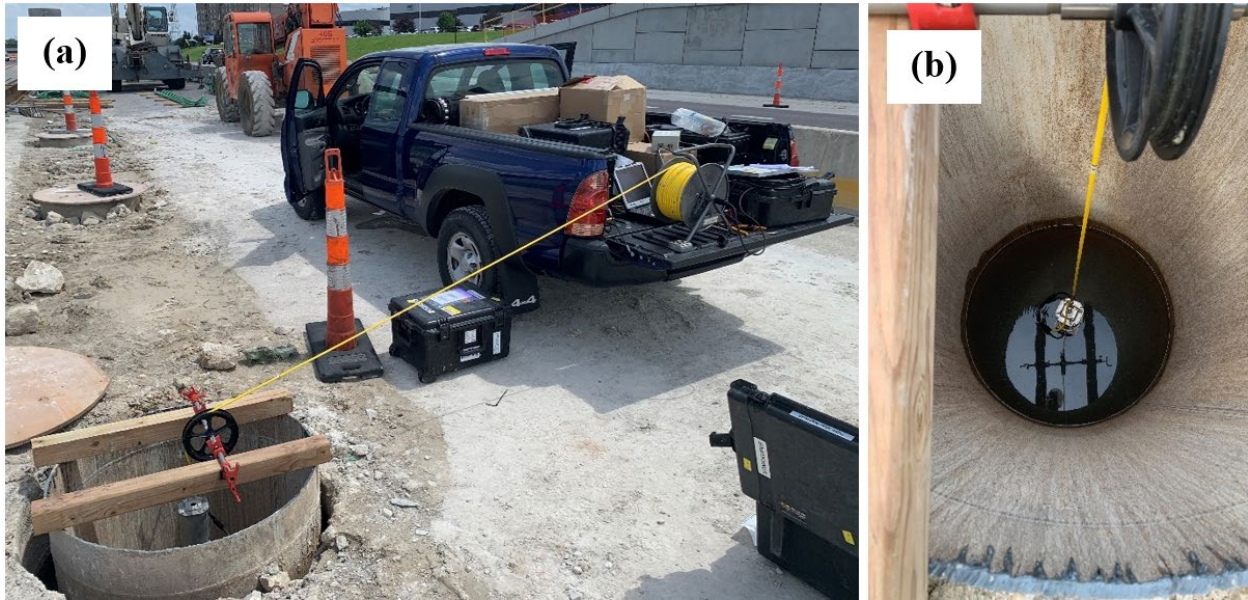


Figure 4-25: Performance of SONICaliper test: (a) overview and (b) caliper device within shaft.

4.5 Cost of TIP and CSL

Actual costs incurred for TIP and CSL testing for this field testing program are presented alongside the cost data presented in Hyatt et al. (2019) (Section 2.8) in Table 4-3, which is an update of Table 2-7. In general, the unit costs from Hyatt et al. are consistent with the costs for this work. One exception is the cost of CSL access tubes. The unit price when most of the tubes were ordered in fall of 2020 and spring of 2021, \$4.47 and \$5.90 per ft, respectively, was less than the unit price from Hyatt et al. However, much greater unit prices (\$15.90 and \$21.00 per ft) were paid for two relatively small orders placed during the summer of 2021, when the tubes were needed in short order and when steel prices globally were remarkably high. Unit costs for conventional TIP testing for this project were the same as those in Hyatt et al. (2019).

Fiber optic (FO) monitoring costs are included in the table are based on the costs for this field testing program as well as experience on previous projects. These costs can vary depending on a) the thermal cable selection and availability; b) on-site supervision during monitoring if a secure location for the analyzer is not available; and c) the analyzer rental depending on the source and capabilities of the analyzer. As compared to conventional TIP, the cable costs for FO systems are generally less expensive, with this differential increasing with longer cable lengths, while the monitoring equipment is more expensive for FO. The installation and engineering analysis costs for the two systems are generally similar.

The similarity of unit price data for this field testing program and Hyatt et al. suggests the observations noted in the discussion of Section 2.8 stand for this project as well. For most projects, TIP testing is likely somewhat cheaper than CSL testing, with the scale of cost differences depending on the project magnitude, details such as who is responsible for data collection, and variability of costs like engineering analysis. Most of the cost differences between the two test methods can be attributed to two items: (1) the cost associated with CSL data collection (compared with wireless collection of data from TIP wires) and (2) the cost of backfilling CSL tubes with grout after testing.

Table 4-3: Summary of average unit price information from Hyatt et al. (2019) and the field testing program of this research.

Test	Item	Unit	Hyatt et al. (2019)	This Project
CSL	Access Tubes	LF	\$6.50	\$5.62 (\$4.47 to \$21.00)
	Access Tube Cap	each tube	\$9.75	\$9.00
	Installation Labor	each tube	\$140.00	
	Post Grouting	LF	\$3.20	
	Engineering	each shaft	\$1,845.00	
Conventional TIP	Wire	LF	\$5.00	\$5.00
	Connector	each wire	\$25.00	\$25.00
	Installation Labor	each wire	\$120.00	\$120.00 ¹
	Engineering	each shaft	\$608.50	\$600 ²
	Data Logging Equipment Rental	monthly		\$3,900 ³
Fiber Optic TIP	Wire	LF		\$0.30
	Connector	each wire		\$10.00
	Cable Preparation	each wire		\$300.00
	Installation Labor	each wire		\$120.00 ¹
	Monitoring	daily		\$1,500 ⁴
	Engineering	each shaft		\$600 ²
	Analyzer Rental	weekly		\$2,750 ⁵

¹Estimate based on actual time of wire installation (1 day for Ewing Ave., 1 day for each Ramp F shaft = 24 hours) and an assumed labor rate of \$100/hour. This estimate does not include travel or mobilization costs.

²No engineering report costs were incurred for this work because analysis was included as part of the research tasks. \$600 is based on previous project experience.

³Rental fees would not be incurred by most testing firms because they typically own their own equipment.

⁴Monitoring fees are incurred due to the need for on-site supervision of the analyzer equipment given the lack of a secure monitoring location. These fees could be offset or eliminated if a secure container with power is available on site, either provided by the owner or contractor, which would allow for unsupervised monitoring.

⁵No rental fees were incurred for this work because the analyzer was included as part of the research task. \$2,750 is based on previous project experience, depending on the specific analyzer, and does not include shipping to/from site.

5. Results of Field Research

Results of the field testing program described in Chapter 4 are presented in this chapter. Results in this chapter are limited to the types of analysis that are typically presented in integrity test reports; additional analysis and synthesis of the data are reserved for the next chapter. Full integrity test reports associated with the results in this chapter are included in the appendices, as referenced throughout the chapter. This chapter is organized by integrity test, with conventional TIP results presented first, fiber optic TIP second, CSL third, and SONICaliper fourth.

5.1 Conventional TIP Results

TIP results are commonly presented as plots of temperature versus depth at two times: the time at which peak temperatures develop, and half of the time at which peak temperatures develop. For this research, the peak temperature was defined based on the average temperature profile, i.e. the profile of temperature versus depth based on the average of all wires at that depth. The peak was defined based on the average profile because the average profile is less sensitive to fluctuations than a single wire. TIP results are sometimes also presented in terms of effective radius, as explained in Chapter 2. TIP reports from PDI's software that include effective radius are presented in Appendix E.

Temperature versus depth plots are presented below for the peak time and half peak time for all four shafts: Ewing Shaft 2 (Figure 5-1), Ewing Shaft 3 (Figure 5-2), Ramp F Bent 5 (Figure 5-3), and Ramp F Bent 6 (Figure 5-4). Evaluation of the temperature profiles results in the following observations:

- Ewing Shaft 2: Above a 2-ft rolloff zone at the bottom of the shaft, temperatures are generally constant within the rock socket. Starting near the top of the rock socket (around depth of 12 ft), the temperature increases moving toward the larger-diameter permanently cased section. Temperatures are greatest at the top of the shaft, most likely due to the overpour (similar to Figure 4-16) resulting in an effective concrete diameter larger than the permanent casing diameter. The greater effective diameter due to overpouring was sufficient to produce greater temperatures at the top of the shaft despite rolloff effects.
- Temperature profiles at peak and half peak for Ewing Shaft 3 are very similar to those for Ewing Shaft 2. This is expected, considering the shafts had nearly identical dimensions and were constructed using the same batch of concrete on the same day. The only notable difference is at the bottom of the shafts, with temperatures at the bottom of Shaft 2 about 10 °F greater than those at the bottom of Shaft 3. The lower temperatures in Shaft 3 could be a result of soft bottom conditions, consistent with softer weighted tape soundings for Shaft 3.
- Similar trends were observed in the temperature profiles for the Ramp F shafts, although the temperatures are greater, as would be expected for larger diameter shafts:
 - The greatest temperatures were observed at the top of the shaft, where significant concrete overpour occurred (e.g. Figure 4-19). Significant rolloff was observed at the bottom of the shafts, with temperature decreases of approximately 25 °F over the bottom 5 ft.
 - The average temperature in the rock socket (bottom 18 ft of each shaft) was generally about 10 °F cooler than the temperature within the permanent casing above the socket.
 - The average temperature was generally about 5 °F greater in the Bent 6 shaft than the Bent 5 shaft. This is a relatively modest difference and is possibly explained by slightly greater placement temperature for Bent 6.

- There is considerably greater variation in temperature across the shaft (i.e. for a given depth) in the Bent 6 shaft compared to the Bent 5 shaft. This suggests cage eccentricity was greater for the Bent 6 shaft. Temperatures in the south and southeast wires are consistently greatest, whereas temperatures in the north and northwest wires are consistently least. This suggests the south-southeast portion of the cage is closest to the center of the shaft, whereas the north-northeast portion of the cage is closer to the shaft sidewall. Cage eccentricity is not surprising given the use of relatively small rebar chairs rather than more robust wheel centralizers and considering deviations from verticality (Section 5.4).
- For both shafts, the temperature data in all wires is more variable above the mechanical bar splice at a depth of 45 ft. A modest temperature increase with depth is observed at this location, too. Both observations are likely explained by the TIP wires being placed outside the reinforcing cage above the splice. The outside of the cage is closer to the shaft sidewall, where temperatures would be expected to be cooler and more variable.

One method for evaluating TIP data is to consider the difference in temperature across the shaft. As explained in Chapter 2, temperature differences generally indicate eccentricity in the reinforcing cage (i.e. the cage is not perfectly centered within the shaft) or an imperfection on one side of the cage (necking, bulging, an inclusion, etc.). The temperature difference from the conventional TIP data was calculated as the difference between the maximum and minimum temperature observed at any given depth and time. For example, for a depth of 2 ft at the peak time for Ewing Shaft 2, the temperature difference is 7 °F, which is the difference between temperatures in Wire 2 (126.7 °F) and Wire 4 (119.6 °F). Temperature difference results are plotted for each of the shafts: Ewing Shaft 2 (Figure 5-5), Ewing Shaft 3 (Figure 5-6), Ramp F Bent 5 (Figure 5-7), Ramp F Bent 6 (Figure 5-8). Each plot includes a profile of temperature difference versus depth at both the peak time and half the peak time.

Evaluation of the temperature difference versus depth data leads to the following observations:

- Temperature differences are generally greater within the permanent casing than within the rock socket. This is likely a result of concrete cover distance being greater within the permanent casing and the use of rebar chairs (Figure 4-13) as centralizers (rather than wheel centralizers).
- Temperature differences in the Ewing Ave. shafts were similar to one another. Surprisingly, greater temperature differences were observed at the bottom of the shaft without any indication of soft bottom conditions, Ewing Shaft 2, than at the bottom of the shaft where weighted tape soundings indicated soft bottom conditions, Ewing Shaft 3.
- Temperature differences in the Ramp F shafts are greater than those in the Ewing Ave. shafts. This is likely because concrete cover distances are greater for the Ramp F shafts: 3 inches in the rock socket and 6 inches in the permanent casing for Ramp F versus 1.5 and 4.5 inches, respectively, for Ewing Ave. The greater cover distance, especially when combined with significantly longer shafts, provides more opportunity for cage eccentricity.
- For all shafts, the temperature differences at half peak time are generally slightly greater than the temperature differences at peak time. The greater differences are in spite of the fact that temperatures, overall, are greater at the peak time. This is likely because temperatures within the shaft concrete begin to equilibrate between half peak and peak time. Because the temperature differences are greater at half peak, when overall temperatures are less, it may be easier to identify imperfections at half peak time than peak time.

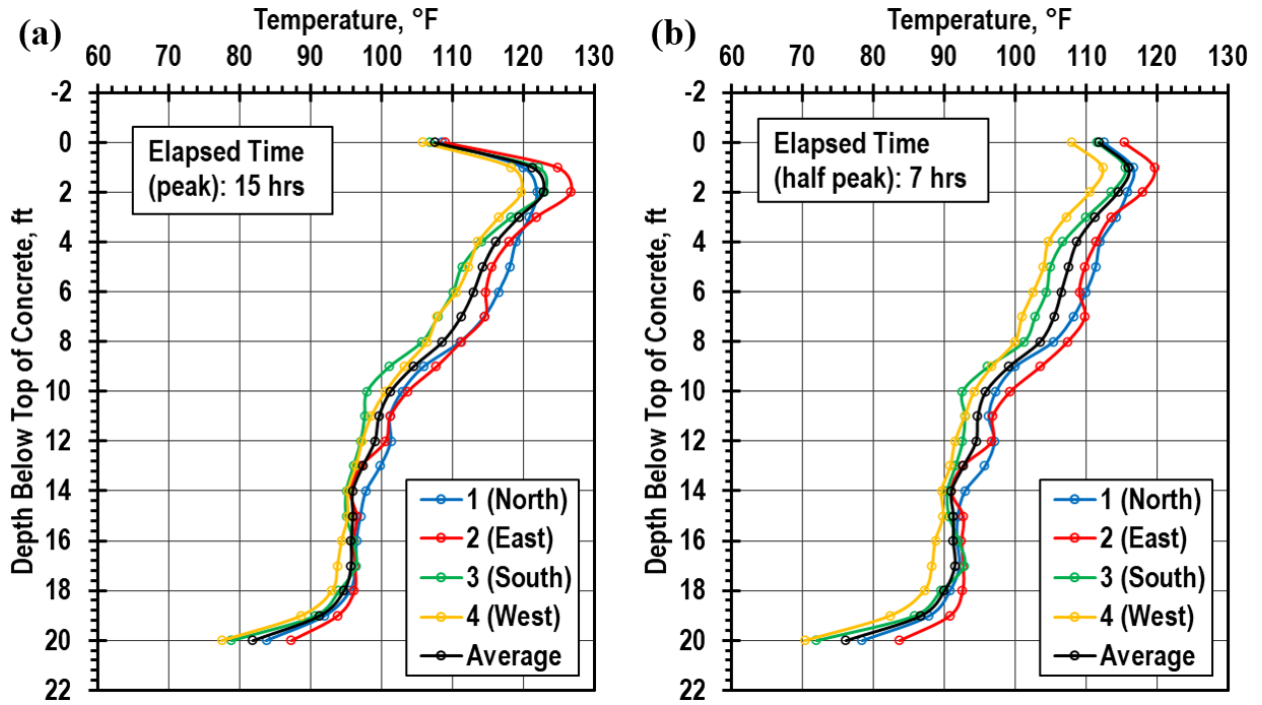


Figure 5-1: Temperature versus depth for Ewing Shaft 2: (a) time of peak temperature, (b) half the time of peak temperature.

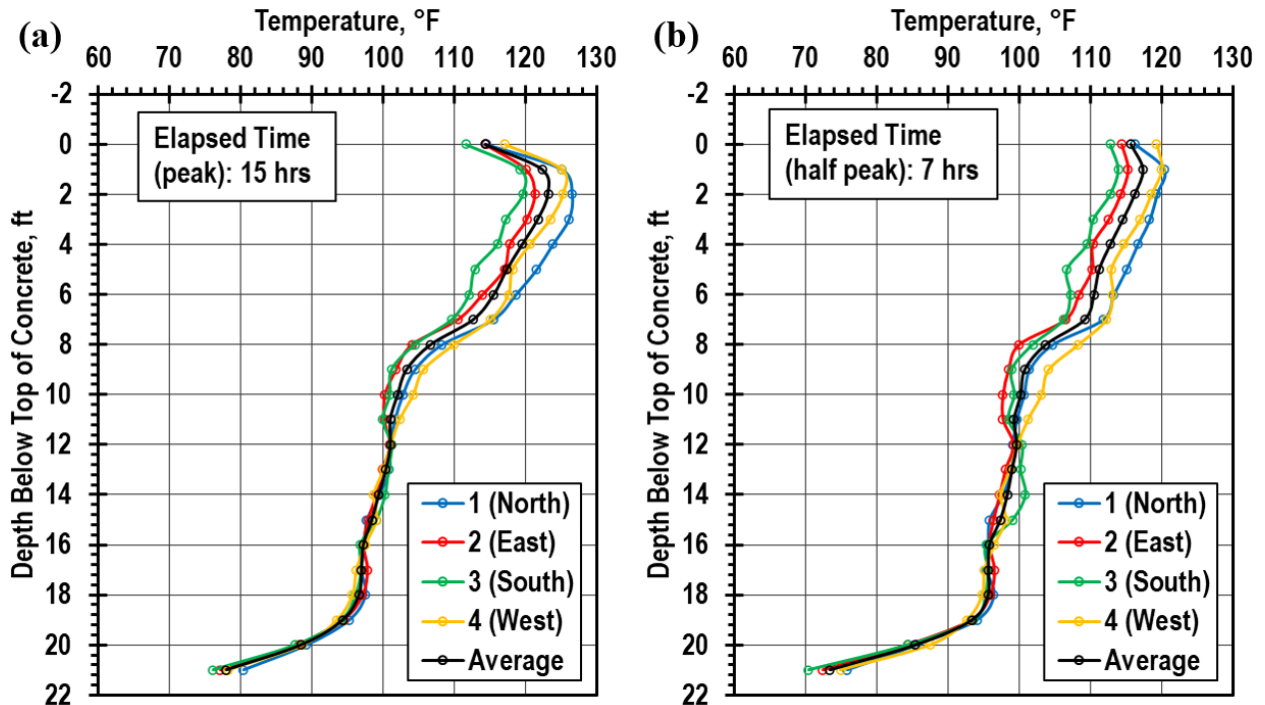


Figure 5-2: Temperature versus depth for Ewing Shaft 3: (a) time of peak temperature, (b) half the time of peak temperature.

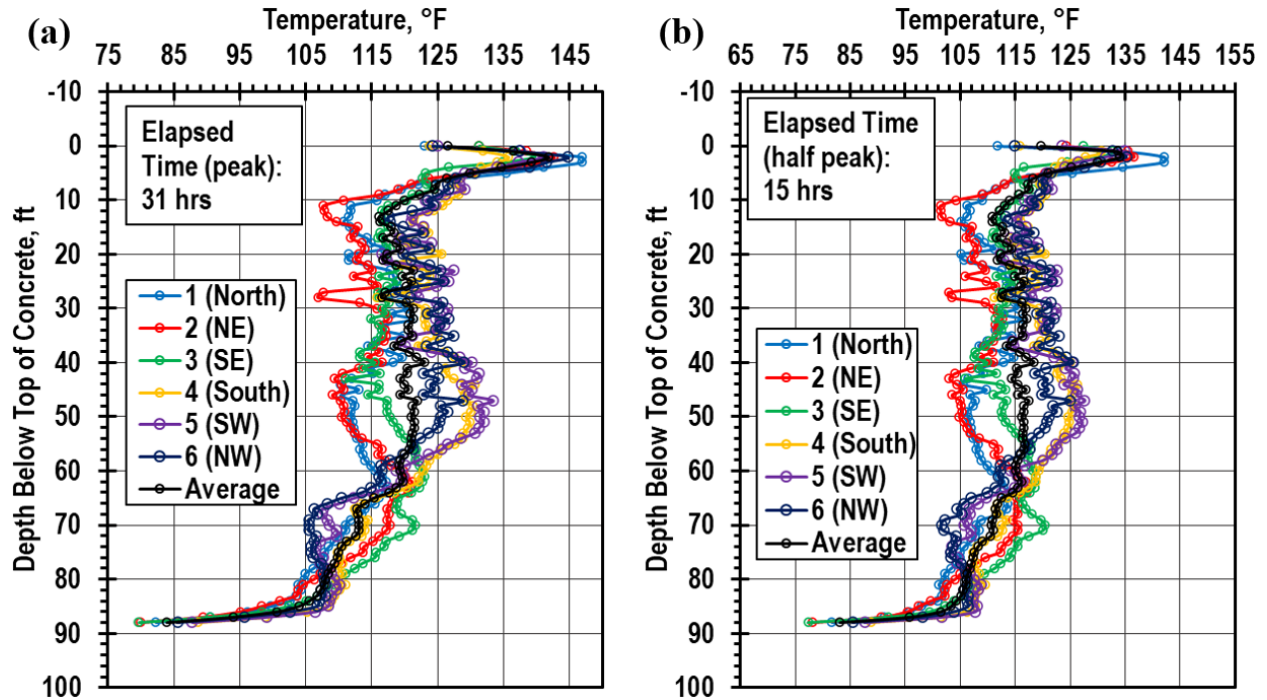


Figure 5-3: Temperature versus depth for Ramp F Bent 5: (a) time of peak temperature, (b) half the time of peak temperature.

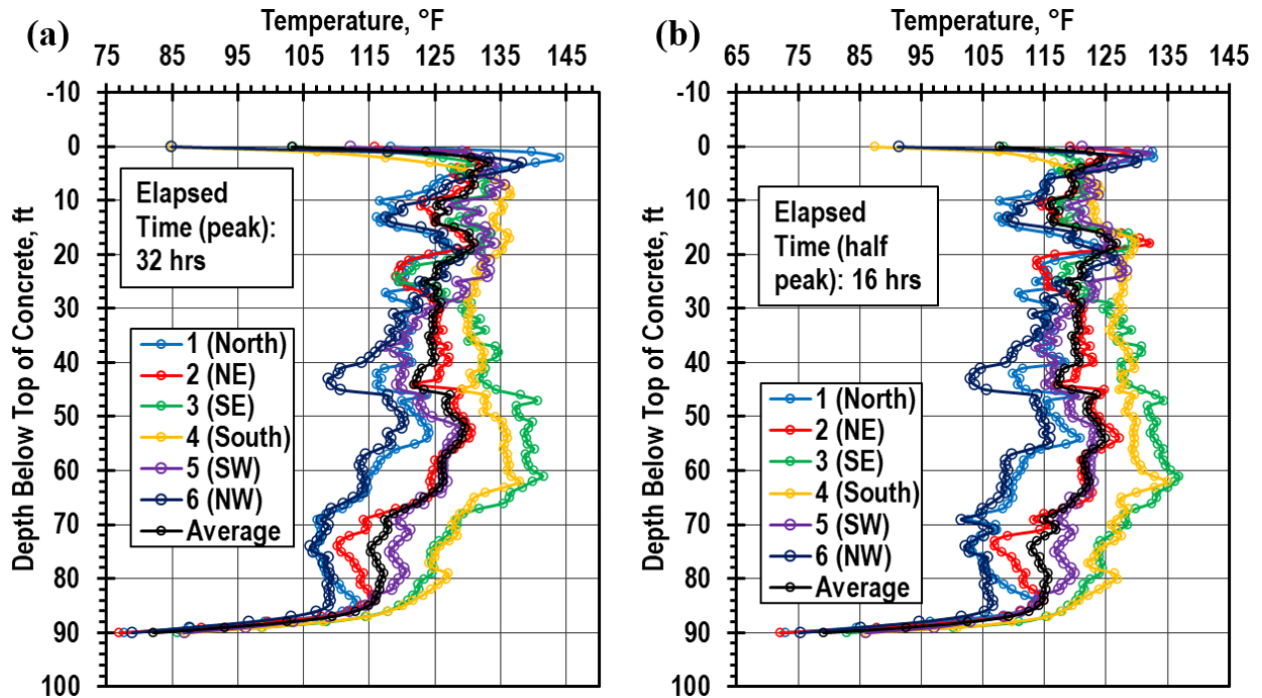


Figure 5-4: Temperature versus depth for Ramp F Bent 6: (a) time of peak temperature, (b) half the time of peak temperature.

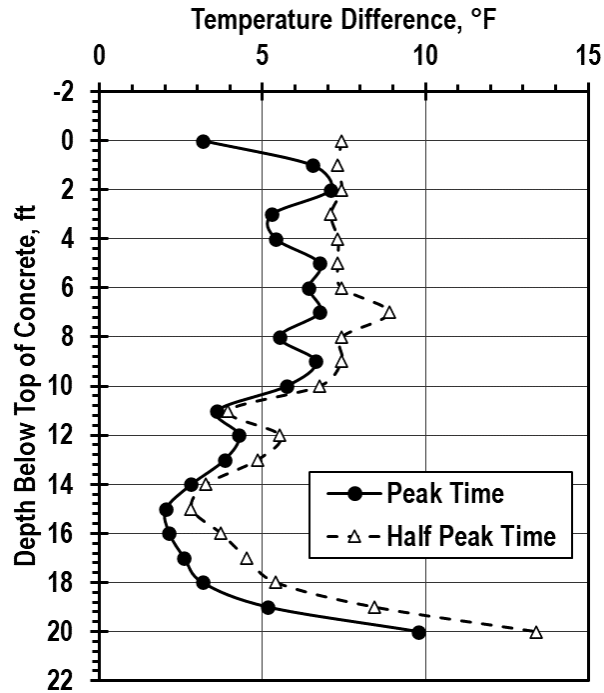


Figure 5-5: Temperature difference versus depth for Ewing Shaft 2.

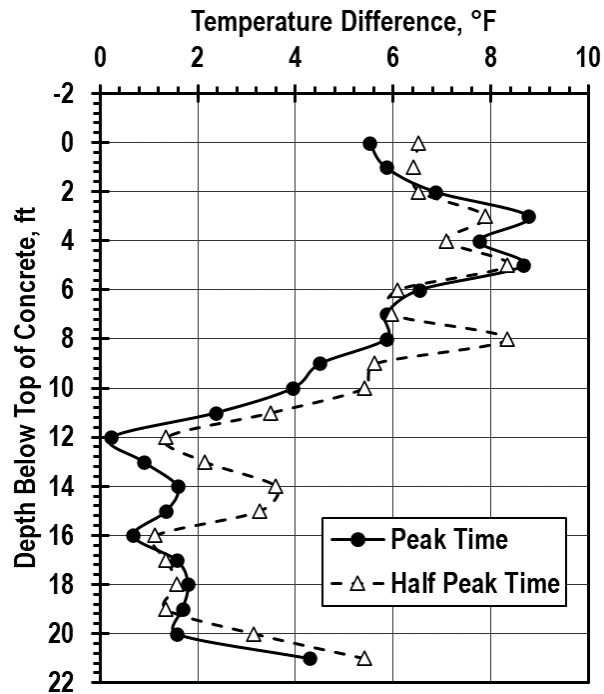


Figure 5-6: Temperature difference versus depth for Ewing Shaft 3.

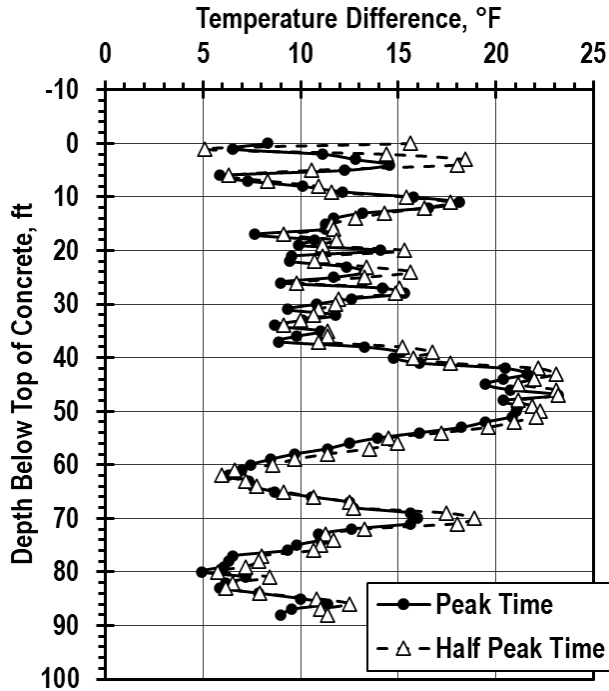


Figure 5-7: Temperature difference versus depth for Ramp F Bent 5.

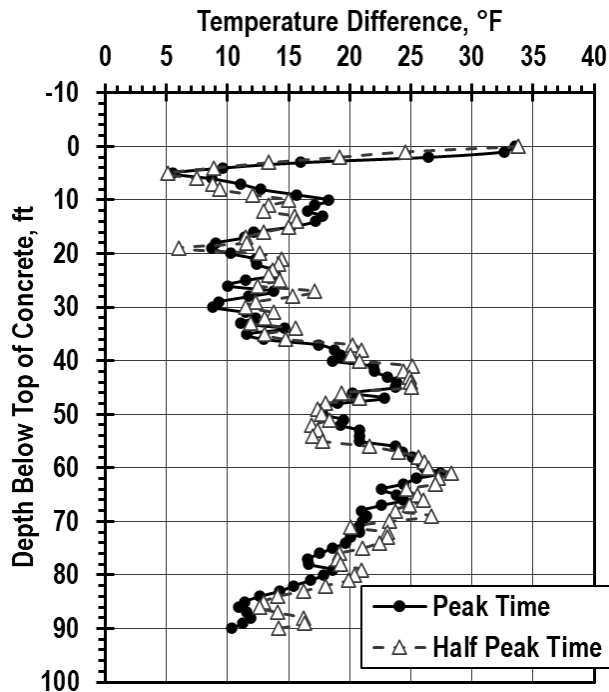


Figure 5-8: Temperature difference versus depth for Ramp F Bent 6.

Results of the conventional TIP testing are summarized in Table 5-1. The table includes peak temperature and the time of peak temperature, the maximum temperature at half the peak time, and the maximum temperature differences observed at peak time and half peak time. As explained above, the temperature profiles for all shafts appear to be impacted considerably by the concrete overpour at the top of shafts. To

limit the influence of the overpour in the summary, the results in Table 5-1 do not consider results above a depth of 4 ft for Ewing Ave. shafts and above a depth of 10 ft for the Ramp F shafts. Results in the table are consistent with the discussions of the temperature profile and temperature difference plots above: generally similar results for similar shafts; greater temperature differences associated with greater opportunity for eccentricity; and similar temperature differences at half peak and peak times.

Table 5-1: Summary of conventional TIP testing results.

	Ewing Ave.		Ramp F	
	Shaft 2	Shaft 3	Bent 5	Bent 6
Peak Average Temperature, °F	116.2	119.6	123.5	131.0
(Depth, ft)	(4)	(4)	(40)	(18)
Peak Time, hrs	15.1	14.8	36.9	31.9
Max. Avg. Temp. at Half Peak Time, °F	108.7	112.8	120.0	126.7
(Depth, ft)	(4)	(4)	(40)	(118)
Max. Temp. Diff. at Peak Time, °F	9.8	8.8	21.8	27.4
(Depth, ft)	(20)	(3)	(47)	(61)
Max Temp. Diff. at Half Peak Time, °F	13.4	8.3	23.9	28.4
(Depth, ft)	(20)	(8)	(47)	(61)

As explained in Chapter 2, effective radius analysis is conventionally included in most TIP reports. Effective radius analysis was performed for each of the shafts using PDI’s TIP Reporter software (version 2021.20.0.0). Results are included in the TIP reports of Appendix E. The effective radius values are based on the methodology described in Section 2.3.4, specifically a Level 2 analysis that models the temperature-radius relationship using average temperatures from TIP and the concrete volume log data from Appendix D. Each temperature-radius model was based on an estimated volume of concrete within the casing and an estimated volume of concrete within the rock socket. For the Ewing Ave. shafts, one truckload of concrete provided sufficient concrete to fill and overtop each shaft. It is therefore impossible to discern the specific shaft volume, never mind the volume within the socket versus the volume within the casing. Accordingly, the theoretical concrete volumes were used in TIP Reporter for its effective radius analysis. For the Ramp F shafts, the results shown in the concrete volume logs of Appendix D were used to estimate the volume of concrete within the rock socket, and the theoretical volume was used within the casing. (The volume information from Appendix D indicates the volume within the casing was generally similar to the theoretical volume.) The effective radius analyses are based on the temperature profiles at half of the peak time. Roll-off corrections were implemented based on findings and recommendations from Johnson (2016):

- For the bottom roll-off, the average temperature just above the roll-off zone was estimated visually. The soil temperature was based on measurements prior to the placement of concrete. The bottom sensor was assumed to be at the base of the shaft based on the information presented in Chapter 4. The scale factor (depth in feet) was estimated as $0.32\sqrt{t}$, where t is the time after concrete placement in hours.
- For the top roll-off, an average ambient temperature of 80 °F at the ground surface was used. The top sensors were within inches of the top of concrete. The average temperature at the top of shaft was estimated visually. The scale factor (height in feet) was estimated as 0.3 ft less than the bottom of shaft scale factor.

Effective radius profiles at half peak are shown in Figure 5-9 for the Ewing Ave. shafts and Figure 5-10 for the Ramp F shafts. For all of the shafts, the effective radius within the cased section is notably less than the actual shaft diameter (i.e. the inner diameter of the casing). The small effective radius values are

a reminder that the effective radius is not the actual radius. Rather, as explained in Section 2.3.4, effective radius is the predicted radius that would produce the observed temperature in the TIP data. Within the cased section, the effective radius values are dominated by the effect of overpouring. The roll-off correction results in smaller effective radius values near the bottom of the casing and effective radius values that are limited by PDI's software to the casing radius near the top of the shaft.

At the bottom of the shaft, the effective radius values are more interesting. Ideally, for a shaft without any imperfections at the bottom (i.e. without soft bottom conditions), the effective radius should not change at the bottom of the shaft. In other words, the roll-off correction should result in adjusted temperatures that are constant with depth. The interpreted effective radius values for the Ewing and Ramp F shafts are generally consistent with construction observations. For Ewing Ave., the effective radius at the bottom of Shaft 2 is variable, but the average value actually increases compared to the rest of the rock socket. For Shaft 3, the average effective radius decreases considerably at the bottom of the shaft, which is consistent with weighted tape observations confirming the presence of soft bottom conditions. For Ramp F, the average effective radius at the bottom of the Bent 5 shaft decreases, but the decrease is consistent with a decreasing trend with depth throughout the rock socket. Evaluation of the bottom conditions for Bent 5 is therefore inconclusive. For Bent 6, there is a dramatic decrease in effective radius values over the bottom 5 ft of the shaft, which supports weighted tape soundings suggesting the presence of soft bottom conditions.

The effective radius interpretation facilitates calculation of concrete cover, but concrete cover is not actually measured with TIP methods. As evidence, there are several locations within the cased sections of the drilled shafts where the effective radius values of Figure 5-9 and Figure 5-10 would suggest total loss of cover (i.e. no concrete outside the reinforcing cage), but such a result is highly unlikely considering the observed construction practices. The computed values of concrete cover are, at best, limited by the reliability of the temperature-radius models, which are typically limited by the reliability of concrete volume estimates, depth measurements, presence of flowing water or groundwater, use of oversized temporary casing, and possibly other environmental conditions affecting the assumed insulation values used in the model. The cover values calculated from effective radius interpretations are better considered as a qualitative assessment of concrete integrity rather than a reliable indication of specific concrete cover distances. Finally, it is also important to consider that many drilled shaft concrete problems (e.g. soft bottom conditions) do not specifically relate to cover.

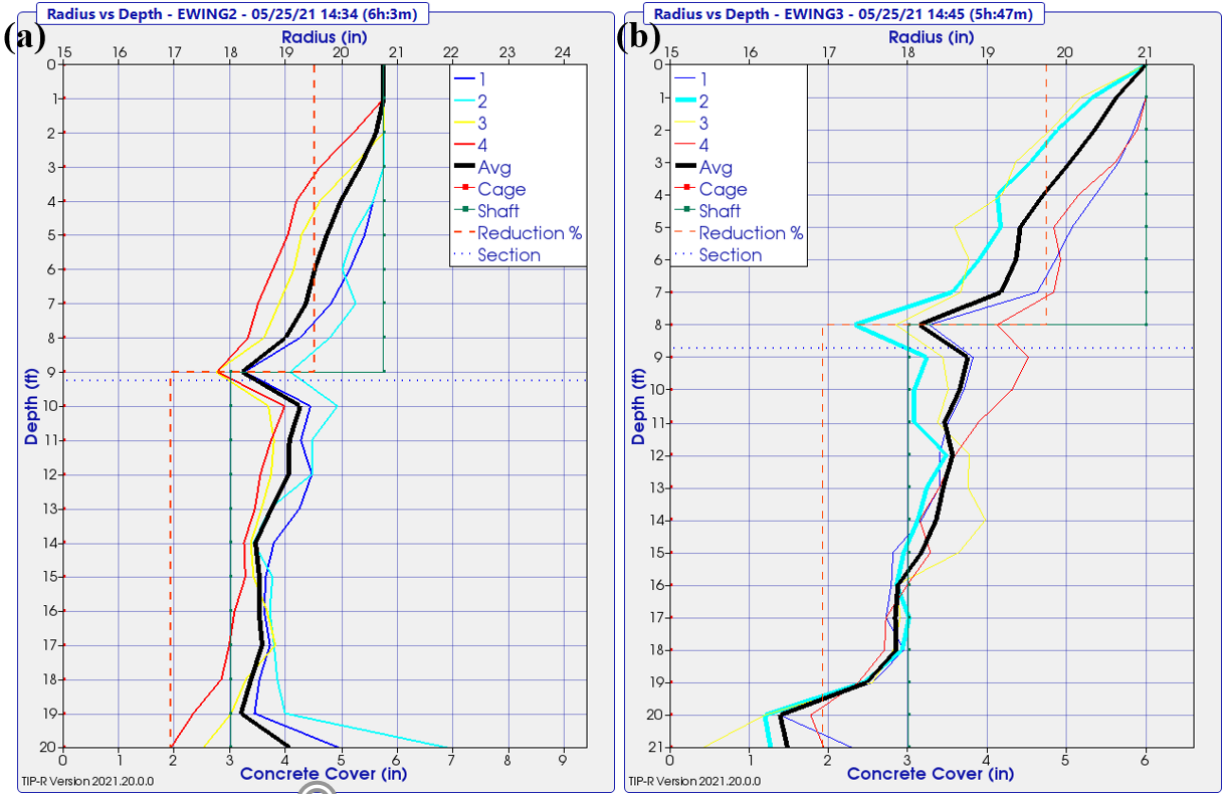


Figure 5-9: Effective radius versus depth at half peak for Ewing Ave. (a) Shaft 2 and (b) Shaft 3.

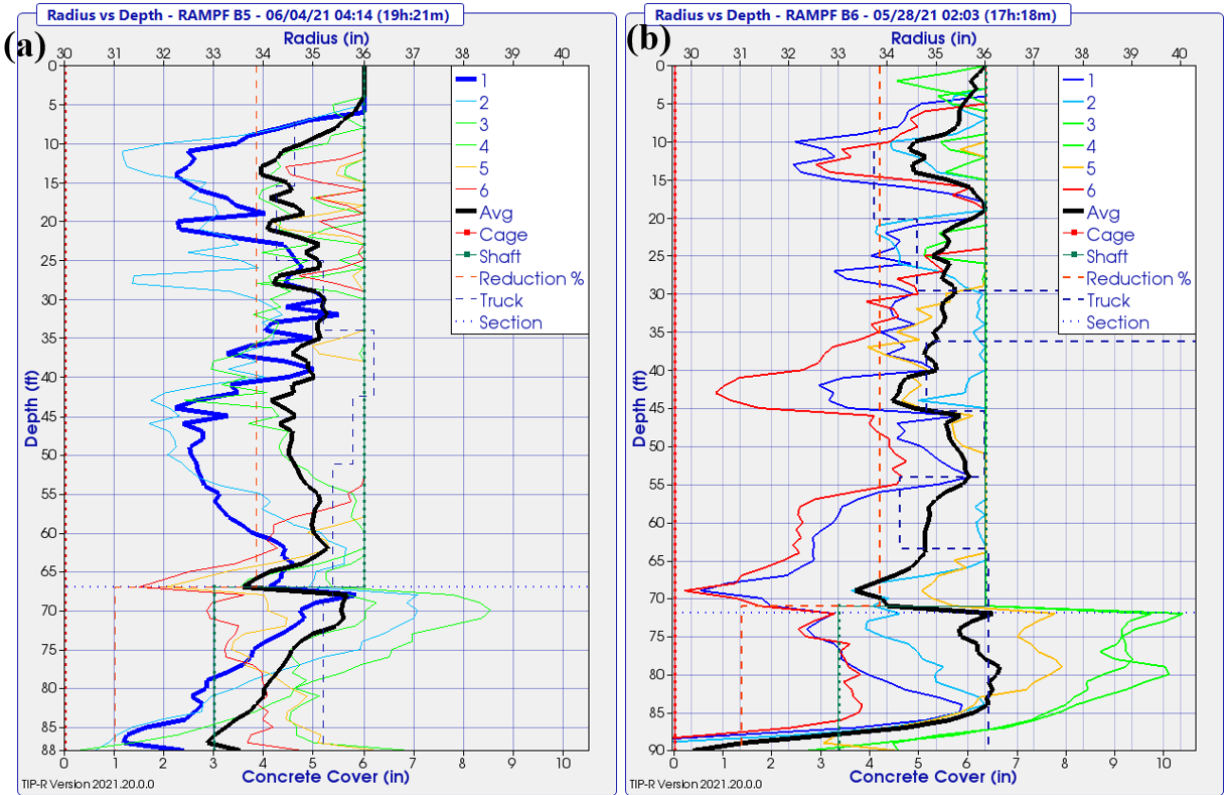


Figure 5-10: Effective radius versus depth at half peak for Ramp F (a) Bent 5 and (b) Bent 6.

5.2 Fiber Optic TIP Results

The fiber optic thermal results for the three monitored shafts are presented as plots of temperature versus depth. Where possible, the times of the data presented were chosen at the peak temperature and half of the peak temperature to match the times for the conventional TIP results in Section 5.1. However, when the timing of the selected plots did not correspond to a period when fiber optic readings were being taken (for example, if the peak occurred overnight), the nearest timed reading is presented instead.

Temperature versus depth plots are presented below for the closest fiber optic thermal readings to the peak time and half peak time for the three shafts: Ewing Shaft 2 (Figure 5-11), Ewing Shaft 3 (Figure 5-12), and Ramp F Bent 6 (Figure 5-13).

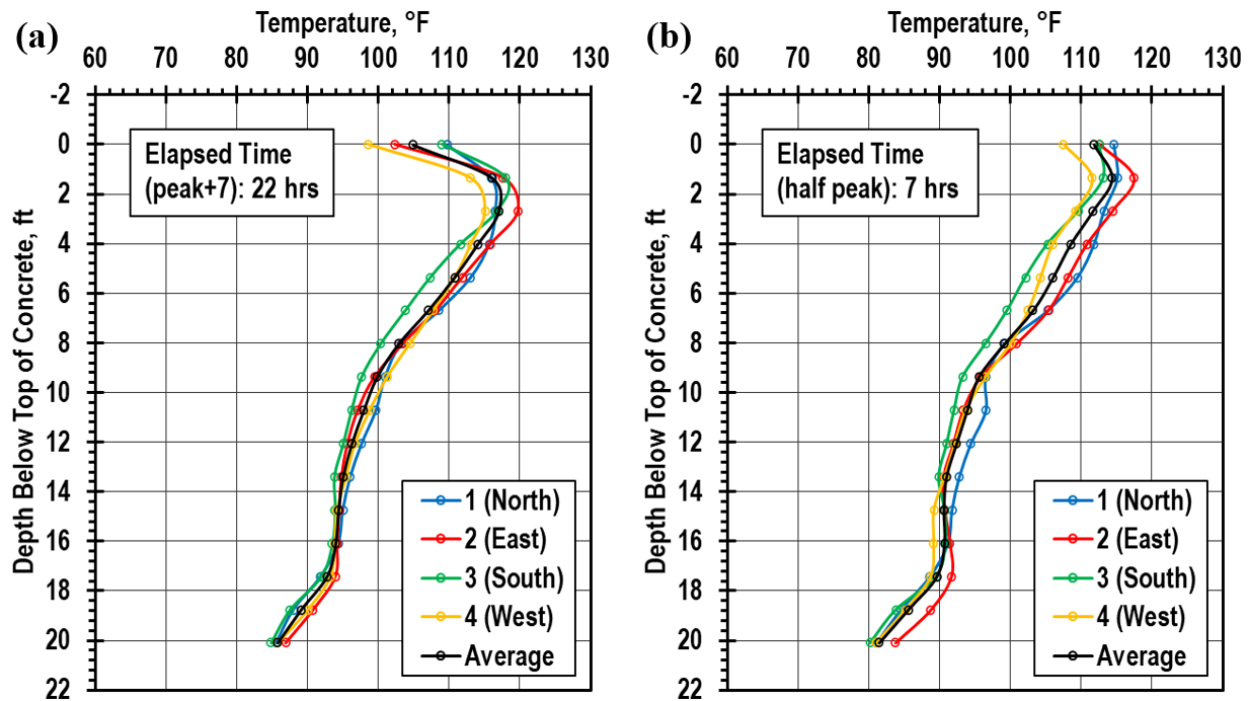


Figure 5-11: Fiber optic temperature versus depth for Ewing Shaft 2: (a) 7 hours after time of peak temperature, (b) half the time of peak temperature.

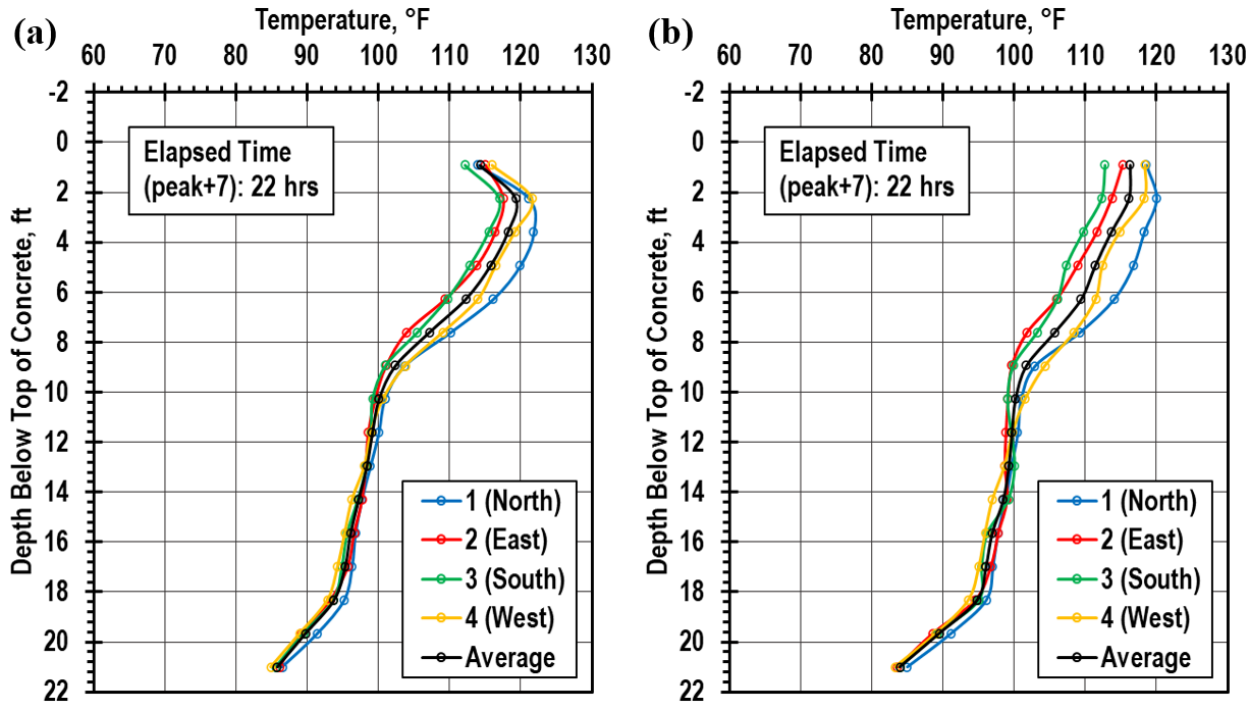


Figure 5-12: Fiber optic temperature versus depth for Ewing Shaft 3: (a) 7 hours after time of peak temperature, (b) half the time of peak temperature.

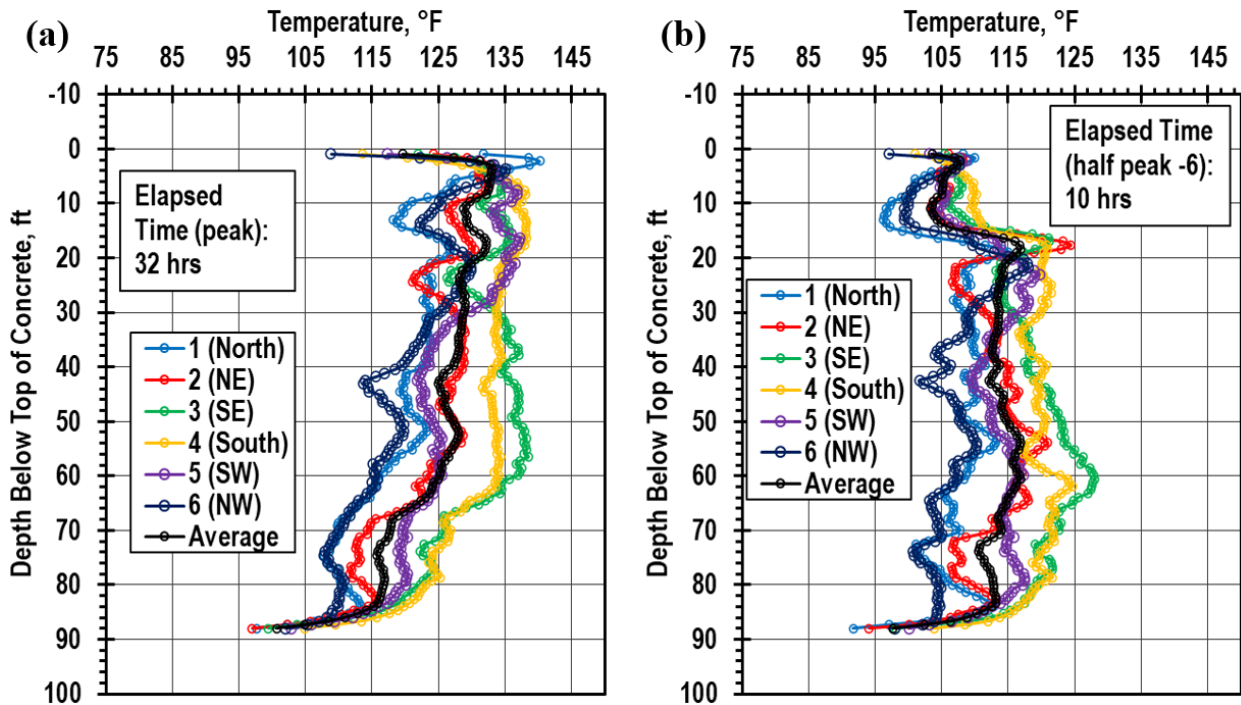


Figure 5-13: Fiber optic temperature versus depth for Ramp F Bent 6: (a) time of peak temperature, (b) 6 hours prior to half the time of peak temperature.

The temperature profiles for the two Ewing Avenue shafts and the Ramp F Bent 6 shafts were in close agreement with the profiles reported by the conventional TIP system. A comparison of the measurements of the two systems is presented in the Section 6.1. Since the temperature results between the two systems are nearly identical, the observations presented in Section 5.1 on the conventional TIP thermal profiles are also applicable to the fiber optic records. For example, this includes the close similarity in the thermal profiles of the Ewing shafts and the relatively larger temperature variation across the shaft in Bent 6 with depth.

The evaluation of the temperature difference has not been recreated for the fiber optic thermal data; however, the results would be similar to those from the conventional TIP results. The effective radius plots of the conventional TIP reports have also not been recreated as the finite element modeling for thermal cross-sectional area in the literature is not yet available as a stand-alone analysis tool. This analysis is the focus of ongoing research and could be incorporated into future processing tools if there is future need for alternative Level 3 and Level 4 interpretation for drilled shaft thermal data.

5.3 CSL Results

CSL reports by others are presented in Appendix F. A summary of the anomalies is presented in Table 5-2. The table is similar to the tables included in the Appendix F reports, but with the addition of relative energy loss and DFI criteria rating (2018) (Section 2.5). The results indicate three potential imperfections:

- Soft bottom conditions on the north side of Ewing Shaft 3.
- Weak concrete at the top of the shaft for Ramp F Bent 5.
- Soft bottom conditions in Ramp F Bent 6.

The soft bottom conditions in Ewing Shaft 3 and Ramp F Bent 6 are consistent with construction observations. At Ewing Shaft 3, weighted tape soundings noted sedimentation on the north side of the shaft, but not the south. At Ramp F Bent 6, soundings indicated even softer conditions than Ewing Shaft 3, which is consistent with the magnitude of energy loss recorded in the Bent 6 CSL reports. The Bent 6 soft bottom conditions were not limited to one portion of the shaft, as indicated by the weighted tape soundings and CSL results. At the top of the shaft for Ramp F Bent 5, three 2-inch diameter cores were performed to investigate the anomaly. The cores did not reveal any problems. The explanation offered by the contractor is that a large volume of air entered the shaft during the overpour when the concrete truck ran out of concrete. The air was removed by vibrating, but likely resulted in access tube debonding. Bleed water could also have produced debonding of the access tubes at the top of the shafts.

An example CSL tube pairing result is shown for Ramp F Bent 6 in Figure 5-14. The results confirm the 25 percent velocity reduction, which is all that is reported in the CSL report table. More striking, however, is the 12-dB relative energy reduction and corresponding loss of signal in the waterfall plot to the right of Figure 5-14. These observations support the DFI approach of considering both velocity reduction and relative energy loss, rather than just velocity reduction. Whereas evaluation of the results in some standards that only include consideration of velocity reduction (including the criteria in MoDOT's Standard Specifications) would classify the result in the second most severe category, consideration of both velocity reduction and energy loss via the DFI criteria puts the defect squarely in the most severe category. The most severe category is likely appropriate considering the construction observations with a weighted tape.

Table 5-2: Summary of CSL anomalies identified in Appendix F.

Shaft	Depth, ft	Tube Pair (Quadrant)	Velocity Reduction, %	Relative Energy Loss, dB	DFI Criteria Rating ¹
Ewing Shaft 2			None		
Ewing Shaft 3	21 to Bottom	1-2 (NE)	18	3	B
	21.2 to Bottom	1-3 (NW)	15	6	B
Ramp F Bent 5	0 to 0.5	1-3 (E)	15	12	C
	0 to 1.2	1-4 (W)	50	12	C
	0 to 1.2	1-5 (NW)	30	15	C
	0 to 1.0	2-4 (SE)	13	12	B
	0 to 1.0	2-5 (N)	50	12	C
Ramp F Bent 6	87.1 to Bottom	1-2 (NE)	25	15	C
	87.8 to Bottom	1-5 (NW)	17	12	C
	86.0 to Bottom	2-3 (SE)	15	12	C
	18.3 to 19.1	3-4 (S)	13	8	A
	88.8 to Bottom	1-3 (E)	17	9	B
	88.9 to Bottom	1-4 (W)	14	7	A
	87.6 to Bottom	2-5 (N)	12	10	B

¹See Chapter 2: A = acceptable; B = conditionally acceptable; C = highly abnormal (Deep Foundations Institute, 2018).

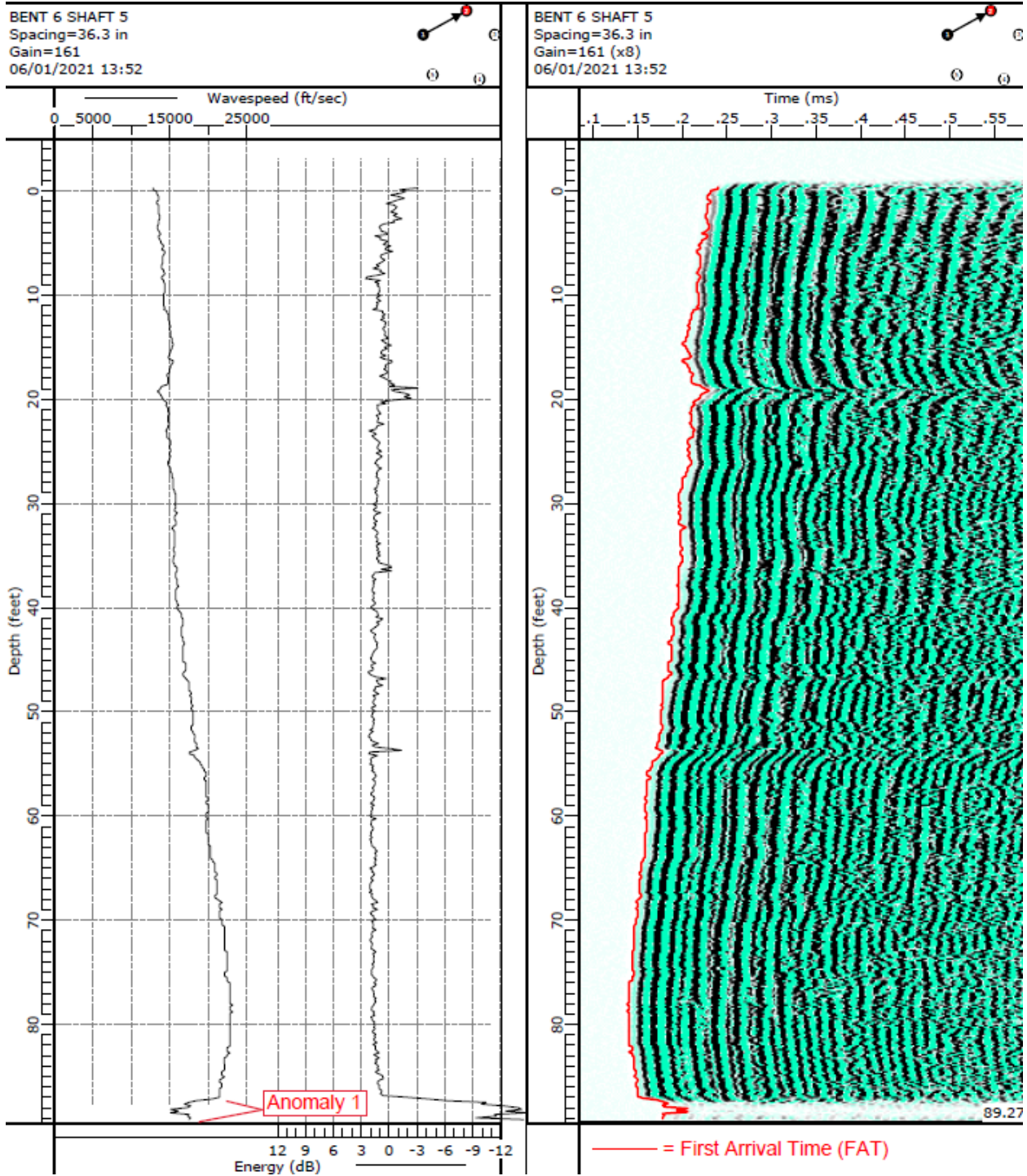


Figure 5-14: Example CSL result for Ramp F Bent 6 (Tube Pairing 1-2).

5.4 SONICaliper Results

Reports of the SONICaliper testing are presented in Appendix G. The results are summarized in the vertical profiles shown in Figure 5-15 for the Ewing Ave. shafts and Figure 5-16 for the Ramp F shafts. The horizontal lines in the figures represent depths at which the caliper device collected data. Within the

casing, only a few depths are necessary to calibrate the measurements. In the rock socket, measurements were collected every 1 ft.

Two important observations are evident from the SONICaliper results:

- Rock socket diameters are generally very close to the design diameters: 36 inches for Ewing Ave. shafts and 66 inches for Ramp F shafts. At Ramp F, the socket diameters are typically slightly under-sized, between 64.5 and 65.5 inches. This is consistent with the measured diameter of the core barrel, which was 64 inches, not including the protrusion of the cutting teeth at the bottom of the barrel. Perhaps the protrusion is sufficient to provide a full 66 inches of diameter when teeth are new, but not when teeth are worn.
- The casings for Ewing Ave. Shaft 3 and especially Ramp F Bent 6 are inclined from vertical. These are the two shafts for which soft bottom conditions were indicated by weighted tape soundings. The observation could be a coincidence; it is also possible that the casing inclination made achieving a proper seal into rock more difficult. Not achieving a proper seal could make soft bottom conditions more likely, although maintaining a positive head and proper cleanout should still be effective bulwarks against soft bottom conditions.

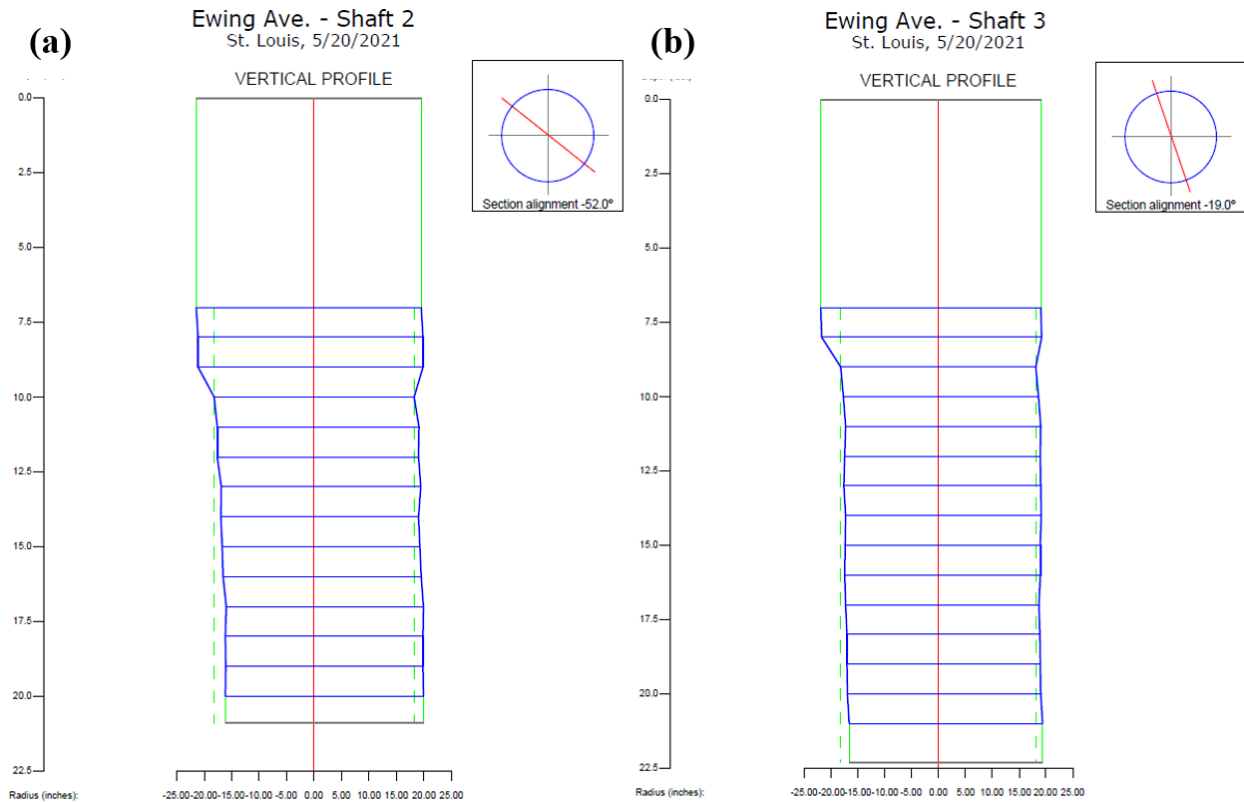


Figure 5-15: SONICaliper shaft profiles for Ewing Ave.: (a) Shaft 2 and (b) Shaft 3.

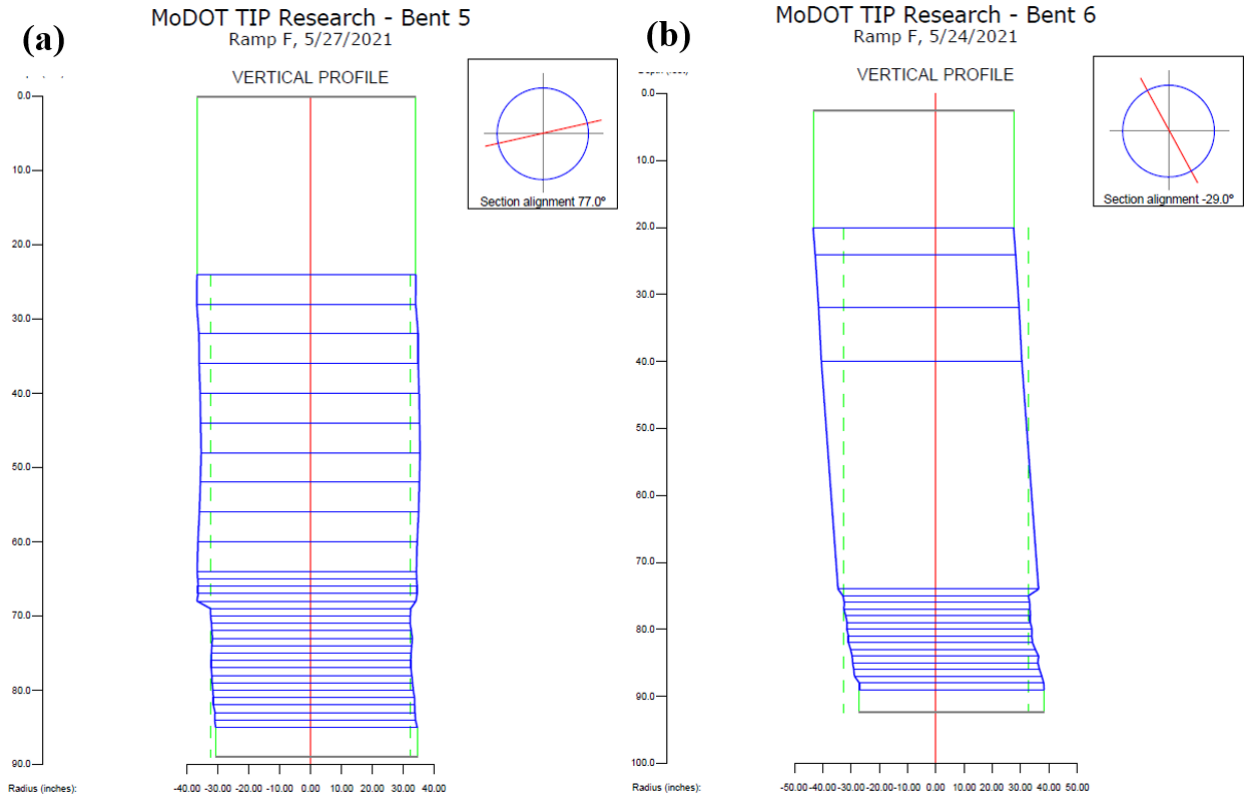


Figure 5-16: SONICaliper shaft profiles for Ramp F: (a) Bent 5 and (b) Bent 6.

6. Interpretation of Results

Results from Chapter 5 are synthesized in this chapter, which includes analysis of the data beyond the analysis methods typically considered in integrity analysis reports. Specifically, comparison of fiber optic and conventional TIP data, analysis of TIP time records at the bottom of the shafts, and analysis of shaft radius information are presented.

6.1 Comparison of Temperatures from Fiber Optic and Conventional TIP

As discussed in Section 5.2, the conventional TIP and fiber optic thermal profiles for the monitored shafts agreed closely in terms of both temperature magnitude as well as shape. To examine this more closely, plots of temperature versus depth for both conventional and fiber optic TIP for Ramp F Bent 6 are presented side-by-side in Figure 6-1. The figure includes six plots, one for each of the six temperature wire locations of Ramp F Bent 6. For each plot, three sets of results are shown, one for each of three times. The plot times represent a range of pertinent time steps for which both sets of data are available: 1.5 hours after pour, 6 hours prior to half peak, and the recorded peak (same data from Figure 5-13).

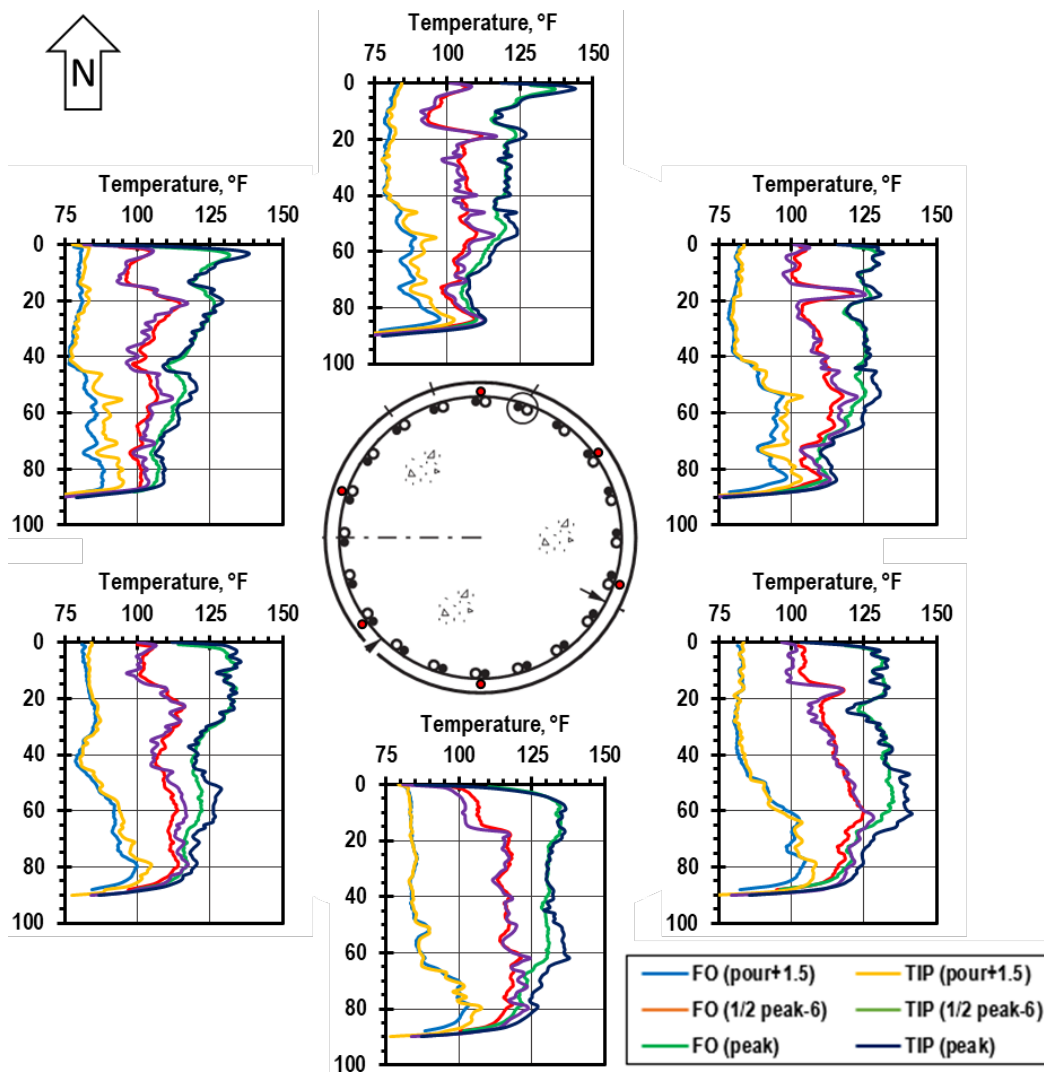


Figure 6-1: Fiber optic and conventional TIP thermal profiles at three times during curing of Ramp F Bent 6.

The measured temperature with depth between the two monitoring systems compares favorably, with an average difference of less than 2 °F. Some specific observations and about the comparison and trends observed are listed below.

- While the temperatures between the two systems agree closely in the upper 43 ft of the shaft, the conventional TIP readings are approximately 4 °F warmer than the fiber readings in the lower half across all verticals. This can be attributed to a change in the installed location of the TIP wires on the reinforcement cage from inside the cage below the splice (42'-8" below top of concrete), to outside the cage above the splice. The thermal fiber optic cables were installed on the exterior of the reinforcing cage for the entirety of the drilled shaft. Since the TIP wires below the splice were located closer to the center of the pile and farther from the perimeter, they registered a higher temperature than the FO thermal cables at the same depth.
- The large spike in temperature at 17 ft present in the north, northeast, and southeast wire locations is observed in both the conventional TIP and fiber optic thermal records with a similar maximum value and temperature gradient. This shows that while the spatial resolution constraints of the fiber optic system can have an effect on the readout of the system, large localized changes in temperature are still accurately detected and reported as compared to the conventional TIP results.
- The temperature variations with depth (within each plot) and across the pile (comparing between plots) were captured in both systems. It is therefore believed that the data can be used for interpretation interchangeably, with both systems providing a similar level of detail, accuracy, and fidelity in the thermal variations within the shaft.

6.2 Analysis of TIP Time Records at the Base of Shafts

Setting aside the top-of-concrete anomaly that was not confirmed by coring, the only imperfections suspected in the shafts were soft bottom conditions in Ewing Shaft 3 and Ramp F Bent 6. For both shafts, weighted tape soundings indicated sedimentation at the bottom of the shaft. The soundings indicated the sedimentation was thicker and more prevalent in the Ramp F Bent 6 shaft than in Ewing Shaft 3, for which sedimentation was primarily felt on the north side of the shaft. The weighted tape findings were supported by CSL results, which indicated anomalies classified as Class B according to the DFI (2018) criteria on the north side of Ewing Shaft 3 and anomalies classified as Class B or Class C across the bottom of the Ramp F Bent 6 shaft. As explained in Chapter 2, Class C are the most severe classification.

As presented in Section 5.1, the TIP temperature profiles versus depth do not necessarily lead one to conclude there may be soft bottom conditions at the base of Ewing Shaft 3 or Ramp F Bent 6. The temperature profiles at the bottom of the shaft are dominated by temperature rolloff associated with heat dissipation through the bottom of the shaft. However, results from Boeckmann and Loehr (2019) suggest evaluation of the TIP time records is potentially more effective for identifying anomalies than evaluating TIP depth profiles. To that end, the results of the field research documented in Chapters 4 and 5 are a useful dataset for testing the ability to identify soft bottom conditions from TIP time records: at both Ewing Ave. and Ramp F, we have two otherwise similar shafts, but one has soft bottom conditions and one does not.

To evaluate the time records for any evidence of soft bottom conditions, plots of temperature versus time were created for the bottom of each shaft using the conventional TIP records. The results are presented in Figure 6-2 for the Ewing Ave. shafts and in Figure 6-3 for the Ramp F shafts. At Ewing Ave., perhaps the most striking difference between Shaft 2 and Shaft 3 is that the variation in temperatures across the bottom of the shaft is considerably greater in Shaft 2. This observation likely is a result of greater cage or rock socket eccentricity in Shaft 2 than Shaft 3, and not a result of soft bottom conditions. However, the

average temperature at the bottom of Shaft 3 is notably less than that in Shaft 2, with maximum temperatures of about 82 °F at the bottom of Shaft 2 and 77 °F at the bottom of Shaft 3. While this is a relatively modest difference, the difference is likely a result of the sedimentation at the bottom of Shaft 3, since the shafts used the same concrete mix and concrete placement for both shafts occurred within an hour of one another. All things considered, however, evaluation of the record at the bottom of Shaft 3 in isolation would not be likely to lead an engineer to suspect soft bottom conditions.

The evidence of soft bottom conditions is stronger in the TIP time record at the bottom of the Ramp F Bent 6 shaft (Figure 6-3). The shape of the time record at the bottom of the Bent 6 shaft suggests a more gradual increase in temperatures compared to the results from other shafts. Whereas the Bent 5 shaft and both Ewing shafts show sharp increases in temperature shortly after concrete placement, the base of the Bent 6 shaft heated up more gradually, with flatter temperature curves, particularly on the north side of the shaft (Wires 1, 2, and 6). (Note for all shafts there is a tendency at the base of the shaft for the temperatures to increase when concrete is placed, then level off or decrease as heat from the fresh concrete escapes to the cooler ground, and then resume temperature increase once the full volume of shaft concrete hydrates.) In contrast to the result for Ewing Ave. Shaft 3, it is possible that an engineer reviewing the time record from the bottom of the Ramp F Bent 6 shaft could identify a potential imperfection based on the shape of the temperature profiles. This is an important finding that reinforces the recommendation by Boeckmann and Loehr (2019) to include consideration of time records in evaluation of TIP results.

One important caveat is that the results from the shafts in this research are somewhat rare in that the reinforcing cages were resting directly on the base of the shafts, rather than using bar boots, suspending the cage from a crane, or resting the cage atop the casing. Because the cage was directly on the base of the shaft, the TIP sensors were closer to the bottom of the shaft – perhaps even buried in sediment – than they would be in most circumstances. Of course, this applies to the CSL results, too: resting the cage on the base of the shaft also results in CSL tubes closer to the shaft bottom. All of that said, resting the cage on the bottom of the shaft promotes cage instability, misalignment, and eccentricity and is therefore generally discouraged, even considering potential integrity test benefits. Many agencies require the CSL pipes to extend within three to six inches of the base of the shaft; this range is considered appropriate based on past project experience. Note that due to the rigid nature of the CSL pipes, they can be extended beyond the termination of the longitudinal reinforcing steel in the event the drilled shaft is over excavated. Due to their non-rigid nature, TIP wires are not suitable for extension beyond the cage.

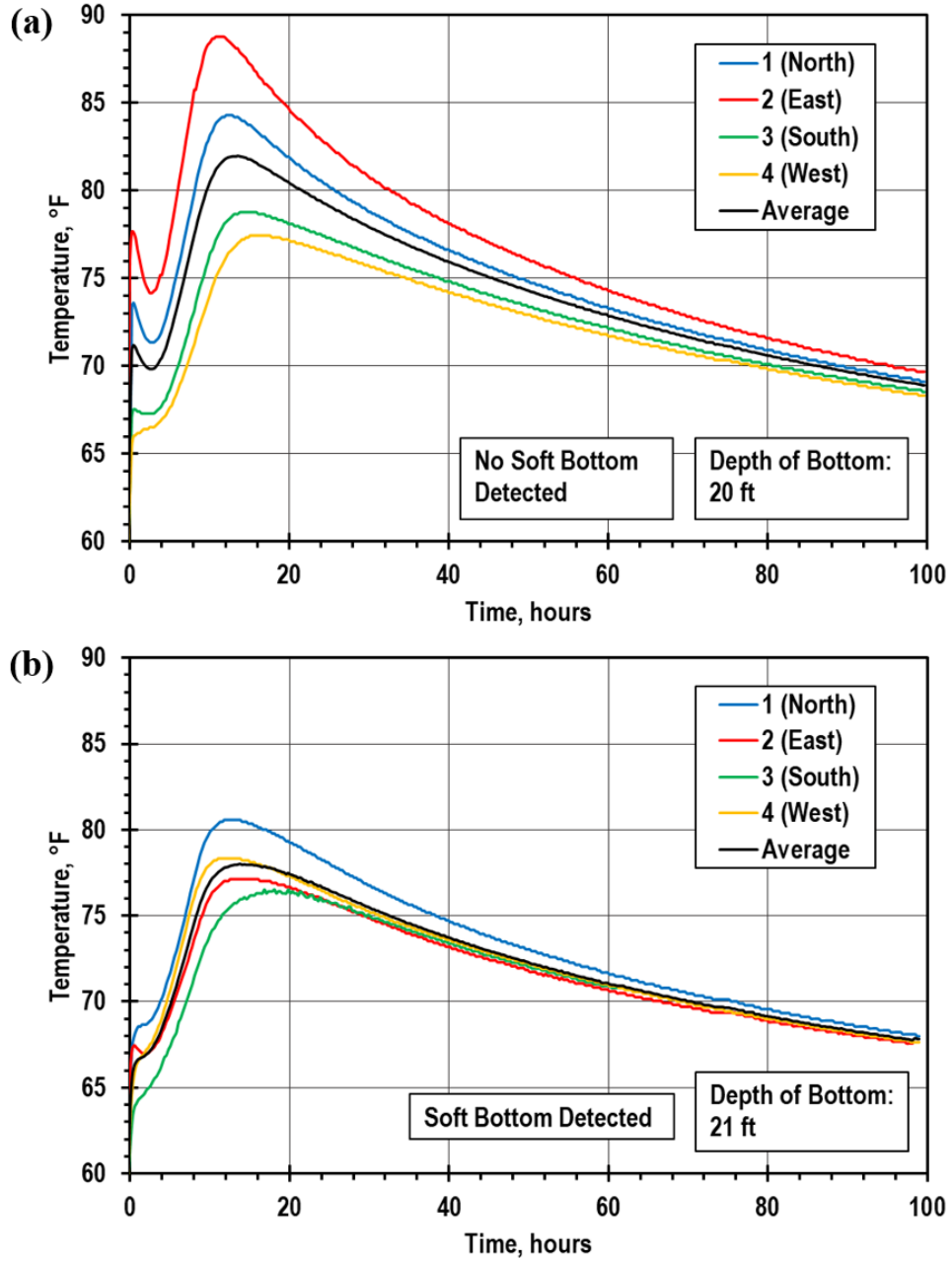


Figure 6-2: Temperature vs time at the bottom of shaft for Ewing Ave.: (a) Shaft 2 and (b) Shaft 3.

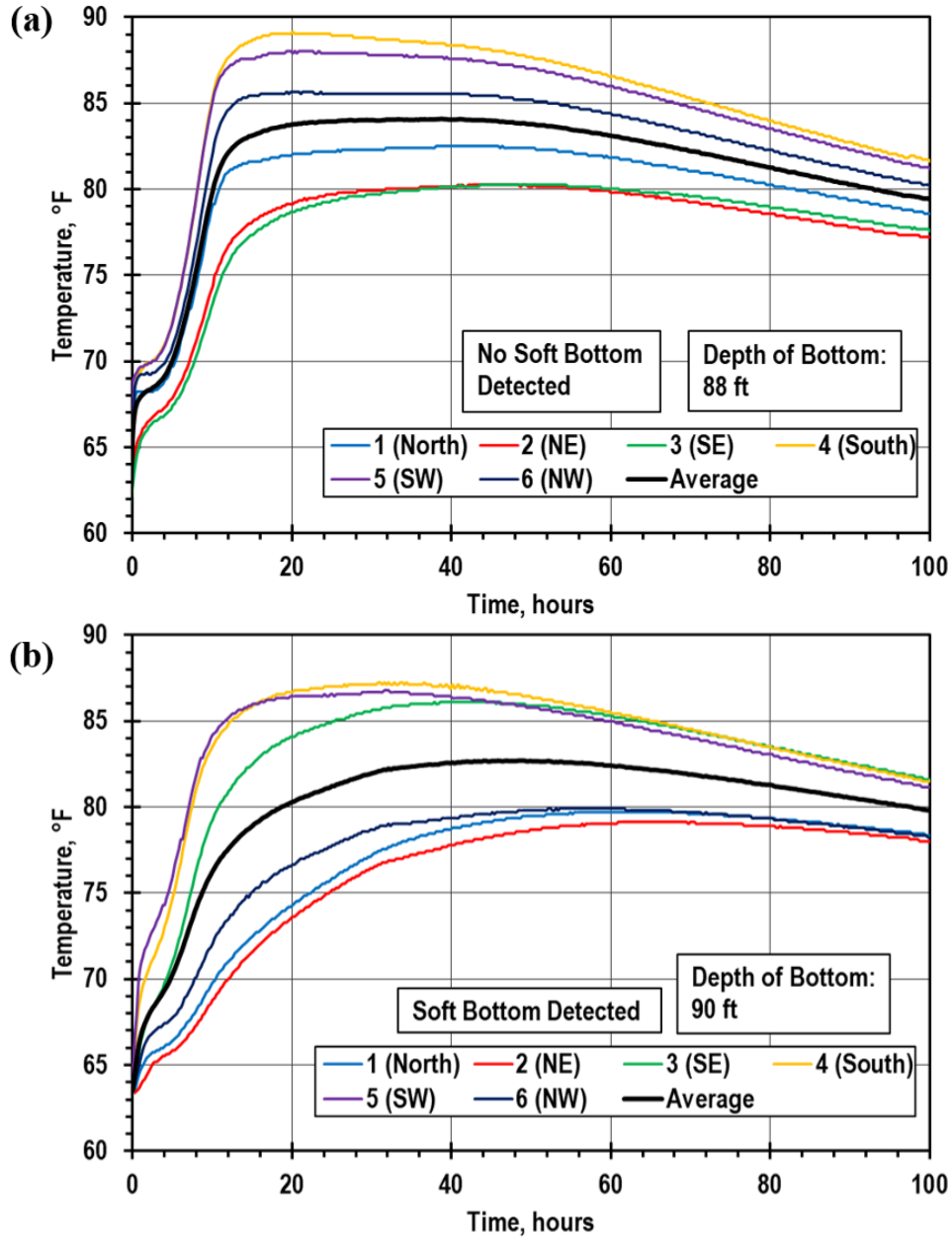


Figure 6-3: Temperature vs time at the bottom of shaft for Ramp F: (a) Bent 5 and (b) Bent 6.

6.3 Comparison of Radius Interpretations: Concrete Volume Log, TIP, and SONICaliper

It is useful to compare results of SONICaliper and TIP since both report results in terms of diameter (or radius). Diameter results from SONICaliper and diameter values from the TIP effective radius results are plotted versus depth in Figure 6-4 for the Ewing Ave. shafts and Figure 6-5 for the Ramp F shafts. The results are limited to the rock socket depths; the cased section of the shafts, where the diameter is known, is not included. For the Ewing Ave. shafts, the SONICaliper diameters are generally consistent with the design socket diameter: slightly oversized in the top portion and spot-on at the bottom. The TIP effective radius values are more variable, generally decreasing with depth, especially at the bottom of the sockets. For Shaft 3, the effective radius 1 ft above the bottom of the socket is 3 inches less than the design socket

diameter, which is an indication of the soft bottom conditions. For both Ewing shafts, the TIP Reporter software does not report an effective radius value at the very bottom of the socket.

At Ramp F, similar trends were observed, with the SONICaliper diameters generally consistent with depth and the TIP effective radius values more variable and generally decreasing with depth. As explained in Section 5.4, the SONICaliper results suggest the Ramp F sockets are slightly undersized. This is consistent with measured core barrel diameters, but not with the diameter interpreted from the concrete volume logs, which suggest the sockets were oversized. TIP effective radius values also suggest the sockets are oversized, but the effective radius interpretations depend on concrete volume inputs, so the oversized TIP effective radius values are to be expected. As for Ewing Ave., the Ramp F shaft with suspected soft bottom conditions (Bent 6) shows effective radius values less than the design diameter. Comparison of design, TIP effective radius, and SONICaliper diameter values for all four shafts serves as a reminder that TIP effective radius values are an evaluation tool and should not be interpreted as representative of the actual diameter.

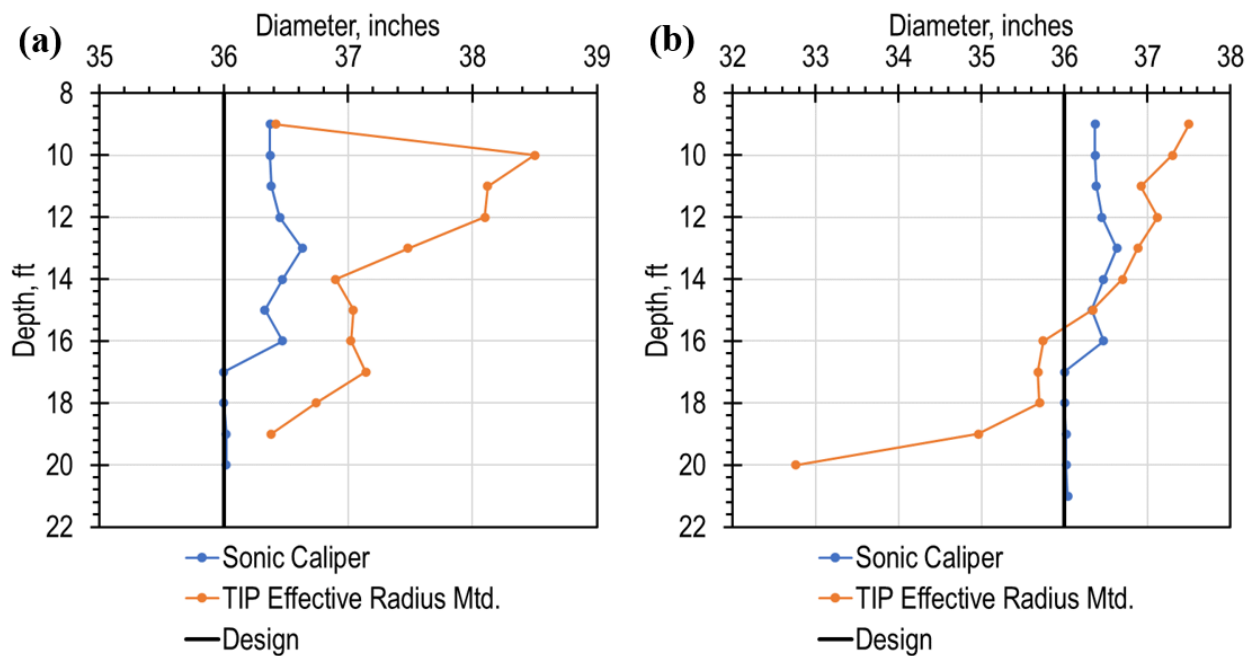


Figure 6-4: SONICaliper and TIP effective radius interpretations in Ewing Ave. rock sockets: (a) Shaft 2 and (b) Shaft 3.

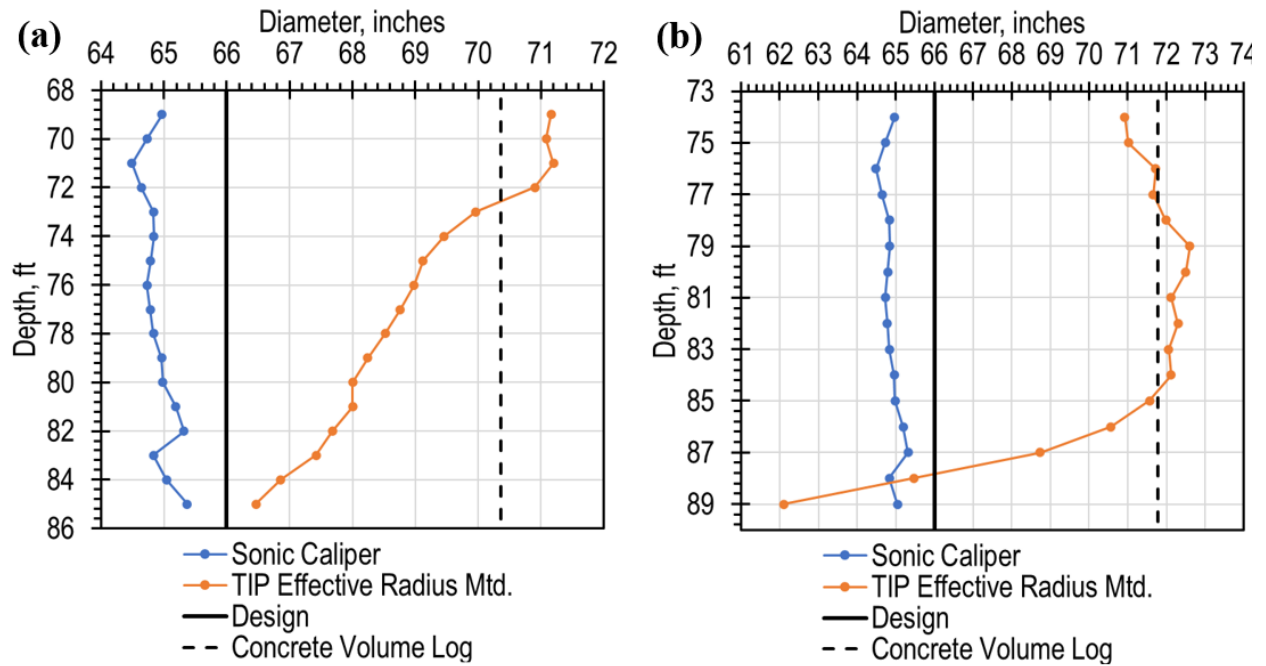


Figure 6-5: SONICaliper and TIP effective radius interpretations in Ramp F rock sockets: (a) Bent 5 and (b) Bent 6.

7. Summary, Conclusions & Recommendations

This chapter begins with a summary of important findings from the literature review, fiber optic lab study, and field research. After the summary, the most pertinent conclusions regarding the effectiveness of TIP and CSL test methods are presented before recommendations for implementing TIP methods are discussed. Additional recommendations regarding CSL are also provided.

7.1 Summary of Findings

This report has documented many significant results regarding TIP and CSL capabilities, limitations, and interpretation methods. The findings are summarized in the list below, which is organized by topic.

7.1.1 TIP and CSL Sensitivity to Defects based on Previous Research

- Schoen et al. (2018) performed TIP and CSL testing on a 5-ft diameter drilled shaft with two defects consisting of gravel bags attached to the inside of the reinforcing cage. For both defects, the bags represented 15% of the shaft cross section. TIP measurements 14 hours after concrete placement indicated temperature drops of 12 and 14° F due to the bags. TIP measurements at time of peak temperature of 34 hours indicated the effect of the gravel bags had diminished to between 3 and 8° F.
- Mullins et al. (2007) performed TIP testing on a 4-ft diameter drilled shaft with intentional defects consisting of sandbags outside the reinforcing cage. The defects represented about 10% of the shaft diameter. For one defect, the bags were on opposite sides of the reinforcing cage; for the other, the bags were all on one side of the cage. The effect of the sandbags was evident from temperature drops of perhaps 3 or 4° F, but difficult to interpret because of significant temperature variation among the access tubes. The timing of the TIP probe measurements is believed to have been close to the time of peak concrete temperatures.
- Ashlock and Fotouhi (2014) performed TIP and CSL testing on two 5-ft diameter drilled shafts with intentional defects. The TIP tests were completed by probe method. For the first shaft, cylinders of hardened but weak concrete were tied to the reinforcing cage. The cylinders represented only 3 to 4% of the shaft cross-section and did not produce any significant anomalies in TIP or CSL tests. For the second shaft, cylinders of aggregate and water representing 8% of the shaft cross-section were included. The TIP response was unclear because cage misalignment led to significant variations in temperature across the shaft, but it is possible to attribute an effect less than 5° F to the defects. CSL testing found a 25% increase in arrival times for the second shaft.
- Boeckmann and Loehr (2018) documented results of TIP testing for WisDOT's Zoo Interchange project outside Milwaukee. Drilled shaft concrete placement issues, primarily soft bottom conditions and tremie breaches, were experienced for the project. CSL detected imperfections at two tremie breaches and three soft bottoms; all five imperfections were confirmed by coring. TIP reports for the project did not recommend further action (e.g. coring) for any of the Zoo Interchange defects. Most of the imperfections were not identified from TIP results because of wire breakage, but a drop in temperature was observed for one of the tremie breaches. The TIP report for that shaft recommended "provisionally accepting" the shaft, contingent on the CSL report for the same shaft and noting adequate concrete cover based on the effective radius analysis.
- Boeckmann and Loehr (2018, 2019) installed ten intentional defects on two test drilled shafts and one control drilled shaft as part of a Wisconsin DOT research study. TIP and CSL were performed on all shafts. The results indicated the test methods are generally complementary, with TIP more effective for identifying weak concrete defects and defects outside the reinforcing cage and CSL more effective

for identifying soft bottom conditions and defects within the reinforcing cage. Boeckmann and Loehr concluded TIP is not effective for identifying soft bottom conditions.

- Boeckmann and Loehr also concluded the ability to detect defects with TIP is greatest at about the time temperatures are rising most quickly, which generally occurs between one third and one half the peak time. For three of four types of defects evaluated by Boeckmann and Loehr, temperature differences attributed to the defects diminished significantly after peaking at the time of maximum rate of temperature increase, in some cases to zero difference at the time of peak temperature.

7.1.2 TIP and CSL Sensitivity to Defects based on this Research

The most significant imperfections suspected in any of the drilled shafts evaluated for the field component of this study were soft bottom conditions detected based on weighted tape soundings of two of the four shafts: Ewing Shaft 3 and Ramp F Bent 6. This outcome – one shaft with and one without soft bottom conditions for each of the two bridge sites – is ideal for evaluating the detectability of soft bottom conditions.

- Contrary to the results of previous studies, including Boeckmann and Loehr (2018, 2019), soft bottom conditions were potentially identifiable in the TIP records from this field study. However, the potential for identification of the soft bottom conditions varies with the TIP interpretation method and possibly the level of expertise of the investigator. Strictly looking at the temperature-depth profile is unlikely to reveal the soft bottom conditions because the effect of the soft bottom is difficult to discern from roll-off. Evaluation of the effective radius profiles is more promising, with notable reductions in effective radius at the bottom of the affected shafts, especially Ramp F Bent 6, which had the more severe soft bottom conditions. However, the effective radius approach is sensitive to curve-fitting parameters and volume inputs. The soft bottom conditions are most evident from evaluation of the temperature versus time records for the bottommost TIP sensors, which revealed a more gradual increase in temperature for the shafts with soft bottom conditions. For Ewing Shaft 3, it is unlikely the gradual increase would be identifiable absent comparison with Ewing Shaft 2 (which had a clean bottom). For Ramp F Bent 6, the gradual response is sufficiently striking that it likely could be detected even without comparison with Ramp F Bent 5. Temperature-time records are not typically presented in TIP reports, but the latest version of PDI's TIP Reporter software includes an option to view the time records and include them in reports.
- The soft bottom conditions were identified as anomalies in the CSL reports. However, the CSL report evaluations are based solely on consideration of arrival time delays. Evaluation based on consideration of both arrival time delays and relative energy reductions (e.g. per DFI's 2018 recommendations) would have led to a more severe categorization of the anomaly.
- Simple weighted tape measurements prior to placement of the concrete confirmed the presence of soft sediment at the base of two of the drilled shafts. This method of inspection is the simplest and most effective way of investigating the potential for soft toe conditions. This activity also occurs at a time in the construction when this potential deficiency can be relatively easily addressed as opposed to discovering the soft to after the concrete is cast and curing.

An important caveat to identification of soft bottom conditions for both TIP and CSL is the need for measurements at or very near the bottom of the shaft. CSL results will not identify soft bottom conditions if the access tubes terminate above the affected zone. Similarly, the effect of soft bottom conditions for Ewing Shaft 3 and Ramp F Bent 6 were likely more evident because the bottommost TIP sensors were just above the base of the shaft and likely surrounded by sediment for Ramp F Bent 6.

Interestingly, the two shafts with soft bottom conditions are the two shafts for which SONICaliper data indicated more significant deviations from verticality in the casing installation. Lack of verticality could have resulted in greater difficulty achieving a proper seal of the permanent casing, which could make soft bottom conditions more likely.

In addition to the soft bottom conditions, TIP results suggest eccentricity of the reinforcing cage based on temperature differences from one side of the shaft to the other. Cage eccentricity would be expected considering the heavy reinforcing cages were supported on the bottom of the shaft (rather than hanging off of the casing or supporting with the crane), and considering relatively small rebar chairs were used as centralizers (rather than wheel centralizing devices).

7.1.3 Conventional TIP Procedures

- Reports of TIP wire breakages in practice are common (e.g. see discussion of Zoo Interchange project above), but improved wire design has significantly reduced the incidence of wire failures, according to users who routinely use TIP wires. None of the 20 wires installed for this project experienced any malfunctions, despite a relatively challenging installation for Ramp F shafts. A new wire design featuring epoxy-encapsulated sensors intended to further reduce the incidence of wire breakage is complete and should be released by PDI soon.
- As documented by Boeckmann and Loehr (2018), the effectiveness of probe measurements depends on the timing of the measurements with respect to the development of temperature differences due to defects. Such timing is very difficult to control. The wire method, in contrast, results in a time record of TIP measurements. The time record, itself, is useful for evaluating potential imperfections, as shown in Boeckmann and Loehr and further supported in the evaluation of soft bottom conditions for this research.

7.1.4 Fiber Optic TIP Methods

- Previous work originating out of the United Kingdom has demonstrated the potential for using distributed fiber optic sensing (DFOS) for performance of TIP methods in drilled shafts. The DFOS approach is an alternative to conventional TIP methods. An advantage of the DFOS is the ability to use the same system to measure mechanical strain as well as thermal strain. Measurement of mechanical strain is useful for load testing as well as long-term performance monitoring.
- The laboratory study demonstrated remarkably close agreement between temperatures measured by fiber optic methods and conventional TIP wires that were submerged in the same water bath.
- During the field study, measured temperature with depth between conventional and fiber optic TIP systems also compared favorably, with an average difference of less than 2 °F. While the conventional TIP system resulted in a continuous record of temperature versus time lasting more than one week, the fiber optic measurements were only recorded during times when testing personnel were on site to operate monitoring equipment.
- The spatial resolution of the fiber optic system limits the ability of the fiber optic TIP method to detect abrupt changes in temperature. For the system used in this research, the spatial resolution was 0.75 m (lab testing) and 1.00 m (field testing), or about 2.5 to 3.3 ft. While the readout distance for the fiber optic system was 0.65 to 1.3 ft, which is similar to the spacing of the conventional TIP sensors of 1 ft, each of the fiber optic readings is influenced by the larger spatial resolution centered upon the readout depth. The effect of this is typically a smoothing of the data, with highly localized spikes in temperature being affected by the surrounding temperatures. However, temperature spikes

of high enough magnitude can still be localized and detected using the fiber optic system, as demonstrated in the results comparison of Ramp F Bent 6.

- The installation of fiber optic thermal cables on the reinforcement cage is similar to the process of the installation of conventional TIP wire. If the fiber optic thermal cable is appropriately selected, it can match or exceed the robustness and resistance to breakage of TIP wire.
- Cable preparation and field repair of breakages requires a more specialized set of tools and skills than electrical connections for conventional field sensors (of note, the proprietary TIP wire design is also difficult or impossible to be repaired in the field).
- Monitoring of the fiber optic thermal cable during curing remains a challenge, relying on both a reliable, “clean” power supply (filtered through a high quality sine-wave inverter) as well as a secure monitoring location for the analyzer given its high value as compared to the TIP data logger. This challenge has been solved in the UK by deploying the fiber optic analyzer in a small CONEX or similar shipping container which can be left on site, unattended, for long periods of monitoring during curing. The range of most Brillouin fiber optic analyzers is in the tens of miles, allowing a single analyzer to simultaneously monitor a number of networked series of piles.

7.1.5 Cost

Published cost data and cost data from the field component of this work suggest the cost of implementing TIP methods may be less than the cost of implementing CSL methods. The cost of TIP wire, generally \$5/ft, is similar to the cost of steel tubes for CSL. However, TIP data is generally collected remotely via datalogging equipment that is simple to install and can generally be managed by personnel already on site. CSL data is generally collected by technicians or engineers, who often incur travel expenses. Requirements to grout CSL tubes also results in greater costs for CSL tests.

7.2 Conclusions

This report has presented evaluations of the effectiveness of TIP and CSL concrete integrity test methods using the results of previous research, documented TIP project experience, and new original research involving testing of four production drilled shafts. Significant conclusions resulting from this effort include:

- TIP is a viable concrete integrity test method. TIP methods have been shown to effectively respond to many types of defects. The test has limitations, but so does every concrete integrity test method.
- Soft bottom conditions are difficult but not impossible to identify using TIP results. Together, results of this study and previous work indicate the detectability of soft bottom conditions with TIP depends on the severity of the imperfection, the proximity of the bottom TIP sensors to the base of the shaft, the method of data interpretation, and the expertise of the investigator. This research indicates relatively severe soft bottom conditions are detectable when sensors are at or just above the base of the shaft and the temperature versus time records are evaluated.
- TIP and CSL are complementary test methods. Neither test provides a perfectly reliable assessment of drilled shaft integrity, but combined, they can be used to detect most conceivable defects. The complementary nature of the two tests is reflected in Table 7-1, which characterizes the ability to detect various types of defects for each test method. The table is an update of Table 2-4, which was originally reported in Boeckmann and Loehr (2018, 2019). The table was revised

to identify soft bottom conditions as potentially detectable for TIP rather than not detectable based on the preceding bullet point.

Table 7-1: Summary of the ability to detect various types of relatively modest defects for TIP and CSL. Modified from Boeckmann and Loehr (2018).

Defect Type	TIP¹	CSL¹
Inclusions in cage interior	Difficult to detect	Readily detectable
Defects outside reinforcing cage	Readily detectable	Not detectable
Soft bottom	Potentially detectable	Readily detectable
Weak concrete	Readily detectable	Difficult to detect
Breach of tremie pipe	Potentially detectable	Readily detectable

¹*Detection ability assessments are generally based on relatively small defects. Detection ability assessments would likely be greater for more significant defects.*

- Evaluation of the TIP time record (temperature plotted versus time for a given depth or set of depths) is important for two reasons. First, temperature differences associated with imperfections vary with time and may not be identifiable at a single point in time. This is especially true if only the peak temperature profile is considered; previous research has shown responses associated with imperfections are greatest between one third and one half of the time to peak. Second, the temperature-versus-time plot associated with various imperfections typically has a shape that is readily distinguishable from sound concrete. These findings were first reported by Boeckmann and Loehr (2018, 2019). The results of this study reinforce their importance as well as their potential application for the identification of soft bottom conditions.
- Evaluation of relative energy for CSL test results can be used to identify defects that are not apparent in CSL arrival time results for the same shaft. This finding was concluded in Boeckmann and Loehr and is supported by evaluation of the soft bottom CSL anomalies in this research.
- Fiber optic thermal monitoring produces comparable temperature profiles as conventional TIP systems. While the material costs for thermal fiber optic cable are generally less than TIP wire, the expense of the system lies with the rental or purchase of the fiber optic analyzer. The benefit of distributed fiber optics is that it can be deployed for strain monitoring as well (with the installation of fiber optic strain cable within the pile), allowing the use of a single monitoring system for temperature monitoring during curing as well as strain monitoring during load testing, construction, or operation of the structure.
- Use of TIP methods for drilled shaft integrity testing may result in cost savings compared to CSL methods. The cost savings are primarily a result of collecting data via remote datalogging equipment for TIP and requirements to fill CSL tubes with grout after testing.

Based on the new conclusions regarding the potential to detect soft bottom conditions using TIP methods, the table of advantages and limitations from Chapter 1 has been revised, as shown in Table 7-2. The updated table notes soft bottom conditions are potentially identifiable, whereas the previous version listed inability to detect soft bottom conditions as a limitation of TIP methods.

Table 7-2: Significant advantages and limitations of TIP and CSL methods. Modified from Boeckmann and Loehr (2018).

	Advantages	Limitations
TIP	<ul style="list-style-type: none"> • Can identify defects outside the reinforcing cage. • In addition to identifying defects, data can be used to indicate misalignment of reinforcing cage. • Significant soft bottom conditions are potentially identifiable, especially if time records are considered. • Tests can generally be performed within a day after concrete placement, resulting in potential construction schedule advantages. • Temperature information may provide additional value for large-diameter shafts subject to mass concrete considerations. 	<ul style="list-style-type: none"> • Ability to detect defects in the center of the shaft may be limited. • Challenges interpreting test data: <ul style="list-style-type: none"> ○ Distinguishing defects from nuisance effects. ○ Acceptance criteria are not well established. • Test window closes within days of concrete placement; optimal test time varies with diameter and shaft boundary conditions. This limitation does not apply to the wire method, which is the predominant method for TIP testing.
CSL	<ul style="list-style-type: none"> • Relatively long history of experience. • Reliably identifies concrete defects within central core of shafts, including soft bottom conditions. • Relatively simple interpretation with well-established evaluation criteria. 	<ul style="list-style-type: none"> • No information outside reinforcing cage: <ul style="list-style-type: none"> ○ Cannot identify defects outside of cage. ○ No indication of cage misalignment. • Relatively frequent “false positives,” particularly due to debonding of concrete from access tubes. • Must wait at least three days to perform test, potentially impacting overall construction schedule.

7.3 Recommendations for Integrity Testing

It follows from the conclusions that TIP methods should be an allowable concrete integrity test method, either as an alternative to or in conjunction with CSL methods. Practical implementation of TIP for routine use requires important, agency-wide decisions regarding appropriate implementation approaches for TIP, procedures for TIP testing and interpretation, and acceptance criteria for TIP measurements. Recommendations for each topic are included in the following sections.

The recommendations in this section form the basis for the proposed TIP specification included as Appendix H. The proposed TIP specification begins with language referencing the ASTM standard, which provides a basis for most of the procedural aspects of TIP test methods. The rest of the proposed TIP specification addresses specific test procedures and interpretation and reporting requirements that follow from the recommendations presented below. The specification is focused on a project-level application of TIP methods. The specification does not address use of TIP versus use of CSL, although recommendations regarding this issue are included in Section 7.3.1.

It is important to recognize and appreciate that drilled shaft integrity testing is not the sole quality assurance measure for drilled shafts. Quality assurance for drilled shafts is also derived from agency requirements and evaluations related to design (e.g. reinforcement restrictions, concrete mix characteristics), shaft construction methods (e.g. methods for maintaining hole stability, slurry control requirements, concrete placement requirements), and controls on characteristics of fresh concrete (e.g. trial batching procedures, workability constraints and measurements). It is important and appropriate to

explicitly consider these requirements collectively to avoid requiring excessive quality assurance that can unnecessarily increase costs and risks associated with drilled shaft construction. In this context, drilled shaft integrity testing is one of several measures for assuring quality for drilled shafts.

Finally, it is also important to emphasize the need for attentive and knowledgeable observation and documentation of drilled shaft construction. Complete and accurate records of drilling, bottom of shaft conditions, and concrete placement are necessary for evaluation and acceptance of drilled shaft construction, not to mention for agency records. In addition, the construction records are critical for understanding and interpreting integrity test results, particularly TIP results. The practices recommended in FHWA's Drilled Shaft Manual (Brown et al., 2018) result in proper documentation.

7.3.1 Potential Approaches to Implementing TIP

There are numerous potential approaches for implementing TIP methods agency-wide. Three specific recommendations below are appropriate considering the conclusions of this research:

1. Both TIP and CSL should be considered allowable concrete integrity test methods.
2. The decision regarding which test method to use for production shafts should be made by the Engineer of Record. The decision should identify which test method will more effectively reduce risks associated with construction defects and should therefore consider project-specific characteristics such as the likelihood of various types of defects, reserve capacity of the design with respect to both lateral and axial loading, and the reliance on base resistance. For example, CSL is probably more appropriate for shafts with design that relies on considerable base resistance or shafts in geologic conditions where base cleanliness has been problematic. In contrast, TIP is probably more appropriate shafts where defects outside the reinforcing cage are more likely or where lateral reserve capacity is limited.
3. In some circumstances, it may be beneficial to perform both TIP and CSL:
 - a. For method/technique shafts, to help identify systematic issues with construction and concrete placement so that techniques for production shafts can be adapted to project-specific conditions and challenges.
 - b. For critical drilled shafts (e.g. non-redundant shafts, shafts supporting major river crossings).
 - c. For drilled shafts where interpretation of integrity test results may be challenging. For instance, many drilled shaft concrete mixes are prone to producing considerable bleed water, generally as an unintended consequence of satisfying workability requirements. For long shafts permanently cased to the top of the rock socket, the bleed water often results in false positive CSL anomalies near the top of the shaft. Including TIP wires for these shafts could help demonstrate the CSL anomalies are false positives, reducing costs and schedule delays associated with coring.

However, if both TIP and CSL are performed on production shafts, care must be exercised in the test evaluation. In many cases, it is more appropriate to use one test to demonstrate that anomalies from the other test are false positives, rather than treating all anomalies from both tests as assumed defects. In all cases, the evaluation of integrity test results should be based on consideration of thorough construction records. For instance, if both CSL and TIP are specified for a permanently cased, large diameter drilled shaft that *may* be prone to bleed, the CSL results should be the primary test method for acceptance of the shaft. The TIP data would be collected and evaluated to augment the CSL results, not to provide a means for acceptance or rejection by itself.

These recommendations are consistent with the conclusion that TIP and CSL are generally complementary in terms of their detection abilities.

7.3.2 TIP Test Procedures and Use of Probe

TIP testing should be performed using sacrificial wires, with data collection beginning just before the time of concrete placement and continuing until at least 24 hours after the peak temperature has been observed. The continuous record of concrete temperatures facilitates the most effective detection of concrete defects because the maximum temperature deviation can be computed by evaluating results throughout the test period. In addition, evaluation of trends in the time record may clarify interpretation of TIP results. These abilities are lost with the probe method, which should not be allowed. In addition, TIP procedures using the wires are simpler to specify and execute.

Although reports of TIP wire breakage are common, wire design has improved recently, and wire breakage should be a rare occurrence when wires are installed by qualified and conscientious personnel. It may be beneficial to add provisions that disincentivize wire breakage to the specifications proposed in Appendix H.

For each wire, the bottommost TIP sensor should be just above the bottom of the longitudinal reinforcing bar it is affixed to. Reinforcing cages should be suspended with the bottom of the cage within 3 inches of the base of the shaft, consistent with the detail of MoDOT EPG 751.37.1.6. If the shaft or rock socket is drilled beyond its design length, the reinforcing cage should be extended accordingly. Alternatively, reinforcing cages can rest on the base of the shafts if appropriate protection is included for the longitudinal bars (i.e. “bar boots”).

7.3.3 TIP Test Interpretation

Interpretation is perhaps the most challenging component of TIP testing. Several recommendations regarding interpretation techniques follow from the results of previous research and this study. The recommended evaluation practice represents an “all of the above” approach wherein temperature versus depth, effective radius, and temperature versus time are all considered:

1. Records of construction, including drilling records, bottom-of-shaft inspection forms, and concrete volume logs should be reviewed to identify potential zones with imperfections (e.g. depths of a tremie breach, potential soft bottom conditions, etc.). If he or she was not on site for construction, the engineer reviewing the TIP results should also discuss the installation with on-site inspection personnel.
2. Temperature versus depth, effective radius versus depth, and results of any other concrete integrity tests should be reviewed to identify potential zones with imperfections (e.g. depths with abrupt temperature changes).
 - Effective radius results can be used to evaluate TIP results but should not be used to infer concrete cover or otherwise determine the precise shape of the shaft.
 - The engineer should attempt to identify causes of suspect TIP results (e.g. abrupt temperature changes) by considering shaft construction records, geologic information, surface water, and groundwater information.
3. Temperature versus time plots should be evaluated for any depths of suspected imperfections identified during Steps 1 and 2. The plots should include records for the depth of the suspected imperfection as well as a nearby depth that appears to be uninfluenced by the potential imperfection (i.e. the baseline measurement).

7.3.4 Acceptance Criteria

The final component of a TIP specification is acceptance criteria, which assign standards for evaluating the interpreted test results. The recommended approach emphasizes engineering judgment rather than applying rigid quantitative criteria, e.g. flagging temperature differences less than X °F or effective radius decreases greater than Y% as anomalies. While a quantitative approach is appealing for uniform implementation, the quantitative approach is generally inappropriate for widespread implementation because of the variability of TIP outcomes. Drilled shaft concrete temperatures vary considerably from one project to the next depending on many factors, primarily diameter and placement temperature. Effective radius results reduce variability but are the result of an interpretation procedure that is partly subjective. For instance, the bottom of shaft rolloff adjustments are critical for effective radius interpretations, but recommendations for the approach are not well documented, particularly when it comes to scale factor calibrations and particularly within the TIP software. Moreover, the specific criteria approach encourages a concrete integrity test report culture that often does not include critical evaluation of test results. In the absence of critical evaluation, it is feasible that potential defects could go unrecognized, especially if the potential defect is not flagged by the specific criterion. For these reasons, an approach emphasizing engineering judgment is recommended.

The recommended approach for acceptance criteria within the TIP specifications is to include open-ended language that relies on the professional judgement of the TIP engineer to flag potential defects. As noted in Table 2-2, this approach was adopted by Florida DOT (2018) and is included in the PDI sample specifications (2017). Both the FDOT and PDI specifications require TIP reports to indicate the presence of any significant temperature deviations, but no definition is provided for what qualifies as a significant deviation. If the engineering judgment approach is adopted, any significant temperature deviations would be identified in a TIP report, and the significant deviations would trigger evaluation by the Engineer of Record for the shaft. The Engineer of Record would deem the deviations as either permissible or requiring further investigation (e.g. by coring or other means).

Review of a substantial volume of TIP project records and TIP literature leads to a primary conclusion that temperature development in drilled shaft concrete is complicated, and temperature differences due to imperfections are rather variable. The degree of complication is perhaps so great that any quantitative approach to TIP acceptance criteria would result in a significant number of inappropriate red flags for some projects and missed defects for others. Moreover, there would be benefits to the judgement approach: avoiding rigid criteria would place the responsibility for interpretation and evaluation of TIP data squarely on TIP professionals, which should promote a greater degree of thoughtfulness in TIP analyses. Such thoughtfulness is frequently missing in concrete integrity reports. In fact, concrete integrity reports for a variety of test methods are sometimes generated by algorithm, a disconcerting practice that is at least compatible with rigid acceptance criteria, if not a direct result of such criteria.

The engineering judgment approach is not without downsides. Not establishing specific criteria could result in a lack of consistency from one project to the next. In addition, while the emphasis of judgment could be beneficial for encouraging more thoughtful evaluations, the approach also places significant responsibility on the TIP engineer, who frequently are contracted to the construction contractor. These tradeoffs are inherent to drilled shaft integrity testing.

7.3.5 Fiber Optic TIP

Thermal monitoring using distributed fiber optic systems is a viable alternative method for measuring temperature profiles during shaft curing. The temperature results are nearly equivalent to those generated by conventional TIP and can be interpreted using the same evaluation approaches. The challenges to the deployment of DFOS for thermal monitoring is the limited number of contractors currently offering fiber

optic monitoring (including none in Missouri), the specialized tools and skill set required for preparation and repair of fiber optic cables, and the high value of the fiber optic analyzer and the associated requirements for safety and protection during monitoring on site. If TIP is being incorporated as a standard integrity testing method over a wide number of projects within an owner's portfolio, the initial investment in adopting a fiber optic monitoring system for deployment can be spread over multiple projects with the added benefit of providing the opportunity for strain monitoring over the lifetime of the structure. If the challenge of deployment and protection of the analyzer is solved (for example, using a secure container or trailer that can be deployed to job sites), fiber optic thermal monitoring can be a comparable alternative to conventional TIP wire systems. Fiber optic TIP is also more practical for high-profile demonstration shafts with load testing, where the fiber optic cable can be used in lieu of strain gages.

An additional complication is the challenge of collecting a continuous time record of temperatures with the fiber optic system. The results of this and previous research emphasize the importance of evaluating TIP results versus time in order to effectively identify potential imperfections. Because the fiber optic system requires personnel presence during monitoring, collecting a continuous time record with the fiber optic system is logistically challenging and likely costly.

7.3.6 CSL Recommendations

CSL test reports should include interpretations based on relative energy, not just arrival time. Interpretations that consider both measures will likely result in better identification of imperfections. The approach recommended in the Deep Foundations Institute's "Terminology and Evaluation Criteria of Crosshole Sonic Logging (CSL) as applied to Deep Foundations" white paper (2018) is one rational approach for evaluating CSL results considering both arrival time and relative energy.

References

- Ashlock, J.C. and M.K. Fotouhi (2014), “Thermal Integrity Profiling and Crosshole Sonic Logging of Drilled Shafts with Artificial Defects,” *Geo-Congress 2014 Technical Papers*, GSP 234, American Society of Civil Engineers, pp. 1795-1805.
- ASTM Standard C39 (2018), “Standard Test Method for Compressive Strength of Cylindrical Concrete Specimens,” ASTM International, West Conshohocken, PA, 2018, DOI: 10.1520/C0039_C0039M-18, www.astm.org.
- ASTM Standard C143 (2015), “Standard Test Method for Slump of Hydraulic-Cement Concrete,” ASTM International, West Conshohocken, PA, 2015, DOI: 10.1520/C0143_C0143M-15A, www.astm.org.
- ASTM Standard D6760 (2016), “Standard Test Method for Integrity Testing of Concrete Deep Foundations by Ultrasonic Crosshole Testing,” ASTM International, West Conshohocken, PA, 2014, DOI: 10.1520/D6760M-16, www.astm.org.
- ASTM Standard D7949 (2014), “Standard Test Methods for Thermal Integrity Profiling of Concrete Deep Foundations,” ASTM International, West Conshohocken, PA, 2014, DOI: 10.1520/D7949-14, www.astm.org.
- Boeckmann, A.Z. and J.E. Loehr (2015), *Concrete Mass Pours for Deep Foundations – Synthesis Report*, Final Phase I Report to Federal Highway Administration, 81 p.
- Boeckmann, A.Z. and J.E. Loehr (2018), *Thermal Integrity Profiling for Detecting Flaws in Drilled Shafts*, Final Report, Wisconsin Department of Transportation, WisDOT ID no. 0092-16-07, 113 p.
- Boeckmann, A.Z. and J.E. Loehr (2019), “Evaluation of Thermal Integrity Profiling and Crosshole Sonic Logging for Drilled Shafts with Concrete Defects,” *Transportation Research Record*, Vol. 2673, No. 8, pp. 86-98.
- Brown, D.A., A. Boeckmann, J. Turner, J.E. Loehr, and R. Thompson (anticipated 2022), *Acceptance Procedures for Deep Foundations of Transportation Structures*, Federal Highway Administration GEC No. 15.
- Brown, D.A., J.P. Turner, R.J. Castelli, and J.E. Loehr (2018), *Drilled Shafts: Construction Procedures and LRFD Design Methods*, Federal Highway Administration GEC No. 10, FHWA-NHI-18-024, 756 pp.
- de Battista, N., K. Kechavarzi, and K. Soga (2016), “Distributed fiber optic sensors for monitoring reinforced concrete piles using Brillouin scattering,” *Proc. SPIE 9916*, Sixth European Workshop on Optical Fibre Sensors, 99160U, 30 May 2016, DOI: 10.1117/12.2236633
- Deep Foundations Institute (2018), “Terminology and Evaluation Criteria of Crosshole Sonic Logging (CSL) as applied to Deep Foundations.”
- Deng, W., R. Zhong, and H. Ma (2021) “Fiber Optic-Based Thermal Integrity Profiling of Drilled Shaft: Inverse Modeling for Spiral Fiber Deployment Strategy,” *Materials*, 14(18), 5377, DOI: 10.3390/ma14185377
- Fisher, A. N., and A. G. Bell (2017), “The Application of Fibre Optic Sensor Technology in the Integrity Testing of Deep Foundations,” *Proc. of the 2018 DFI-EFFC International Conference on Deep Foundations and Ground Improvement*, Rome, Italy.
- Florida Department of Transportation (2022), *Standard Specifications for Road and Bridge Construction*, January 2022 eBook.

- GRL Engineers (2015), “Sample Specification for Crosshole Sonic Logging (CSL),” September 2015, accessible via <http://www.grlengineers.com/specifications/>
- Hyatt, T., D. Belardo, R. Melker, and J. Webster (2019), “Cost and Technical Comparison of Non-Destructive Test Methods for Drilled Shafts,” Proceedings of the 44th Annual Conference on Deep Foundations: Chicago, IL, Deep Foundations Institute, 11 p.
- Likins, G. and G. Mullins (2011), “Structural integrity of drilled shaft foundations by thermal measurements,” *Structural Engineering*, p. 46-48.
- Johnson, K.R. (2014), “Temperature Prediction Modeling and Thermal Integrity Profiling of Drilled Shafts,” *Geo-Congress 2014 Technical Papers*, GSP 234, American Society of Civil Engineers, pp. 1781-1794.
- Johnson, K.R. (2016), “Analyzing thermal integrity profiling data for drilled shaft evaluation,” *DFI Journal – The Journal of the Deep Foundations Institute*, Vol. 10, No. 1, pp. 25-33, DOI: 10.1080/19375247.2016.1169361
- Klar, A., P. J. Bennett, K. Soga, R. J. Mair, P. Tester, R. Fernie, H. D. St John, and G. Torp-Peterson (2006), “Distributed strain measurement for pile foundations,” *ICE Proceedings Geotechnical Engineering*, Vol. 159, Issue 3, July 2006, pp. 135-144, DOI: 10.1680/geng.2006.159.3.135
- Mullins, G. (2010), “Thermal integrity profiling of drilled shafts,” *DFI Journal – The Journal of the Deep Foundations Institute*, Vol. 4, No. 2, pp. 54-64, DOI: 10.1179/dfi.2010.010
- Mullins, G. (2013) “Advancements in drilled shaft construction, design, and quality assurance: the value of research” *International Journal of Pavement Research and Technology*, Vol. 6, No. 2, pp. 93–99, doi:106136/ijprt.org.tw/2013.6(2).93
- Mullins, G., K. Johnson, and D. Winters (2007), *Thermal Integrity Testing of Drilled Shafts*, Final Report Prepared for Florida Department of Transportation, 214 p.
- Mullins, G. and D. Winters (2011), *Infrared Thermal Integrity Testing Quality Assurance Test Method to Detect Drilled Shaft Defects*, Final Report Washington State DOT, WA-RD 770.1, 176 p.
- Mullins, G., D. Winters, and K. Johnson (2009), *Attenuating Mass Concrete Effects in Drilled Shafts*, Final Report to Florida DOT, Report No. BD-544-39.
- Ouyang, Y., A. Bell, M. Elshafie, C. Kechavarzi, R. Fernie, and R. Mair (2015), “The history of UK experience in the use of fibre optic monitoring of geotechnically associated installations” *Geotechnical Engineering for Infrastructure and Development*, January 2015, pp. 637-642.
- Pile Dynamics, Inc. (2017), “Sample Specification for Testing Foundations with the Thermal Integrity Profiler (TIP),” October 2017, accessible via <http://www.grlengineers.com/specifications/>
- Piscsalko, G., G. Likins, and G. Mullins (2016), “Drilled Shaft Acceptance Criteria Based Upon Thermal Integrity Profiling,” Proceedings of the 41st Annual Conference on Deep Foundations: New York, NY, Deep Foundations Institute, 10 p.
- Rui, Y., C. Kechavarzi, F. O’Leary, C. Barker, D. Nicholson, and K. Soga (2017), “Integrity Testing of Pile Cover Using Distributed Fibre Optic Sensing”, *Sensors* 2017, no. 12: 2949, DOI: 10.3390/s17122949
- Schoen, D.L., G.J. Canivan, and W.M. Camp III (2018), “Evaluation of Thermal Integrity Profiling (TIP) Methods—Probe, Embedded Wire, and Wire Suspended in CSL Tubes,” Proceedings of IFCEE 2018, ASCE GSP 294, pp. 550-560.

Soga, K. (2014), "Understanding the Real Performance of Geotechnical Structures Using an Innovative Fibre Optic Distributed Strain Measurement Technology," *Rivista Italiana de Geotechnica*, April 2014, Vol. 4, 42.

Washington State Department of Transportation (2022), Standard Specifications for Road, Bridge, and Municipal Construction 2022, M 41-10.

Zhong, R. and W. Deng (2020) "Influence of Aggregates in Concrete on Fiber-Optic Based Thermal Integrity Profiling Analysis of Concrete Structures," *Front. Matter.* 7:227, DOI: 10.3389/fmats.2020.00227

Appendix A – Construction Plans for Ewing Ave. Bridge (A8851)

Appendix B – Construction Plans for Ramp F Bridge (A8854)

Appendix C – As-built Drawings for Drilled Shafts with TIP

Appendix D – Concrete Placement Logs

Appendix E – Conventional TIP Reports from PDI TIP Reporter Software

Appendix F – Crosshole Sonic Logging Test Reports

Appendix G – SONICaliper Test Reports

Appendix H – Proposed Specification Language

The proposed TIP specification language below is based on the recommendations presented in Chapter 7. The proposed specification is likely best implemented as a subsection of 701.4.17 Integrity Testing or as a project special provision.

1. General

Performance of Thermal Integrity Profiling (TIP) test methods shall conform to ASTM D7949, Method B. In the event of any conflict between this specification and ASTM D7949, this specification shall control over ASTM D7949.

The TIP probe method (Method A of ASTM D7949) shall not be used, except as a supplemental test when crosshole sonic logging (CSL) is the primary concrete integrity test method. When the probe method is used as a supplemental test to CSL test methods, the probe method test shall be performed according to ASTM D7949, Method A. When the probe method is used, temperature measurements shall be collected twice, once at half the anticipated peak time and once at the anticipated peak time.

The TIP testing organization is the party responsible for overseeing performance of the TIP test methods and for preparing the final TIP report. The testing organization shall have documented prior experience with TIP testing by the wire method on at least five deep foundations projects. Final TIP reports produced by the TIP testing organization shall be prepared and sealed by a professional engineer licensed in the state of Missouri.

Peak temperature is defined as the maximum temperature at any depth for the average temperature profile (i.e. the profile defined by averaging results from each of the wires).

2. TIP Wires and Wire Placement

Each TIP wire shall consist of a cable with one temperature sensor per foot of cable length. TIP wires shall be connected to data acquisition equipment capable of recording and storing temperature data from each sensor every 15 minutes for a recording period of at least one week.

The number of TIP wires per shaft shall be one per each foot of shaft diameter or four, whichever is greater. For the purposes of determining the number of TIP wires, shaft diameters shall be rounded up to the next greatest whole number. The TIP wires shall extend from within 1 inch of the bottom of the reinforcing cage to at least the top of concrete, with an additional 10 ft of slack wire above the top of concrete. The bottom TIP sensor shall be within 4 inches of the base of the drilled shaft, even if the shaft is overexcavated. TIP wires shall be evenly spaced around the circumference of the reinforcing cage. The TIP wires shall be installed parallel to the longitudinal axis of the reinforcing cage. TIP wires shall be affixed to the shaft reinforcing cage using plastic cable ties, with at least one tie per temperature sensor. Cable ties shall not be placed directly on the temperature sensors, except for the bottommost sensor of each wire. The TIP wires shall be affixed to the cage tautly but with sufficient slack to prevent damage during lifting of the reinforcing cage.

After the reinforcing cage has been placed in the shaft but prior to the placement of concrete, each TIP wire shall be checked to ensure temperature data can be read and recorded for each sensor. Any defective TIP wires shall be replaced prior to placement of concrete.

3. Recording Period

Recording of temperature data from all TIP wires in a shaft shall start prior to concrete placement for the shaft. Recording of temperature data shall continue until at least 24 hours after the peak

temperature has been observed. Temperature measurements shall be recorded for each sensor every 15 minutes during the recording period.

4. Results and Reporting

TIP reports shall be submitted within three working days of the end of the recording period.

TIP reports shall include for each shaft at least two temperature profile plots. Each temperature profile plot shall present temperatures on the horizontal axis versus depth or elevation on the vertical axis. On each temperature profile plot, one line shall be included for each TIP wire, and an additional line shall be included for the average of all TIP wires. One temperature profile plot shall present temperatures at the time of peak temperature development, and another temperature profile plot shall present temperatures at approximately half of the time to peak temperature development. Depths corresponding to the top of shaft, bottom of shaft, and any of the following features shall be indicated on the temperature profile plots: top of temporary casing, bottom of temporary casing, top of permanent casing, bottom of permanent casing, shaft diameter change, and any other installation details deemed relevant to the TIP analysis (e.g. depth of tremie breach). The date and time of analysis and the time elapsed since the completion of concrete pouring shall be noted on each temperature profile plot. Each temperature profile plot shall also include a legend noting the location of each TIP wire with respect to North.

TIP reports shall also include a plot of effective radius versus depth or elevation based on temperatures at approximately half of the time to peak temperature development. The effective radius values at the top and bottom of the shaft shall include roll-off corrections. Average temperature parameters for the top and bottom shall be based on measurements from nearby depths at the time of analysis. The soil temperature shall be based on TIP measurements just prior to placement of concrete. The bottom scale factor in feet shall be estimated as 0.3 times the square root of the elapsed time in hours since concrete placement. The top scale factor shall be 0.3 feet less than the bottom scale factor.

TIP reports shall also include plots of temperature versus time for the bottom two levels of sensors and for depths of any suspected defects. Suspected defect depths shall be identified from shaft installation records (e.g. depth of tremie breach, potential soft bottom conditions) or from the temperature profile plots (e.g. depth of low observed temperatures). The temperature versus time plots shall include at least three lines: (1) a line representing temperatures for the depth of the suspected defect, (2) a line representing temperatures for a nearby depth that appears to be uninfluenced by the potential defect, and (3) a line representing the temperature difference between (1) and (2). The line for (3) shall be plotted on a secondary axis. Alternatively, the line for (3) may be plotted on a separate plot.

Effective radius profiles may be included in TIP reports. Effective radius profiles shall not be used as a means for evaluating the data or for inferring specific values of concrete cover.

5. Evaluation and Recommendation

Evaluation of TIP data shall consider any available records of drilled shaft installation, including concrete yield plots. TIP report conclusions regarding the interpretation of TIP results shall consider observations from drilled shaft construction records.

TIP reports shall include a conclusion stating either that no imperfections were indicated in the TIP records or listing specific locations and characteristics of potential imperfections. If imperfections are

suspected, the depth of each suspected defect shall be indicated in the report. If possible, the cross-sectional location of each suspected defect shall also be indicated in the report in terms of cardinal direction (e.g. northwest quadrant of the shaft).

TIP reports shall include a recommendation to accept the shaft as-is, a recommendation for further review, a recommendation for further investigation, or a recommendation for repair. The Engineer of Record shall consider the recommendation when making the final acceptance decision.

6. Acceptance

Note: this section should apply to all integrity test methods, not just TIP.

The Engineer of Record shall make the final determination of shaft acceptance based on review of the shaft installation records, concrete integrity test results, and any subsequent analysis, investigation, and repair of the shaft.